

AD

AD718086

A STUDY OF
FRICTION FUNDAMENTALS
IN EXPLOSIVES

DECEMBER 1970

Final Technical Report
Contract DAAA21-69-C-0558

by

JOHN A. BROWN
Berkeley Heights, New Jersey

for

United States Army
PICATINNY ARSENAL
Dover, New Jersey

Reproduced by
NATIONAL TECHNICAL
INFORMATION SERVICE
Springfield, Va. 22151



THIS DOCUMENT IS APPROVED FOR PUBLIC RELEASE
AND SALE; ITS DISTRIBUTION IS UNLIMITED.

8.

TABLE OF CONTENTS

	<u>Page</u>
1. FOREWORD -----	i
Objectives	
Scope	
Acknowledgements	
2. SUMMARY -----	1
3. THE NATURE OF MECHANICAL FRICTION -----	3
The Classical Understanding of Friction -----	3
The Nature of Solid-Solid Contact -----	9
The Generation of Heat between Sliding Solids -----	18
4. FRICTION HAZARDS TO EXPLOSIVES -----	29
Laboratory Friction Sensitivity Testers -----	29
Hazard Reduction Techniques -----	35
5. SUGGESTED FRICTION RESEARCH TOPICS -----	39
A Mathematical Model of Friction Ignition -----	39
Experimental Test of the Model and Application to Hazard Control -----	41
Development of Improved Friction Sensitivity Testers -----	41
Fracture and Electrostatics -----	42
Summary Outline of Suggested Research -----	43
6. BIBLIOGRAPHY -----	45
General -----	45
Asperities and Solid-Solid Contact -----	45
Heat Generation and Temperature Statistics -----	47
Studies on Explosives -----	48
Rubber and Polymeric Solids -----	50
Lubrication -----	51
Crushing and Fracture -----	51
Electrification -----	53
Abrasion -----	53
Other -----	53
7. APPENDIX -----	55
Francis: <i>Interfacial Temperature Distribution Within a Sliding Hertzian Contact.</i> -----	55
Beerbower: <i>A Critical Survey of Mathematical Models for Boundary Lubrication.</i> -----	65

1. FOREWORD

The objective of this study is to transplant some new understanding of friction phenomena into the science of explosives initiation and safety, and to suggest fruitful new research programs which will go beyond the empirical and enhance basic understanding. It is essentially a planning study.

Mechanical engineers have been studying friction since the fourteenth century, and they have gained a degree of competence in dealing with it by lubrication and by modification of surfaces. Their actual understanding of friction is still fragmentary; but some of the mechanical and lubrication art can be applied to the problems of explosives, and this report gives an introduction to that art.

The art selected for presentation is the generation of heat and hot-spots by mechanical friction. In recent years, a number of investigators have addressed themselves to quantitative, mathematical models of this phenomenon in metals; and it appears feasible to adapt their treatments to explosives. Successful adaptation would lead to a quantitative understanding of frictional initiation and to a concomitant delimitation of what can and cannot be done about it. This report includes a suggested Research Plan to do that.

This study has searched the general literature on lubrication and micromechanics through the year 1970, and has included personal consultation with selected authorities in the fields of friction and lubrication. So much material was found that it was necessary continually to narrow the scope of this review in order to preserve adequate depth in the selected topic; the literature is enormous, and one could literally spend a career studying it and adapting it to explosives. Future workers wishing to range wider than the scope of this report will find an excellent starting point in the general references cited.

This report is the product of Picatinny Arsenal Contract DAAA21-69-C-0558, carried out by the author on a non-profit, spare-time basis. The courtesy of Esso Research and Engineering Company in approving this outside activity by a full-time employee and in providing library access is gratefully acknowledged, as is the invaluable counsel of the author's colleague, Mr. Alan Bearbower. The contract was sponsored by the Explosives Laboratory and monitored by Dr. Joseph Hershkowitz and Dr. Bernard Pollock of the Applied Physics Branch thereof.



JOHN A. BROWN
Principal Investigator

2. SUMMARY

This study introduces the knowledge of asperity and flash temperature statistics which has been contributed by the engineering and lubrication fields and gives an anthology of primary and summary sources to support a sound theoretical investigation of its application to the explosives field. It outlines a Research Plan to derive an integrated mathematical model of frictional ignition and to test its validity with empirical data. It suggests how a validated model will lead to better safety data and to better and safer explosives handling techniques.

Solids do not contact each other over their entire touching surfaces, as they appear to do, but rather only on the tips of the higher surface *asperities*. The total *area of real contact* is such a small percentage of the total surface area that the touching asperities are loaded to their yield point and deform until their aggregate cross section is just adequate to support the load.

Most of the surface is not even touching; but the tiny areas which do touch - the *junctions* - are in such intimate contact that van der Waals, electrostatic or even interatomic bonds form and lead to strong *adhesions*. When one solid body is forced to slide over another, the adhesions are forcibly sheared; and the work required to shear them is the major component of the frictional resistance.

The heat generated between two sliding bodies, which is equal to the work expended in making them slide, necessarily appears in and only in the junctions; and since the total area of the junctions is quite small, the resulting temperatures can be quite high - hundreds or even thousands of degrees. If one knew the size of each junction and the fraction of the total frictional power it consumed, one could readily calculate the resulting temperature in that particular *hot-spot*.

The size of individual junctions is usually not known; but the average size can be estimated, and the distribution of sizes appears to be Gaussian or nearly so in a broad range of cases, so that at least a *statistical description* of the *flash temperatures* on the asperity tips can be derived. This function, coupled with published models of the growth of hot-spots to explosion, offers a way to calculate the probability of ignition of a given explosive in a given frictional situation, entirely from first principles. Comparison with empirical data will then serve to test the validity of the model.

A number of alternate models can be postulated, involving different assumptions as to physical mechanisms of heat generation and as to what surfaces are and are not critical; and there is a *laboratory friction sensitivity tester* either existing or suggested for each. Calculation of ignition probabilities as above offers a new and powerful way to test the validity both of the assumptions and of the testers, and thus to gain a deeper understanding of the entire frictional initiation process.

INTENTIONALLY

BLANK

3. THE NATURE OF MECHANICAL FRICTION

The classical concepts of friction coupled with modern concepts of the nature of solid-solid contact open up a new approach to understanding the basic nature of the frictional initiation of explosives.

THE CLASSICAL UNDERSTANDING OF FRICTION

Friction is the resistance to motion which exists in varying degree whenever one solid object is caused to slide over the surface of another one. It is a universal attribute of matter, and its application has its roots in prehistory. The use of sleds, rollers and wheels, often supplemented by liquid lubricants, dates back more than 3000 years; although the scientific study of frictional phenomena is much more recent.

Leonardo Da Vinci was probably the first purposeful observer of friction phenomena. He noted that the friction of two sliding bodies is *independent of their contacting areas* and that the total frictional force is *proportional to the normal load* between the contacting surfaces (113). These two principles, still valid today, are usually called "Amontons' Laws", after the French scientist Amontons who rediscovered them in 1699 (114). (There are limits to their validity, but mainly they are true.)

Amontons (114), Coulomb (115) and Euler (116) further quantified the studies of friction; and by 1785 most of today's general understanding was established. These scientists hypothesized that friction is due to the interlocking of mechanical protuberances or *asperities* on the surfaces of the contacting material like two pieces of sandpaper face to face. This "Roughness Hypothesis" explained Amontons' laws and remained the majority view right through the nineteenth century and into the twentieth.

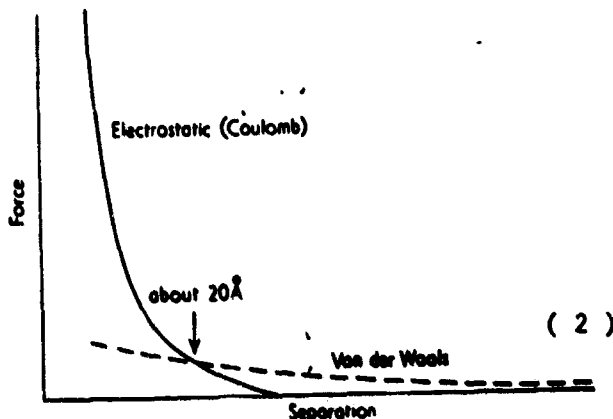
Beginning about 1920, however, interest began to revive in the "Adhesion Hypothesis" as growing precision in measurement revealed more and more weaknesses in the Roughness Hypothesis. "Adhesion" hypothesizes that actual "welding" occurs wherever two surfaces touch and that the frictional resistance to sliding is the force required to break the welds. Interestingly enough, Adhesion had been considered by the original workers and rejected because they could not reconcile it with the observed fact that the frictional force was independent of the contacting area.

Today, it is almost universally accepted that frictional force is due to a combination of the two effects: "Adhesion plus Plastic Deformation", wherein only a few of the higher asperities of each surface actually contact a few asperities of the other surface. As the normal

load is increased, the high asperities are squashed down so that the next smaller asperities begin to contact each other; and this process continues until there is enough contact area to support the load. This *actual area of contact* is very much smaller than the *apparent area of contact* (the gross size of the object's face); in fact, it has nothing to do with the size of the face, which neatly explains why the frictional force has nothing to do with the size of the face but is proportional to the normal load.



As the asperities contact one another, they adhere; and the nature of the adhesion varies widely. Objects of like composition can often form actual welds or interatomic crystal bonds, but there are smaller adhesive forces which act between any two materials. Bowden (2) describes them as Coulombic and Van der Waals. Closer than about 20 Å, the force is mainly coulombic and is relatively strong. Beyond about 20 Å, the force is mainly Van der Waals and is weaker but longer range.



Force-separation curves between solid bodies as a function of separation. The electrostatic forces are very large for small separations but fall off to a negligible value for separations greater than about 30 Å. For greater separations the only discernible forces will be the relatively weak van der Waals forces.

It can therefore be seen that forced sliding requires the rupture of asperity adhesions and that there will indeed be some asperity interlocking just as Amontons had thought. Quantitatively it turns out that most of the observed frictional force is due to adhesion, and only a small amount of it is due to asperity interlocking or deformation.

A complication resides in the fact that adhesion is usually greatly inhibited by the presence of an interfering film of something such as a surface oxide, or moisture, or a foreign material, or even adsorbed air. Indeed, were it not for these interfering films, things could scarcely be slid at all. Atomically-clean metals placed in contact in a good vacuum adhere so strongly that they seize and are permanently welded. So do bearings which are run under such heavy loads that the protective films are stripped off. Almost everything in familiar experience is protected by some kind of film, so that the observed adhesion is very much less than welding - it is usually more akin to Van der Waals forces than to interatomic bonding - nevertheless, adhesion still dominates over interlocking of asperities.

Lubrication, of course, is simply the deliberate interposition of an interfering film of oil or some other liquid. The resulting reduction in friction owes something to reduced interlocking of asperities, since the oil takes up some space; but it is mainly due to reduced adhesion, particularly in slowly-moving or essentially stationary systems.

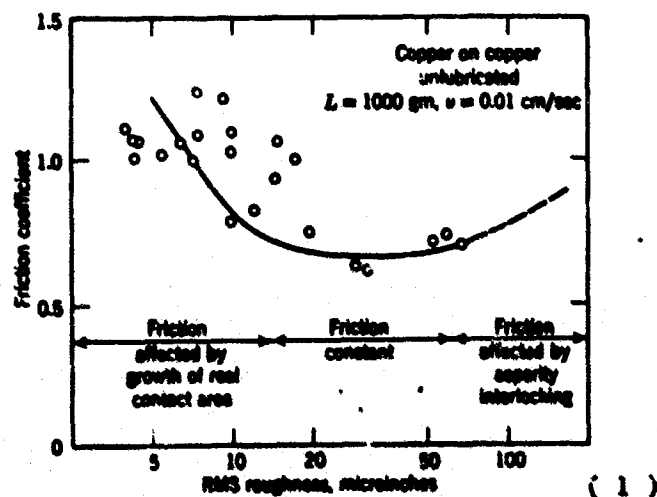
The most useful quantitative concept is that of the *coefficient of friction*, the proportionality constant between the frictional force required to slide a given object and the normal load:

$$F = fL$$

The coefficient of friction is a property of the particular materials involved but not of the physical size of the system. It says, for example, that the same force is required to slide a brick across a table regardless of whether the brick is lying flat, resting on one edge or standing on end. It takes twice as much force to slide a stack of two bricks and ten times as much force to slide a stack of ten bricks. It takes the same force to slide two stacks of five bricks each as to slide one stack of ten bricks. The coefficient is, in principle, a true constant and is independent of either the load or the contacting surface area. Thus, large and small objects have the same coefficients of friction.

It is frequently stated that the coefficient of friction is also independent of the sliding velocity, but this is only approximately true. It is well known that the friction force required to start sliding is usually greater than the force required to maintain sliding, and this has given rise to the notion that there are two coefficients of friction - *static* (for surfaces at rest) and *kinetic* (for surfaces in motion). These are normally shown separately in tables of friction coefficients. Recent work has shown that this is a gross oversimplification (1). The static coefficient is a function of the time of contact, and it increases as the contacting asperities slowly yield and the real area of contact increases. The kinetic coefficient varies with sliding velocity, but only slightly, usually by just a few percent as the sliding speed is raised by a factor of ten. For most practical purposes of interest here, the kinetic friction coefficient may be considered to be a constant independent of the sliding velocity.

To a good approximation, the friction coefficient is independent of the roughness of the sliding surfaces - at least it is in the roughness range normally encountered in engineering practice. Very smooth surfaces give abnormally high friction coefficients because the area of real contact is abnormally high. Very rough surfaces give abnormally high coefficients because asperity interlocking becomes excessive. But in the roughness range in which we actually find most surfaces, the friction coefficient is at a minimum and almost independent of roughness.



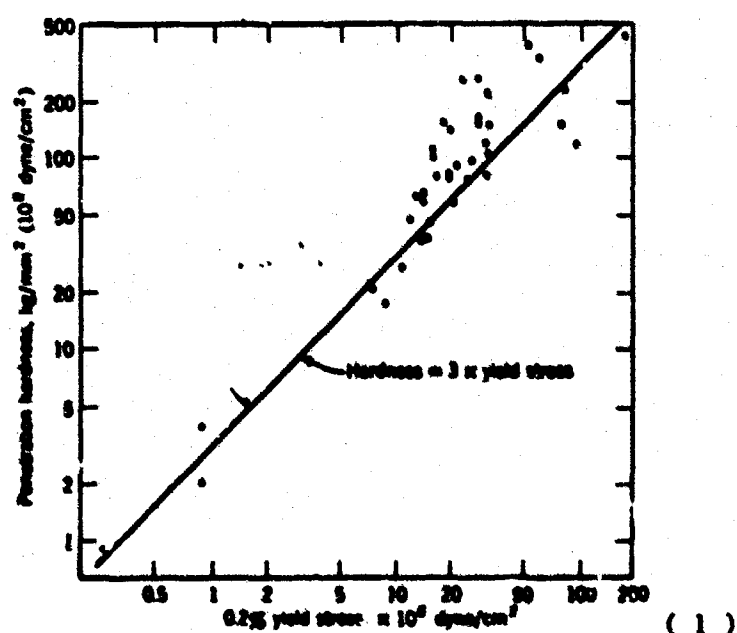
Another exception occurs when a rough hard body slides on a much softer one. Here the asperities of the rough surface dig into the softer material and the ordinary "friction" is augmented by gouging and plowing.

All elementary texts on friction point out that the coefficient of friction of a given material is approximately equal to the ratio of the material's shear strength and penetration hardness

$$f = s/p$$

because the sliding process involves the *shearing* of adhesions which are limited in size by the *hardness* of the material (1,2). This says that friction can be reduced by decreasing the shear strength of the interface, and of course one of the effects of lubrication is to interpose a low shear strength interface between two relatively hard materials. It also says that, if one has two different materials sliding on one another; it is only the strength and/or hardness of the *softer* of the two which matters.

The s/p relationship is neither exact nor fundamental. It is vitiated by involving assumptions which are only approximately true and by ignoring effects such as surface energy and asperity interlocking which become important just when ones gets into unusual regimes and needs theoretical guidance the most. Moreover, s and p are not really independent quantities; they are very similar quantities which depend in almost the same way upon such factors as bond strength, nature of dislocations, etc., so that one goes up with the other and the ratio is quite similar for a wide range of materials. For example, lead and low carbon steel vary by nearly a factor of 100 in shear strength and penetration hardness, but f is nearly the same for steel (1.0) as for lead (1.2). This point is shown graphically by the following figure which plots penetration hardness vs. yield stress for pure metals (1).



Coefficients of friction do not vary as greatly from material to material as might be expected. Most common metals exhibit coefficients of 0.1 - 0.3 when tested as one normally sees them. Most non-metals run slightly higher at 0.3 - 0.4. Wood-on-steel is about 0.5, as is wood-on-stone, iron-on-stone and leather-on-iron. Most solid explosives run about 0.6 - 1.1. Carefully cleaned metals run about 0.7 to 1.3 in air. This is not a large range of variation; many physical properties vary by orders of magnitude from material to material.

Wider variations are known. Teflon, for example, is anomalously low at 0.04 due to its exceptionally low surface energy; and freshly-prepared copper surfaces in high vacuum can run from 5 to 200 due to cold welding on contact. Nevertheless, these cases are wildly exceptional; and the fact remains that most materials have about the same coefficients of friction - about 0.5.

To some extent, the striking uniformity of coefficients of friction is due to the fact that most materials are handled and tested in air, and rather contaminated air at that. The visible "surface" of a bar of iron, for example, is not iron at all; it is iron oxide, covered with a layer of adsorbed moisture and atmospheric gases and most likely a layer of oily materials from adjacent machinery and/or human beings. Non-metals may lack the oxide layer (many of them are oxides themselves); but they will have the moisture, gassy and oily layers. Consequently, the interface is the same, or nearly the same, in most cases; and one should expect the friction to be similar even on dissimilar materials.

For most ordinary materials of experience - probably including explosives - most of the frictional force is due to adhesion. The "roughness component" is small, approximately 0.05 in an overall coefficient of 0.5. Other conceivable effects, such as plowing and electrostatic attraction, are usually negligible.

It should be noted for the record that there are important difficulties with the adhesion explanation of friction; and most modern workers feel that while it is essentially correct, it is also a gross oversimplification of the friction process. Nevertheless, it serves so well for all but the most exacting purposes that most workers in the friction field would rather amend it than abandon it.

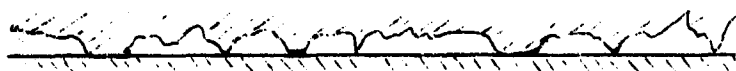
The foregoing discussion is intentionally simplified to serve as a first introduction for personnel who are scientifically trained but unfamiliar with this field. Those who wish to delve deeper will find excellent resources listed in the general bibliography. The books by Rabinowicz (1) and Bowden and Tabor (2,3) are particularly recommended, as is the NASA publication *Interdisciplinary Approach to Friction and Wear* (4). Other, more specific, references will be found in the specific citations.

THE NATURE OF SOLID-SOLID CONTACT

To the human eye, it appears that two flat surfaces placed in contact actually touch each other over their entire areas; but this is far from the truth. Visually smooth surfaces, even optically polished ones, are quite rough on a microscopic scale. General workshop surfaces or metals, for example, have asperities on the order of 15 microns high; and even the smoothest metallic surfaces have asperities 100 - 1000 Angstroms high. If such a surface were slowly lowered onto one which was truly flat on the atomic scale, it would first make contact only on the peaks of the highest asperities, and the remainder of the surface would not be in contact at all.



If the material were ideally rigid, only point contact would be made on only the three highest asperities, and the upper object would be supported on a tripod; but in actuality, the asperities are so small that the weight of the object far exceeds the yield strength of the material, and the asperities squash down and permit other, lower asperities to contact also. These in turn squash down and permit still more contacts until finally there is enough total area of contact to support the load without further yielding.



The total *area of real contact* is only a small percentage of the total area of the surface; most of the surface is not touching at all and never will touch, even if the load is increased enormously. The total area of contact is approximately equal to the normal load L divided by the penetration hardness p of the material:

$$A_r = L/p$$

As an example, consider a smooth, 100-gram cube of copper resting on a smooth steel plate. The load is 0.1 Kg, and the penetration hardness of copper (the softer material) is 6000 Kg/Cm². This gives $A_r = 1.67 \times 10^{-5}$ Cm², compared to a total area of the cube face of 5.0 Cm².

Actual cases, of course, are not as simple as pictured above. The formula $A_r = L/p$ is for purely plastic deformation, and is an approximation anyway. Real asperities no doubt deform elastically over part of their travel, and elastic deformation is described by the more complex Hertzian equations (117), of which

$$A_r = \pi \left[\frac{3LR}{2E'} \right]^{2/3}$$

Where:

- A_r = Real area of contact
- L = The normal load
- R = The relative radius of curvature of the two surfaces
- $E' = E/(1-\nu)^2$
- E = Young's modulus
- ν = Poisson's ratio

is a simplified example. Also, in real cases, both surfaces are rough, and the contact pattern is much more complex as asperities contact other asperities on their shoulders or even in the opposing valleys.



Nevertheless, the *total area of real contact* must remain that given by the appropriate deformation equation, since it is a function only of the load and the strength of the material, not its shape. The total area of real contact is distributed among all the asperity junctions. The individual contacts will range all the way from some just barely touching to others widely squashed out, and the resulting junction sizes will range all the way from mere points up to a circle proportional to the size of the largest and highest asperity.

It must not be thought that asperities are anything like as high and jagged as the sketches above would suggest. The vertical scale of the sketches is greatly exaggerated for clarity. Actual asperities tend to be low and broad, with contact points widely spaced. Early metallographic studies of metal surfaces showed that solid metal surfaces have asperities which are typically 10 to 300 μ in. high; that their slopes are shallow, so that their bases can be 50 to 3000 μ in. across; and that individual contact areas are about 100 to 1000 μ in. wide. The following electron micrographs of a gold surface show dome-like asperities. The largest are roughly 400 μ in. across and 50 μ in. high; the smallest are less than 20 μ in. across and 5 μ in. high. These data are from Williamson (4); other authors have reported similar findings on a wide variety of materials.

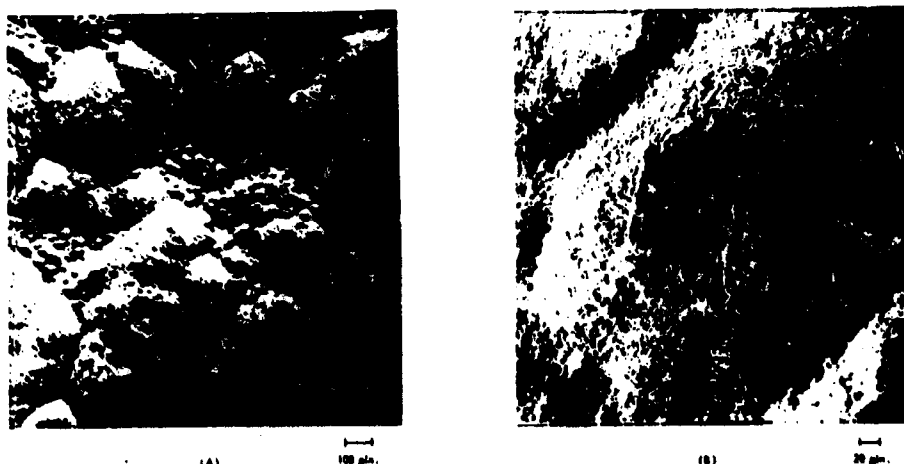


FIGURE 1.—Electron micrograph of plated gold surface. (a) General view at X 4000. (b) A single contact area X 18000. (4)

One would like to know the size of each individual junction and the number of junctions of each particular size, and much effort has gone into studying these parameters in real systems. People have pressed opaque solids against glass plates and observed the junctions through the glass (3), and other people have prepared contour maps from electron micrographs of aluminum surfaces (4); but the most promising technique for our purposes appears to be statistical.

Greenwood and Williamson have shown (8) that a wide variety of surfaces have asperity height distributions which are very nearly Gaussian, and that even in surfaces which are strongly non-Gaussian as a whole, the upper 50% usually is accurately Gaussian. For example, they report the following data for bead-blasted aluminum (8):

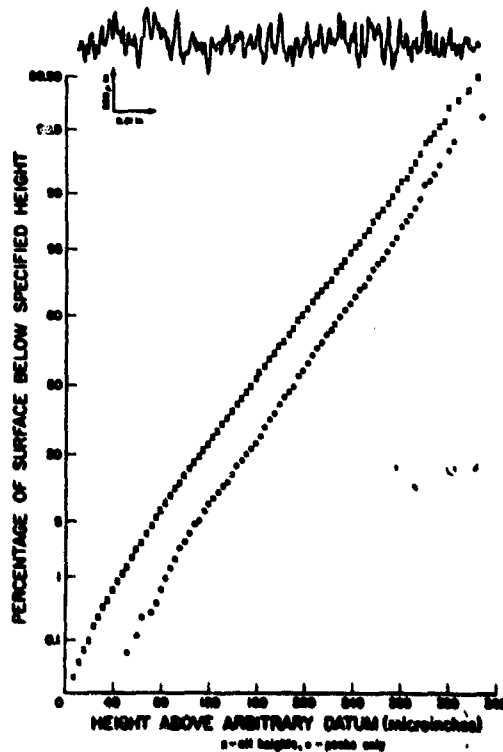


FIGURE 4.—Cumulative height distribution of bead-blasted aluminum. Both the distributions of all heights (X) and of peak heights (O) are Gaussian. The profile of the same surface is shown in the upper diagram; the vertical magnification is 50 times the horizontal magnification. (4)

and the data on the following page for abraded steel (8):

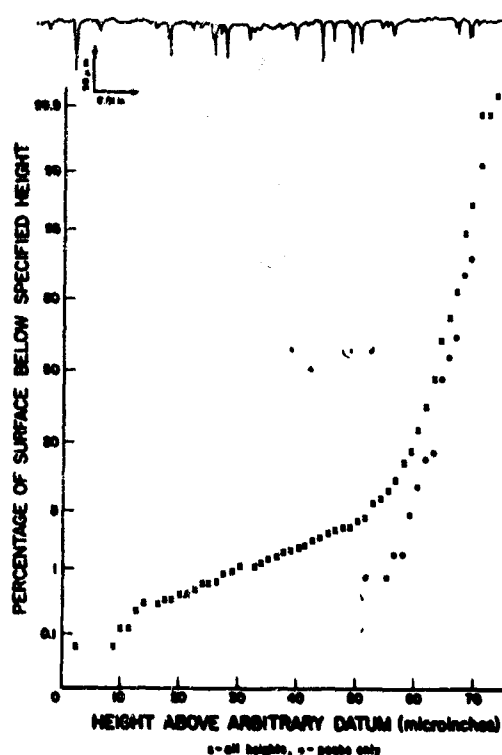


FIGURE 5.—Cumulative height distribution of mild steel specimen. Distribution of all heights, X. Distribution of peaks, O. This specimen was abraded on 400 grade carborundum paper, then slid against a copper block flooded with oleic acid, at approximately 10 kg, 130 cm/s for 30s. Although the distribution at first sight appears highly non-Gaussian, in fact nearly 90 percent of the surface is Gaussian: the surface, with an actual standard deviation of 50μ in., would behave in contact as if Gaussian with a standard deviation of half this. The profile of the same surface is shown in the upper diagram; the vertical magnification is 200 times the horizontal magnification.

(4)

Williamson also argues that most surfaces indeed *ought* to be Gaussian because of the statistical principle that any quantity which is the result of a large number of random increments and decrements will tend to follow a Gaussian distribution (the Central Limit Theorem of statistical theory) (4). Most engineering surfaces are indeed the end result of a large number of independent deforming processes (grinding, machining, sandblasting, polishing, etc.); and many other surfaces are made by such processes as casting against engineering surfaces or processing in equipment made from materials having engineering surfaces. Moreover, the Central Limit Theorem argues that in almost *any* attempt, human or natural, to produce

uniformity, the residual errors will be Gaussian provided the attempt is good enough to exclude systematic or periodic errors. And Williamson's findings seem to say that even systematic errors leave a Gaussian distribution in the higher asperities, which are the ones that participate in solid-solid contacts.

So it seems likely that we can arrive at a useful *statistical* description of asperity and junction sizes even if we cannot determine the sizes of individual junctions during the sliding process. Inasmuch as the frictional initiation of explosives is itself a statistical phenomenon, a statistical description of the junctions may well be quite good enough.

A number of investigators have attacked the problem of deducing the statistics of junction sizes from statistical descriptions of asperity heights. Greenwood, for example, has shown (9) that the *average* junction size does not change with the applied load if the asperity size distribution follows any kind of exponential law. The original junctions grow, of course; but new, tiny ones form at just the rate needed to keep the average constant and the distribution essentially normal. Tabor has pointed out in a comment on Greenwood's paper (9) that Gaussian distributions, which as we have seen we expect to find on real surfaces, are close enough approximations to exponential distributions to make the arguments valid for them as well.

We already know the *total* junction area - it is the area of real contact. If we could determine the total *number* of junctions, we would then have the average junction area; and Greenwood's statistics would tell us the entire distribution of junction sizes.

Rabinowicz (1) has investigated the number of junctions existing during sliding by several techniques, including some statistical ones. He argues that the real area of contact (the sum of the asperity junctions) is constant as long as the load remains constant, but that individual junctions are continually being made and broken in a random fashion. This gives rise to random variations in the instantaneous coefficient of friction over a sliding distance which is a function of the average junction size. Rabinowicz derives the diameter of the average junction from an autocorrelation analysis in which the friction coefficients $f_1 \dots f_i \dots f_k \dots f_n$ are measured at intervals off a friction-distance plot, and the autocorrelation coefficient

$$r_k = \frac{n}{n-k} \frac{\sum_1^n (f_i - \bar{f})(f_{i+k} - \bar{f})}{\sum_1^n (f_i - \bar{f})^2}$$

is calculated (22). The distance k at which the autocorrelation drops to zero is equal to twice the average junction diameter. For copper on steel, he finds an average junction diameter of 9×10^{-4} cm., which is in reasonable agreement with values derived from measurements of wear debris.

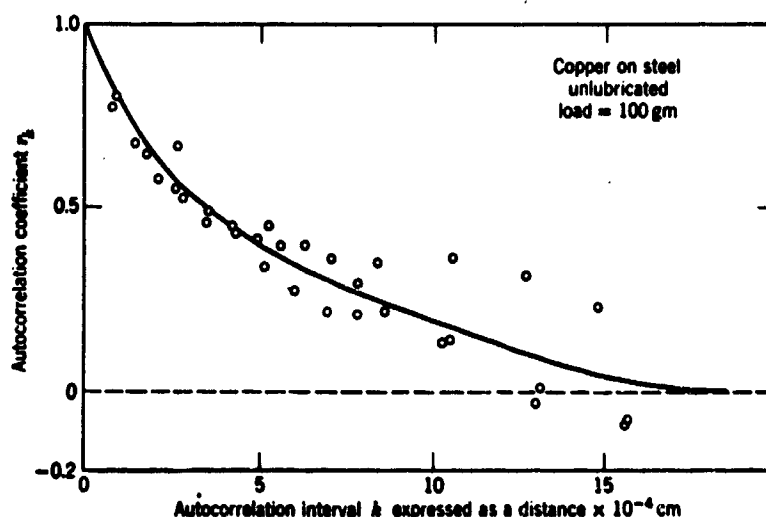


Fig. 3.13. Autocorrelation coefficient of friction traces as a function of distance along the sliding track. Since r_k drops to zero in 18×10^{-4} cm, the average junction diameter is 9×10^{-4} cm.

(1)

Table 3.1 Estimates of Junction Diameter

(1)

Combination	Load	Lubricant	Method	Junction Diameter	Reference
Copper on steel	1 kg	None	f_s - distance	7μ	Rabinowicz, 1951
Steel on copper	1 kg	None	f_s - distance	6μ	Rabinowicz, 1951
Copper on copper	1 kg	Cetane	f_s - distance	8μ	Rabinowicz, 1951
Copper on steel	2 kg	None	Particle size	31μ	Rabinowicz, 1953
Copper on copper	0.1 kg	None	f_k autocorrelation	10μ	Rabinowicz, 1956
Copper on copper	0.1 kg	None	f_k fluctuations	5μ	Rabinowicz, 1956
Steel on steel	80 kg	Contaminated	$f_s - t$ vs. $f_k - v$	10μ	Rabinowicz, 1958
Copper on copper	Any	None	$24000 \gamma/p$	26μ	Eq. 3.15
Steel on steel	Any	None	$24000 \gamma/p$	13μ	Eq. 3.15

Rabinowicz also estimates the total number of junctions from a different treatment of the same statistical data (1). He points out that if an assumption is made as to the range in strength between the weakest and strongest junctions, and a factor of 2 seems plausible in many cases, it is possible to estimate from the amplitude fluctuations how many junctions must have been present at any time. He derives the expression

$$\frac{\sigma}{\bar{f}} = \frac{1}{4\sqrt{n}}$$

Where:

σ = standard deviation of friction values
 \bar{f} = the mean friction coefficient
 n = the number of junctions

Rabinowicz also deduces the size distribution of junctions from autocorrelation data by using all the autocorrelation coefficients, not just the one at which the correlation reaches zero; and he finds size distributions in good agreement with those deduced from wear particle measurements (22).

Ling has also done calculations in this area (13), although his work has been more concerned with the deformations of asperities during sliding and is better considered in the next section under the generation of heat between sliding solids. In general, his results are consistent with those discussed above.

Jones, *et.al.*, (10) and Whitehouse and Archard (20) have also recently published reviews of methods of obtaining areas of real contact and of the properties of random surfaces in contact. Their conclusions are essentially those already stated, starting from slightly different initial assumptions.

Tsukizoe and Hisakado, in a recent trilogy of papers (16, 17, 18), present detailed calculations of the separation, the real area of contact, the number of contact points, the average radius of the contact points, and the distribution of radii of the contact points between two metal surfaces. They assume that the surfaces contain a large number of asperities in the form of cones of equal base angles, that the heights of the cones are Gaussian, and that the metal deformation is plastic. They also report empirical measurements on aluminum surfaces, with good agreement with the calculated values. These papers are too mathematical for review in this introductory discussion, but they deserve the most careful study by anyone who may wish to pursue this line.

In summation: although there are still a number of unresolved problems, there is general agreement that real surfaces consist of arrays of asperities with a Gaussian distribution of peak heights, that such surfaces contact each other only at junctions of aggregate area much less than the total apparent area of the surfaces, and that there are techniques for calculating the number and the size distribution of the junctions.

There are some fairly dubious assumptions built into some of these derivations, for example the assumption of purely plastic deformation of asperities; but other mathematical analyses have shown that it really does not matter if certain other assumptions, such as an exponential distribution of asperity heights, are true (9). There are also some contradictory assumptions in some of the complementary arguments; for example Rabinowicz assumes all junctions the same size in his autocorrelation treatment (22) which was used above to derive a junction size distribution; but the invocation of Gaussian distributions can rationalize a lot of that kind of thing too.

All the models have been criticized on the basis that real surfaces do not consist of idealized cones or wedges or sphere sections; but it has been shown that it really does not make much difference what the asperity shape is or what the exact deformation law is - one still gets an acceptably-Gaussian distribution of junction sizes, and one gets reasonable agreement with empirical data in test cases.

Nothing is yet known about the topography of the surfaces of explosive blocks, and some measurements should be early on the agenda of any program to adapt these insights to the study of explosives; but it would be surprising to find that explosive surfaces did not consist of asperities Gaussianly distributed.

THE GENERATION OF HEAT BETWEEN SLIDING SOLIDS

The generation of heat between sliding solids has been familiar since the first caveman slid down a vine and burned his hands. Boy Scouts use it when they rub two sticks together and start their campfire. We contend with it daily in the bearings of all our machines. In fact, in many machines such as automotive or helicopter transmissions, only an infinitesimal amount of the oil used is actually needed to lubricate the gears - all the rest is required solely as a coolant to carry away the heat generated by the friction between the gears. If the heat is not removed, the result can quickly be disastrous for the gears. In the case of sliding explosives, failure to deal with frictional heat can be even more dramatically disastrous.

It is easy to determine the heat generated in a simple sliding situation. It is simply the thermal equivalent of the work expended in making the object slide against friction: one calorie for each 4.18×10^7 ergs. This datum is seldom easy to obtain in a hazard situation where one might have a shower of complex shapes cascading down under gravity, but it is easy to obtain in a laboratory situation where one can set up simple, measureable operations and collect quantitative data.

The gross *amount* of heat is not the datum of interest for an explosive, though; one wants to know the resulting *temperature* in a given volume of explosive and the *size* of the volume which reaches the given temperature.

The interface temperature can be estimated from conventional heat flow equations by assuming that the heat is generated in the interface and conducted away into each of the two sliding objects according to their respective thermal conductivities. For the case of an infinitely long cylinder rubbing end-wise on a flat plate at moderate sliding speeds:

$$\Delta T = \frac{fLv}{4Jr(k_1 + k_2)} \quad (\text{Equation A})$$

Where:

- ΔT = Mean temperature rise above the rest of the material
- f = The coefficient of friction
- L = The normal load (in force units)
- J = The mechanical equivalent of heat
- r = The radius of the rubbing cylinder
- and k_1 and k_2 are the thermal conductivities of the two contacting surfaces.

The simple equation above needs many corrections and elaborations for real situations. At high sliding speeds, far more heat flows into the plate, which continuously sends new, cool material into the zone where heat is generated, than into the cylinder, the same part of which always remains at the interface. This problem has been attacked by many investigators, including Blok (31), Jaeger (40), Bowden and Thomas (33), and Archard (32).

Francis, in a forthcoming paper (41), derives an analytic expression for the steady-state interfacial temperature field in a sliding circular Hertzian contact, taking into account the difference in bulk temperatures of the two bodies and the ellipsoidal distribution of the frictional power in the contact area:

$$T_s(x, y) = \frac{2Q}{\pi^{1/2} k R^3} \left(\frac{2a}{\pi} \right)^{1/2} \left(1 + \pi^{-1/2} \left[0.65 \left(\frac{a}{\pi L(y)} \right) + 0.44 \left(\frac{a}{\pi L(y)} \right)^{2/3} \right] L^{1/2}(y) \Omega(u) \right)$$

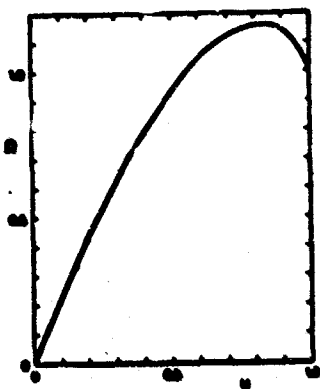


Fig. 4—The dimensionless function $\Omega(u)$ which prescribes the shape of the surface temperature profile across an infinitely fast moving band source having an elliptical power density profile. The leading edge of the band is on the left.

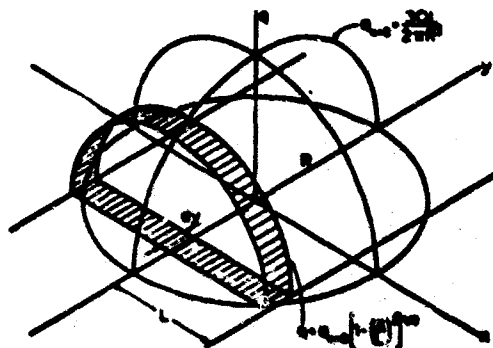


Fig. 5—Isometric view showing the fast moving ellipsoidal power density distribution, a differential strip (width dy , length $2L$), and its equivalent semi-infinite band source (width $2L$).

He derives a formula for the maximum interfacial temperature T_{max} in terms of the total frictional power Q , the radius of the contact R , the thermal conductivity k , and a dimensionless parameter B which describes the power distribution.

$$T_{max} = T(x=0, 0) = \frac{1.852Q/\pi Rk}{1.996 - 1.091B^{-0.818} - 0.537B^{-0.871} + B^{1/2}}$$

Francis' paper, in the form of a preprint of his presentation to the 25th ASLE Annual Meeting in Chicago, May 4-8, 1970, is included in its entirety in the appendix because it is not yet readily available from standard sources.

For hot-spot calculations, the radius r and the load L of equation (A) should be those for a single asperity junction, and their sums should equal the area of real contact and the total load, respectively. If one knew the total number of junctions and the size of each, one could pro-rate the load on each and the amount of heat flowing into each, and calculate the resulting temperature rise at each. One in general does not know much about individual junctions, but some approximations are possible.

Rabinowicz (1) shows that the radius of a junction is related to the surface energy γ and the hardness p of the softer material by the order-of-magnitude relation:

$$r = 12,000 \frac{\gamma}{p}$$

and that the load L an asperity will carry is its area times its hardness:

$$L = \pi r^2 p$$

Substituting in equation (A), he obtains the final expression:

$$\Delta T = \frac{9400 f \gamma v}{J(k_1 + k_2)}$$

and calculates flash temperatures on individual junctions as follows:

Material	f	γ	k	$\Delta T/v$ ($^{\circ}\text{C}/\text{cm}/\text{sec}$)
Brass on brass	0.4	900	0.26	0.15
Steel on steel	0.5	1500	0.11	0.75
Bakelite/Bakelite	0.3	100	0.0015	2.2
Glass on glass	0.9	500	0.0007	70.6

The approximations involved are rather gross, and they include the assumption that the total load is not a factor; but they give an idea of the magnitudes obtainable.

One could also plug in a Gaussian distribution function, as discussed in the preceeding section, and obtain a statistical description of the entire array of junctions. This should be quite adequate for the explosive situation, since explosive initiation is also statistical in nature. (In fact, the statistical nature of explosions is one of the strong arguments for Gaussian distributions of asperities.)

Ling has done a good bit of this (36), and has derived expressions for the instantaneous temperature of an asperity junction using a stochastic model of junction formation and breaking during the sliding process. At a sliding velocity of 5000 ft/min, he calculates flash temperatures of around 1800 °F for steel-on-steel, with variations from approximately 500°F to 2000°F.

For explosives, still another factor becomes important in attempting to calculate the temperature of a frictional hot-spot: the explosive will begin to decompose quite exothermically at some elevated temperature, and the temperature will run away, perhaps explosively. Fortunately, this process at least has been well studied, and expressions are available to calculate the thermal evolution of a hot-spot as functions of both the hot-spot size and temperature. For example, Zinn (48) expresses the progress of an exothermic reaction proceeding by first-order kinetics in a medium of thermal diffusivity k by:

$$\partial T / \partial t = k \nabla^2 T + (QZ/C) w e^{-E/RT}$$

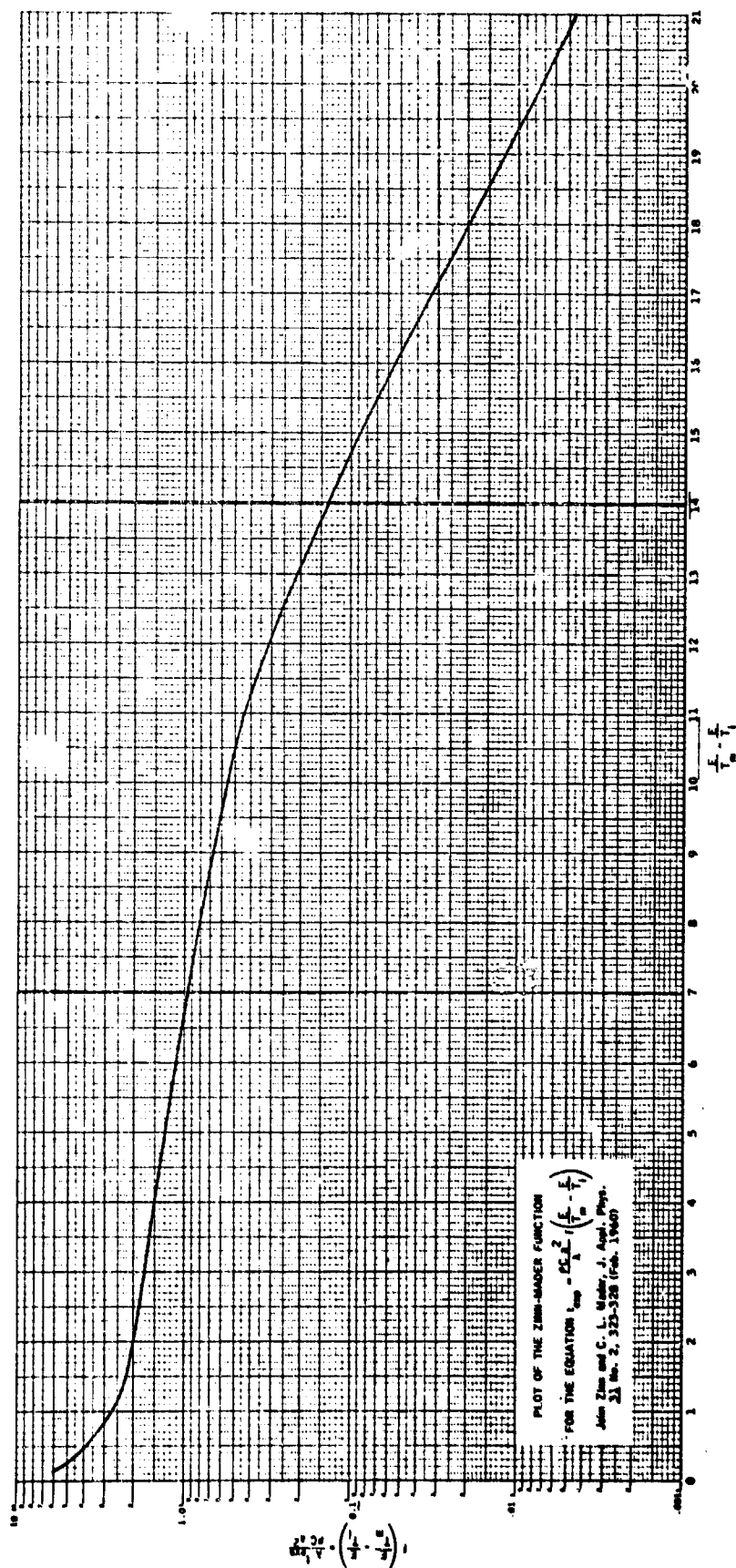
where the symbols have the usual meanings. A more useful expression is the Zinn-Mader (49) formulation for the minimum explosion temperature:

$$t_{\text{exp.}} = \frac{a^2}{\alpha} f(E/T_m - E/T_1)$$

where:

t_{exp}	= time to explosion	
a	= sample thickness	
α	= thermal diffusivity = $\frac{\lambda}{\rho c}$	λ = thermal conductivity
E	= activation energy	ρ = density
T_m	= minimum temperature for explosion	c = specific heat
T_1	= surface temperature	

The function f is a complex one best handled graphically:



It still remains for someone to integrate all these approaches into a coherent, quantitative description of the formation of hot-spots between sliding blocks of explosives. Expressions are available for the amount of heat generated, for the number, size and distribution of asperity junctions, for the temperature profiles in and between the junctions and their variation with time, for the flow of heat through the junctions and into the bulk of the explosive blocks, and for the thermal evolution of hot-spots in the explosive. This would be an ambitious undertaking, and its execution is far beyond the scope of this study.

Physical mechanisms for heat generation

The foregoing discussion has dealt with the fate of heat generated between sliding solids to the neglect of the actual generation of that heat. One does not need to know the origin of heat in order to understand its flow and effects, but some consideration of the mechanisms of heat generation is useful in understanding friction.

Viscous flow can take place in either a liquid or a solid, and the resultant heating is directly proportional to the work expended in causing the flow. For example, for shear in a thin film:

$$H = \mu AU^2/h$$

where:

- H = work per unit time dissipated into heat
- μ = viscosity of the flowing material
- A = area of the sheared film
- U = sliding speed
- h = thickness of the sheared film.

For a typical oil in a reasonable machine bearing, one can plug in appropriate values of 3.3×10^{-6} for μ , 25 Sq.In. for A, 300 in/sec for U, and 10^{-3} in. for h, and obtain a value of 7430 in-lb/sec, or 1.125 HP, or 840 watts of heating.

If all the heat remained in the oil, and the oil stayed in the clearance space, the temperature would rise at the rate of H/Vc , where V = the volume of the film and c = the heat capacity of the oil per unit volume. Taking $c = 140$ in-lb/cu.in. $^{\circ}$ F for a typical petroleum oil, one calculates 2120° F/sec.

Such drastic heating rates do not occur in normal practice because heat is lost into the massive heat sink of the metal parts and because hot oil is continuously extruded and fresh, cool oil is continuously supplied. In cases of lubrication failure, the reality of the above numbers is quickly apparent as bearings overheat and seize. One observes actual melting of even hardened steel surfaces.

Such heating rates may also be entirely realistic in the case of a sliding explosive, where the "lubricant" is molten explosive or even the surface layers of the solid itself, the shearing rate may be extremely high and the heat conductivity of the solid is low.

Calculation of heating for cases other than that of a well-defined, lubricated bearing is difficult, because it is seldom possible to pin down the properties or the dimensions of the material being sheared. In fact, even the calculation for the bearing is only grossly correct. It gives the *averaged* temperature for the entire volume of the oil film; but the oil film is not sheared uniformly, it contains a shear *gradient* and a consequent temperature gradient. The local heating in zones of highest shear can be very much greater than the overall heating.

Non-uniformity of heating has been studied by Appeldoorn, *et.al.*, for fluids forced through a capillary (46). For adiabatic, incompressible flow, the bulk heating is a function of the driving pressure, and the specific heat and the density of the fluid:

$$\Delta T_b = P/C_v \rho J$$

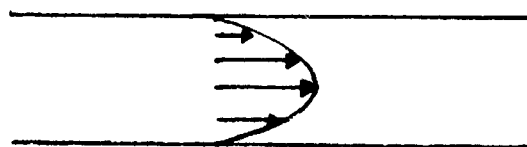
where:

- ΔT_b = the bulk temperature rise
- P = the driving pressure
- C_v = the specific heat of the fluid
- ρ = the density of the fluid
- J = the mechanical equivalent of heat

ΔT_b for a typical hydrocarbon oil is about 7°F for each 1000 psi.

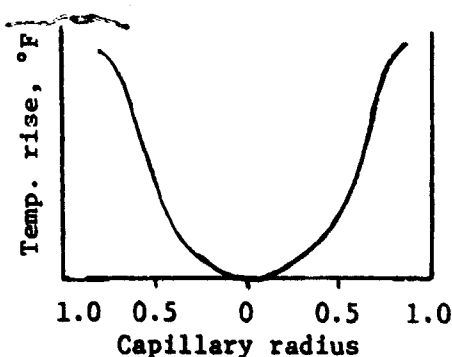
But this is only an *average* value; the actual temperature profile is very non-uniform across the capillary because the shear is very non-uniform. It is well known that the flow profile across

a pipe is approximately (not exactly) parabolic, with the fluid at the wall essentially motionless and that at the center essentially not in shear.



(Arrows indicate velocity vectors)

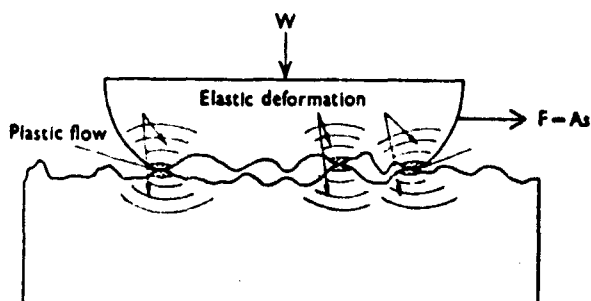
Appeldoorn, *et.al.*, have shown experimentally (46, 47) that this flow (and shear) profile is reflected in a temperature profile which is similar:



and they have measured temperature rises at the wall as high as 140°F for the case where the bulk rise was only 7°F.

For the case of one solid sliding upon another without lubrication, the shear gradient may be very steep indeed; and the area of shear may be very small, *i.e.*: the area of real contact, which is vastly smaller than the bulk area of contact; so that the local hot-spots due to shear may be very hot indeed.

Nothing limits the above phenomena to liquids. Solids can flow too, under sufficient pressure; and sufficient pressure specifically exists in an asperity junction already loaded to the plastic flow point. The following diagram which has been used repeatedly by Bowden (3) illustrates the point:



Two solids placed in contact are supported on the summits of surface irregularities. The pressure exceeds the yield pressure p_m of the solid, which flows plastically until the area of contact A is sufficient to support the load W . Hence $A = W/p_m$. The material around the regions of contact will be elastically deformed. If s is the shear strength of the junctions, $F = As$.

Solid flow also exists whenever a high asperity of a hard surface plows a furrow in a softer opposing surface. In addition to cutting shavings, such plowing usually leaves a ridge on either side of the furrow, and this has to be due to the plastic flow of solid material. The pressures in psi are tremendous; so are the shear gradients, and so are the local temperatures.

Note also that the melting point of a rubbing material does not limit the temperature rise, as is so often stated. If the pressure and the sliding speed are maintained, the molten material will be in severe shear and will be heated further by viscous flow. This is the reason why organic explosives which cannot be ignited by slow sliding can be ignited by fast sliding; fast sliding forces the molten layer into severe shear. It is also the reason why grit increases the friction sensitivity of an explosive: a melting asperity collapses and reduces the pressure somewhat, while a rigid grit particle maintains the local pressure and forces the molten material into severe shear through narrow clearances.

The phenomena of viscous and plastic flow probably account for most of the heat produced in solid and in lubricated sliding. The breaking of asperity adhesions may involve other phenomena such as surface energy effects (see Rabinowicz, chapter 6); but this too may be accountable by the heat of the plastic deformation of the asperity just prior to rupture.

Elastic hysteresis has been mentioned as a possible source of heating as an asperity deforms elastically under load and then recovers its initial shape with release of its stored energy. In most cases, most

of the stored energy probably goes back into the deforming asperity to boost it on its way as it departs, but at least one case has been reported (45) of glass particles becoming incandescent apparently *after* the deforming slider had departed. In viscoelastic materials such as rubber - and perhaps some PBX - there is a *bulk* hysteresis loss which is significant. In fact, it is the major mode of energy loss in a rubber tire on a wet or icy pavement, and it accounts for nearly all of an automobile's traction in such cases (68, 69, 70). As every motorist knows, the effect is very small compared to the normal dry adhesion of a tire to pavement.

It should also be noted that "elastic" is a deceptive word. Few, if any, materials are perfectly elastic. A repeatedly flexed spring will get hot, not from elastically stored energy which is given back to the deforming source, but from hysteresis losses which are really flow losses. So will a rubber tire. Nevertheless, the heating is still real; and hysteresis losses may make their contribution in some cases. Most authorities, though, feel that it is a minor contribution compared to plastic and viscous flow.

There are two other important phenomena associated with sliding and grinding processes: fracture and electrostatic discharges. They are both outside the scope of this study, and they are probably of minor consequence in most frictional initiations; but mention of them needs to be made.

Fox and Soria-Ruiz, of the Cavendish Laboratory, have studied the "apparent temperatures" generated in the leading edge of a crack propagating in an explosive, and have found them to reach values as high as several thousand degrees (81). These are not actual temperatures; they are those temperatures one calculates from the observed rate data using kinetic parameters derived from more ordinary experiments, and they may or may not correspond to thermal temperatures. Nevertheless, they are most provocative; and they suggest that surface energies may play significant roles in brittle explosives.

It has also been reported (118) that the work required to form one square centimeter of new surface on Al_2O_3 is highly dependent upon the method used:

Method	Ergs
Pulling	500
Zero creep	700
Dry crushing	100,000
Crushing under liquid	75,000

Clearly, crushing requires the expenditure of much more work than is recovered in the formation of new surface. The rest must appear as heat. The 25% reduction by wetting is also provocative, and has similar implications.

At this writing, Fox has an active program on the subject, and he has promised a paper specifically directed toward fracture initiation of explosives.. It is recommended that interested investigators await Fox's paper. This study contains no further reference to fracture except a bibliographic listing of publications which were encountered in the field in the course of the literature search.

Electrostatic discharges are frequent concomitants of sliding, and they may be important initiation sources, particularly for primary explosives; but they are not "friction", and they are beyond the scope of this study. Piezoelectricity and the emission of exoelectrons from freshly broken or abraded surfaces are closely related phenomena which may also be important, but they too are beyond the scope of this study. The entire subject of electrical friction phenomena is a large one, and could easily absorb a study larger than this one. The bibliography contains a number of excellent starting places for anyone interested in pursuing it.

4. FRICTION HAZARDS TO EXPLOSIVES

This study has found no magic for reducing friction or friction hazards - except for the ancient magic of lubrication - and the study and control of friction hazards remains very much a Black Art. For the time being at least, the testing and the safe handling of explosives remains highly empirical; and innovations should be made only with the greatest caution.

LABORATORY FRICTION SENSITIVITY TESTERS

There is a bewildering variety of friction sensitivity testers, and the number of variations is approximately equal to the number of active laboratories. The testers are all highly empirical,* and their value is usually limited to a particular application in a particular time and place; they do not yield fundamental data. They are only partially successful even in yielding empirical data, partly because the hazardous stimulus is usually quite difficult to identify and simulate, but mostly because the essential nature of friction is only dimly understood. In these circumstances, it is neither practical nor profitable to review each tester in detail: it seems better to review the principles of operation and critique them. Detailed descriptions of individual testers may be found in the literature through the attached bibliography.

Most friction sensitivity testers are attempts to produce a realistic, usually small-scale, simulation of actual processing operations or accident situations; and they can be grouped into three categories:

- (1) Those which shear a thin layer of explosive between two rigid plates of steel or other material of construction. Some of these are lineal and single-pass, and some are rotary and continuous.
- (2) Those in which a block of explosive is rubbed violently on a hard or abrasive surface.
- (3) Those in which a sample of explosive is subjected to extreme deformation in an impact or extrusion event.

* The word "empirical" is not used in derogation. The writer is an enthusiastic empiricist, on the grounds that empiricism is necessary to keep theoreticians honest. But it is also true that sound theory is necessary to keep empiricists relevant, and this study attempts to emphasize fundamentals.

The Shear tests are the most popular, and they are represented by the (British) Explosives Research and Development Establishment Mallet Friction Test (51), the E.R.D.E. Emery Paper Friction Test for Sensitive Explosives (51), the E.R.D.E. Sliding Block Friction Test (51), the U.S. Bureau of Mines Pendulum Friction Test (51), the USNOTS Pendulum Friction Test (51), the Picatinny Arsenal Pendulum Friction Test (51), the Allegany Ballistics Laboratory Sliding Friction Machine (56, 57, 58), the Esso Friction Screw (66), and others.

All the Shear tests squeeze the sample between two tool faces of steel or other material of construction and subject it to shear by means of a sliding motion of the two tools. They use varying degrees of pressure from weights, springs or hydraulic cylinders; and they use varying sliding speeds. The pinching surfaces can be steel, fiber, aluminum, glass, or any other material the investigator thinks realistic of a potential real event. The surfaces can be smooth or rough, and they can incorporate added grit of varying hardnesses.

Most of the Shear tests are intended to be simulative of process or accident hazards, such as the pinching of a sample between the blade and the wall of a sigma blade mixer, or the pinching of a sample between the threads of a bolt and its bolt-hole. The ABL Sliding Friction Test (56, 57, 58) is probably the best of these, and it has been widely copied in this country.

The common weakness in all the Shear tests is that they have little to do with the friction properties of the explosive itself; the friction is mainly between the two plates, or the mallet and the anvil, with the explosive playing a minor role as a lubricant or as an acceptor of heat generated by the rubbing of the two plates. The explosive is doubtless sheared like a viscous liquid to some extent, but it is never clear to what extent. The tests are simulative of real pinching events, and they do furnish empirical estimates of degree of hazard, which is their intention; but they are not susceptible of detailed analysis, and they cannot give fundamental insights. They combine too many, too complex, phenomena.

One Shear test, the Esso Friction Screw (66), was developed as a purely empirical test to correlate with accident experience in the laboratory handling of NF compounds; but it has promise of yielding fundamental data, given some further development. It subjects the sample to slow shear between two plates under ever-increasing pressure and in the presence of added grit. The main friction is emphatically not that between the two plates; because it makes no difference whether the plates are steel, aluminum or Teflon in most cases, and it makes little difference how rapidly the screw is turned. The overriding independent variable is the hardness (not the melting point) of the added grit.

One can speculate that the grit particles act as the contacting asperities between the two plates, and that the explosive acts as the lubricant or separating film between asperities. Pressures are such as to crush the grit particles, so that the grit hardness (= crush strength) controls the asperity-asperity contact pressure. Sliding speeds are so low as to preclude gross bulk heating, so that the temperatures generated must be simply the Flash Temperatures on the asperity tips. The flash temperatures are probably not calculable from the dry friction models discussed in Section 3, since the contacts are lubricated by the sample; but they may be calculable from models currently being developed at Esso Research and Engineering Company for Boundary Lubrication. This work is incomplete at this writing; but it will be published during 1971 (80), and a preliminary version is given in the Appendix of this study.

Violent rubbing of a block of explosive on a hard external surface does involve the frictional properties of the explosive itself; because the explosive is the softer material, and its shear strength and penetration hardness will be the ones of importance. Such tests are typified by the Pantex Skid Test (51) and the A.W.R.E. Oblique Impact Test (51). The Canadian Friction-Impact Test is also an example.

The Skid Test and the Oblique Impact Test hardly qualify as small-scale laboratory tests, since their sample is on the order of 20 pounds; but they are controllable experiments, and they could yield fundamental data if coupled with mathematical modeling such as is recommended herein. A somewhat different mathematical analysis of the Pantex Skid Test is currently being carried out at Lawrence Radiation Laboratory (62), and it should appear soon.

The Canadian Friction-Impact Test, in which a torpedo slides down an inclined track to strike a 50-mg sample a glancing blow (51), probably uses too small a sample for satisfactory isolation of effects; but 20 pounds is certainly not necessary, and some intermediate size ought to be both optimum and convenient.

Dyer and Taylor have recently reported a new test wherein a 25 mm cube of explosive is pressed against a friction surface which is suddenly jerked away with a sliding motion (61). This is about the right size, although it may be just a bit on the large side for laboratory work. This test ought to be subjected to careful analysis coordinated with a mathematical modeling such as is suggested in Section 5. It has great promise.

Dyer and Taylor also report interesting studies with grit, and their data somewhat parallel those from the Esso Friction Screw. These studies also ought to be extended, in the light of the Esso results and in the light of the principles discussed in this report.

Violent, extreme deformation is employed in the SUSAN Test (51), wherein a one-pound sample of explosive contained in a special projectile is fired against a hard target at controlled velocities. This is, of course, an "impact" test; and LRL, the originator, classifies it as one; but it has been reported that the sample undergoes extreme deformation, expanding to several times its original diameter with a corresponding reduction in thickness before exploding. This sounds very much like plastic or viscous flow with consequent heating, as described in Section 3.

For that matter, any impact test, including the BuMines, the NOL and the Picatinny Arsenal impact tests, look to this writer as if they had a large component of violent deformation via plastic flow. This may be one reason impact tests are so notoriously hard to analyze.

There are several other friction tests currently under development by various groups, but none of them show much promise of breaking new ground. The AEC has one in which an abrasive band pressed against an explosive sample is suddenly pulled away with a sliding motion while the pressure is maintained (119). The "friction" is greatly confounded with gross wear of the explosive, and one does not know whether the friction is between the abrasive and the explosive or between the explosive and other explosive loaded into the abrasive band.

There are also several rotary friction machines in various stages of development. There was one at Thiokol a number of years ago, McDonnell Douglas Corporation built one a couple of years ago (59), E.R.D.E. announced one in February 1970 (60), and one is under development at Picatinny Arsenal (120).

These machines in general shear the sample between rapidly rotating plates for various periods of time. The shear is something like that in a journal bearing, and the heat generation may be subject to analysis in a similar manner. The treatment is discussed briefly in Section 3.

Some suggested new approaches

The planning of the development of improved friction sensitivity testers requires the identification of the factors which are really controlling in frictional initiation of explosives, and that may have to await the outcome of the theoretical studies recommended in Section 5. For planning purposes here, let us make several alternate assumptions and see where they lead us.

Assumption 1: The important friction characteristics are those of the solid explosive surface itself. This assumption is plausible because of the high coefficients of friction and the low thermal conductivities of most explosives compared with those of most metallic materials of construction. If this be the case, then testers typified by the ABL Sliding Friction Machine are on the wrong track; and testers such as the Dyer and Taylor machine would be better. The assumption requires that container-on-container friction be eliminated and that sliding be confined to explosive-on-explosive or explosive-on-container.

If the assumption is verified, then further development of the Dyer-Taylor machine is indicated. It needs to use a smaller sample for laboratory safety and convenience, and it certainly could since most of the present sample is far removed from the surface. It also needs to have the capability of higher sliding speeds and higher pressures up to the strength limit of the explosive block. A slightly modified apparatus could also measure the coefficient of friction of the explosive surface, and that should be done by adding a strain gauge to the slider.

Assumption 2: The important friction characteristics are those of the container surfaces, not the explosive itself. This assumption is also plausible because of the generally low strength of explosive solids. They abrade and melt under friction, and the temperature rise is strictly limited. If this be the case, then the ABL machine is on the right track and the Dyer-Taylor machine is wrong. Moreover, the hot-spots must be generated on the asperities of the test tool faces; and the important characteristic of the explosive is simply its thermal sensitivity, which can be evaluated more directly in other ways (for example, the modified Picatinny Arsenal Autoignition Test developed by Coburn and Brown (67)).

If this assumption is verified, then construction of an ABL machine is recommended, with provision to interchange tool faces of any given material of construction. The thickness and disposition of the explosive sample layer probably needs to be optimized too.

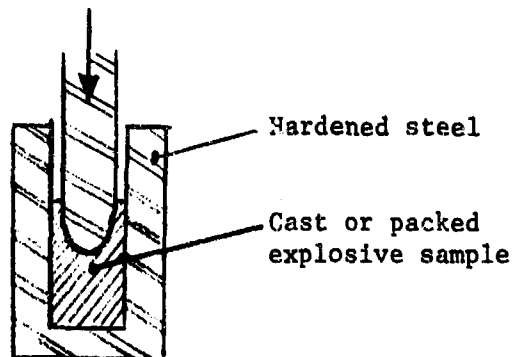
The Esso Friction Screw provides an alternate, or perhaps a complementary, approach to this assumption; and it is a lot cheaper than the ABL machine. It is likely that the Esso Friction Screw produces its hot-spots by grit-on-grit friction, with the explosive acting as a heat acceptor; and the thickness of the explosive film is controlled by its film strength and viscosity. The grit could be metallic particles, and the problem of surface finish and flatness is obviated.

Still another alternate under this assumption is to measure the friction characteristics of the container materials without any explosive present and measure the thermal sensitivity of the explosive separately. This requires the success of the Section 5 theoretical studies, and it is probably not empirical enough to inspire confidence in safety decisions.

Assumption 3: The important factor is not sliding friction at all, but rather heating from viscous or plastic flow of the explosive. If this be the case, then none of the existing friction testers can be very good; because they all involve a great deal of sliding friction, and the flow of explosive is only what results incidentally.

A machine designed to test this factor should provide a fixed clearance large enough to preclude container-container contact, and should provide a controlled pressure to cause the flow. One approach would be to squirt the explosive out through a jet like a hypodermic syringe, with the test flow occurring in the needle. This would be easy to analyze by the calculations discussed in Section 3, but it would be difficult to construct mechanically. There would be sliding friction between the plunger and the barrel, and quite a bit of plasticity would be required of the explosive.

A better approach would be to force the explosive up through an annular orifice as a plunger drives down into a closed cup:



The plunger needs to have a short stroke to avoid collision with the bottom of the cup, and it needs to move with a controllable high speed.

It also needs very rugged guides in order to maintain close clearance without danger of accidental contact with the cup wall.

Such a test is obviously workable with liquid or soft explosives; it is not so obvious how well it would work with granular or brittle explosives. It might be that their strengths will be small compared to the loads imposed by the test fixture, so that they too will flow. There might also be a large amount of particle-particle surface friction, but the assumption here is that that is not important anyway.

Another variation of this concept would be to crush a pellet of explosive so as to force it to *flow* out into a thin disk. This might be done in a hydraulic or pneumatic press with a short, powerful stroke, or the pellet might be crushed under the rim of a wheel. It might also be done in an impact tester; in fact, an impact tester may actually *be* nothing more than a friction tester after all. The writer has yet to see a satisfying analysis of its action on solid samples in terms of compression or shock waves.

Crushing has certain attractions from an empirical point of view because it is a realistic process and because it automatically adjusts itself to widely different physical properties of the explosive. A liquid or soft sample will flow, with heating due to viscous shear; a brittle sample will crush, with whatever effects the formation of new surface entails; and a rubbery sample will deform and recover, with attendant heating due to hysteresis losses. The same considerations make it less attractive for the gathering of fundamental data.

HAZARD REDUCTION TECHNIQUES

There is no magic to eliminate friction or its effects. Friction is basic to the very nature of matter, and about the best we can do is to moderate its effects by suitable mechanical design and operating limitations.

Lubrication is nearly magic, though. It provides a low shear strength interface and thereby drastically reduces the coefficient of friction, and it also provides a heat sink to cool the hot-spots which do form. The best lubricant is one with a high film strength so that it will separate the solid surfaces and *keep* them separated, but the materials which are best for this (fatty or petroleum oils) are difficult to get rid of when their function is finished; so a better choice for explosive processing is water or a volatile hydrocarbon or halocarbon, or a lower alcohol. A still better choice, when it can be done, is to use a liquid which can remain in the finished composition, such as the plasticizer in a composite explosive.

There is nothing new about lubrication, of course. It has always been the practice to handle primary explosives only when they are wet with water or alcohol, even though it has been demonstrated that wetting does not reduce their sensitivity to impact or *severe* friction (55). It does reduce their sensitivity to *gentle* friction, which is what one has in normal handling.

Limitation of rubbing pressures and velocities is also obvious and has always been practiced. Clearances between mixer blades and walls should be as wide and blade speeds should be as slow as is consistent with adequate mixing. Extruder plungers and screws should move slowly. On the other hand, bearings and compression rams should fit as closely as possible in order to keep explosive materials from entering the clearance space.

Grit should be carefully excluded, because it can introduce severe friction where there would be none in its absence. It may even be desirable to substitute softer materials for ingredients of the explosive itself. For example, powdered aluminum is a safer choice than powdered boron for high-energy rocket propellants because of the hardness of the boron (67). Similarly, the use of aluminum hydride gives very friction sensitive materials because of the hardness of the aluminum hydride (121).

Low-friction tool and container surfaces are desirable on principle because of the danger of generating hot spots by their rubbing on one another. Brass-on-brass is better than steel-on-steel because the lower coefficient of friction and the higher heat conductivity both act to reduce the flash temperatures attainable. It is even better to make one surface Nylon. But not Bakelite - Bakelite's very low heat conductivity leads to very high flash temperatures. Surface finishes should preferably be around 20 to 50 microinches, because both smoother and rougher surfaces give higher friction coefficients.

It is also good to make the two contacting surfaces of dissimilar materials which have little or no mutual solubility. Steel-on-steel can seize if the parts rub hard enough to cause asperity-asperity welding, but lead-on-steel cannot because lead is insoluble in iron. Nylon and steel are similarly insoluble and cannot seize. Most plastics, however, are poor choices against another plastic surface, because there is often mutual solubility with high coefficients of friction.

Dissimilar materials are good from another point of view as well. They give an opportunity to use one material with a favorable surface energy and/or yield strength and another with a favorable surface finish and/or heat conductivity, and have the best of both worlds.

Actually, it should not be surprising that this study has not produced startling new insights. After all, intelligent people have been facing these problems for a very long time; and they have come empirically to most of the right answers. It would be surprising if this study had found them wrong.

What this study can do is to illuminate the reasons for the empirical rules of thumb and to guide the choice of new materials such as plastics when plants are modernized and the old rules of thumb do not cover the situation. Plant designers should get up to date on the science of friction by studying the authorities in the field, and Rabinowicz (1) is an excellent place to start. It would also be well to retain expert consultants to review the friction aspects of the design of new facilities, and Rabinowicz himself would be a good choice.

INTENTIONALLY

BLANK

5. SUGGESTED FRICTION RESEARCH TOPICS

This review has turned up a number of places where the science of friction and friction sensitivity is not yet adequate but where there are clear opportunities for advancement and where the logical next steps are clear. This section outlines some of the more attractive and better defined ones.

A MATHEMATICAL MODEL OF FRICTION IGNITION

The foregoing discussion has mostly been rather qualitative, partly because a quantitative analysis of the various processes was beyond the objectives of this study and partly because the kind of quantitative analysis which is really needed has not yet been made. Nevertheless, a quantitative study is needed if the findings are to be of maximum use. It is necessary to determine just how large the various frictional effects discussed really are in situations involving explosives and to compare their magnitude with those of empirically observed explosion hazards.

A quantitative theoretical program is recommended to integrate the approaches sketched out in Section 3 into a complete, quantitative model of the formation of initiating hot-spots. Mathematical expressions are available for the amount of heat generated in sliding, for the number, size and spatial and size distribution of asperity junctions, for the temperature profiles in and between the junctions and their variation with time, for the flow of heat through the junctions and into the bulk of the explosive blocks, and for the thermal evolution of the hot-spots in the explosive. This is essentially a job for a mathematician, or a very mathematically inclined Materials Scientist. It might be an excellent project for a selected Materials Scientist on a post-doctoral year.

Most of the mathematical models required have been introduced in Section 3, including the Zinn and Mader models (48, 49) of the growth of hot-spots in an explosive. The only additional model needed is one for the critical conditions for a hot-spot to lead to explosion, and this is furnished by the work of Boddington (50). He has calculated the critical sizes and temperatures for runaway in a number of common explosives by procedures more rigorous than those of Zinn and Mader, and they are summarized in the following figure:

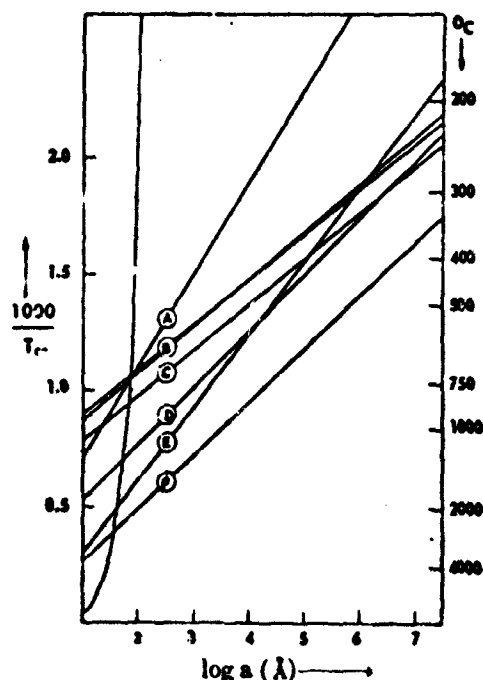


FIG. 3. Critical temperature as a function of hot-spot size for some common explosives. Straight lines are for $k = 0$ and should be displaced to the right by the amounts 0.301, 0.477 for $k = 1, 2$ respectively. A: AgNO_3 ; B: HMX, PETN (greatest slope); C: RDX; D: tetryl; E: ethylenedinitramine; F: ammonium nitrate. The steep curve represents decay of a thermal spike caused by a fusion fragment (corrected to k equals 1).

Successful execution of the program envisioned should enable the quantitative prediction of the probability of explosive initiation by any given frictional process without recourse to empirical testing, knowing only the fundamental material properties of the materials involved and the speeds, pressures, etc., of the mechanical events. Comparison with empirical reality will reveal whether the chosen frictional processes are indeed the critical ones, as is discussed in the following paragraphs.

EXPERIMENTAL TEST OF THE MODEL AND APPLICATION TO HAZARD CONTROL

The validity of the model developed in the first suggested project will depend completely upon the relative importance of the processes chosen for incorporation, and this furnishes a way to determine which process or processes actually are dominant in any given hazard situation.

For example, if a model assuming the generation of heat by explosive-explosive friction is found not to correspond to reality; it would imply that that assumption is not valid and suggest the substitution of a different assumption such as the generation of heat by metal-metal friction or by viscous shear. The model which best describes empirical reality is by definition the one which incorporates the frictional processes which really are controlling.

Once the critical processes are identified, the lessons for in-plant hazard reduction will be obvious. For example, if the study were to show that metal-metal friction was not important and that only explosive-explosive friction would lead to trouble, we could quit worrying about materials of construction and concentrate on preventing the sliding of one block of explosive on another. Similarly, if viscous shear turned out not to be important, we could quit worrying about maintaining wide clearances and concentrate on preventing actual metal-to-metal contact. Nature being what she is, conclusions will probably never be that clear-cut; but there should still be lessons for hazard control.

Modeling will also reveal whether still other phenomena such as fracture or frictional electrification need to be studied. If the models account adequately for the empirical observations, "other effects" can pretty well be forgotten; however, if they do not, it will be a clear indication that the "other effects" need to be explored in depth.

DEVELOPMENT OF IMPROVED FRICTION SENSITIVITY TESTERS

As discussed in Section 4, there is at present a wide variety of empirical friction sensitivity testers, none of which is really very much good. The modelling studies proposed above will help to weed out some of them by revealing which ones' principles of operation are valid and which are not. They will also help to guide the development of new and better ones. This subject has already been discussed in Section 4, and it will only be recapped here.

It is suggested that three, perhaps four, different types of testers be studied, embodying different basic assumptions as to the critical friction process or processes. These would be (1) A Dyer-Taylor type machine in which an explosive block is rubbed on a hard surface at controlled pressures and speeds, (2) an ABL machine in which the explosive is a thin film between two hard rubbing surfaces, (3) the Esso Friction Screw in which the explosive is a thin film between grit particles rubbing without bulk heating, and (4) an extrusion-type machine in which viscous and/or plastic flow can be studied, or alternatively a crushing machine to study the same processes.

This study is complementary to the modelling study in that each machine emphasizes some basic friction process and some one model ought to be appropriate to each; so the experimental and the theoretical programs serve as tests of each other.

Again, nature being what she is, it is unlikely that results will be clear-cut enough to discard any one approach completely; and it may be that all the testers should be retained and used where appropriate. It may be best to match the tester to the particular hazard problem, with the guidance of the theoretical models.

FRACTURE AND ELECTROSTATICS

This report is believed to be fairly complete* inasregards friction itself, but there are other phenomena associated with sliding and grinding, and they are not covered herein. Among these phenomena are crushing and fracture, and frictional electrification. They may or not be important effects, and the modelling studies above are designed partly to determine whether such additional processes need to be invoked to explain frictional initiation of explosives. If they are needed, then programs are needed to investigate them in depth; and each program will be at least as large as this one.

Fracture and electrostatics are beyond the scope of this study, and no attempt was made to cover the literature on them. Nevertheless, articles on them were inevitably encountered; and the ones which were encountered are included in the bibliography to serve as a starting point for any future detailed survey.

* Not exhaustive. It was necessary to restrict the scope of this study in order to preserve useful depth; but it is believed that no major insights into friction have been missed. If any have been missed, it is hoped that reviewers will bring them to attention.

SUMMARY OUTLINE OF SUGGESTED RESEARCH

A MATHEMATICAL MODEL OF FRICTION INITIATION

- The amount of heat available from sliding
- The statistics of junction number and size
- The statistics of junction temperature
- Critical hot-spot size and temperature

EXPERIMENTAL TEST OF THE MODEL AND APPLICATION TO HAZARD CONTROL

- Calculation of frictional conditions to cause ignition
- Comparison with empirical tests
- Conclusions as to whether the model adequately predicts events or whether additional phenomena need to be taken into account.
- Conclusions as to permissible process conditions

DEVELOPMENT OF IMPROVED FRICTION SENSITIVITY TESTERS

- Construction of devices embodying different basic processes

- Dyer-Taylor type machine
- ABL type machine
- Esso Friction Screw
- Extrusion or crushing type machine

- Cross-checking with the predictions of the models and comparison with known handling hazards

- Matching of the tester to the problem

POSSIBLE NEW PROJECTS

- Fracture and surface energy
- Electrostatics

INTENTIONALLY

BLANK

6. BIBLIOGRAPHY

GENERAL

1. E. Rabinowicz, Book: *Friction and Wear of Materials*, John Wiley and Sons, NY 1966.
2. F. P. Bowden & D. Tabor, Book: *The Friction and Lubrication of Solids*, Clarendon Press, Oxford 1964.
3. F.P. Bowden & D. Tabor, Book: *Friction and Lubrication*, John Wiley and Sons, NY 1956.
4. P. M. Ku, editor, Book: *Interdisciplinary Approach to Friction and Wear*, NASA SP-181, U.S. Government Printing Office 1968.
5. P. A. Thiessen, K. Meyer and G. Heinicke, Book: *Grundlagen der Tribochemie*, Akademie-Verlag, Berlin 1967.
6. M. J. Furey, *Friction, Wear and Lubrication*. Industrial and Engineering Chemistry, Vol. 61, No. 3, 12-29 (1969).

ASPERITIES AND SOLID-SOLID CONTACT

7. J. A. Greenwood and J. B. P. Williamson: *The Contact of Nominally Flat Surfaces*. Proc. 2nd Int. Conf. on Electric Contacts (Graz, Austria), 1964.
8. J. A. Greenwood and J. B. P. Williamson: *Contact of Nominally Flat Surfaces*. Proc. Royal Soc. (London) Vol. 295A, 1966, pp 300-319.
9. J. A. Greenwood: *The Area of Contact Between Rough Surfaces and Flats*. J. Lubn. Techn., ASME, Vol. 89F, pp 81-91.
10. M. H. Jones, R. I. L. Howells and S. D. Probert: *Solids in Static Contact*. Wear, Vol. 12 (1968) pp 225-240.
11. F. F. Ling: *On Asperity Distributions of Metallic Surfaces*. Jour. Appl. Phys., Vol. 29, 1958, pp 1168-1174.
12. F. F. Ling: *Mechanics of Sliding Surfaces*. Metals Engineering Quarterly, Vol. 7, pp 1-3 (1967).
13. F. F. Ling: *The Deformational and Geometrical Aspect of Surfaces in Sliding Contact*. Fundamental Phenomena in the Materials Sciences, Vol. 2, 1966, Plenum Press, pp 57-71.

14. A. J. W. Moore: *Deformation of Metals in Static and Sliding Contact*. Proc. Royal Soc. (London), Vol. 195A, 1948, pp 231-243.
15. A. P. Green: *The Plastic Yielding of Metal Junctions due to Combined Shear and Pressure*. J. of the Mechanics and Physics of Solids, 1954. Vol. 2, pp 197-211.
16. T. Hisakado: *On the Mechanism of Contact Between Solid Surfaces (1st Report, The Initial Separation and the Distributions of Slopes of Facets on Surface and on Profile Curve)*. Bulletin of JSME, Vol. 12, No. 54, 1969, pp 1519-1527.
17. T. Tsukizoe and T. Hisakado: *On the Mechanism of Contact Between Metal Surfaces: Part 2 - The Real Area and the Number of Contact Points*. J. of Lubn. Techn., January 1968, pp 81-88.
18. T. Hisakado: *On the Mechanism of Contact Between Solid Surfaces (3rd Report, The Number and the Distribution of Radii of Contact Points)*. Bulletin of JSME, Vol. 12, No. 54, 1969, pp 1537-1515.
19. T. Tsukizoe and T. Hisakado: *The Influence of Surface Roughness on the Mechanism of Friction*. J. of Lubn. Techn., April 1970, pp 264-273.
20. D. J. Whitehouse and J. F. Archard: *The Properties of Random Surfaces in Contact*. ASME - Surface Mechanics, Winter Annual Meeting, Los Angeles, Calif., 16-21 Nov 1969, pp 36-57.
21. E. Rabinowicz, et.al.: *The Statistical Nature of Friction*. Trans. Am. Soc. Mech. Eng., 77 981-984 (1955).
22. E. Rabinowicz: *Autocorrelation Analysis of the Sliding Process*. J. Appl. Physics, Vol. 27, No. 2, Feb., 1956. pp 131-135.
23. E. Rabinowicz: *Investigation of Size Effects in Sliding by Means of Statistical Techniques*. Proc. Conf. Lubn. & Wear, IME. London, 1957. pp 276-280.
24. E. Bickel: *Some Fundamental Problems in the Measurement of Surface Roughness*. ASME - Proc. Int. Production Engineering Research Conf. 1963. pp 667-674.
25. I. M. Pesante: *Determination of Surface Roughness Typology by Means of Amplitude-Density Curves*. CIRP Annalen, Vol. 12, 1964, pp 61-68.
26. F. P. Bowden: *Adhesion and Friction*. Endeavour 16 5-18 (1957).

27. F. F. Ling: *On Some Implications of a Bifurcation Phenomenon of Friction*. *Wear*, 5 158-160 (1962).
28. D. Tabor and R. H. S. Winterton: *Surface Forces: Direct Measurement of Normal and Retarded van der Waals Forces*. *Nature*, Vol. 219, Sept 14, 1968, pp 1120-1124.
29. P. E. Fowles: *A Thermal Elastohydrodynamic Theory for Individual Asperity-Asperity Collisions*. Paper No. 70-Lub-25 presented at the 12-15 Oct 1970 ASME-ASLE Lubrication Conference in Cincinnati, Ohio. To be published.
30. Y. P. Chiu: *On the Contact Problem of Cylinders Containing a Shallow Longitudinal Surface Depression*. Paper No. 69-WA/APM-23 presented at the 16-20 Nov 1969 Winter Annual Meeting of the American Society of Mechanical Engineers in Los Angeles, Calif. To be published.

HEAT GENERATION AND TEMPERATURE STATISTICS

31. H. Blok: *Theoretical Study of Temperature Rise at Surfaces of Actual Contact under Oiliness Lubricating Conditions*. *Proc. Gen. Disc. Lubrication and Lubricants, IME*. 1937. pp 222-235.
32. J. F. Archard: *The Temperature of Rubbing Surfaces*. *Wear* 2, pp 438-455. (1958/59).
33. F. P. Bowden and P. H. Thomas: *The Surface Temperature of Sliding Solids*. *Proc. Royal Soc. London*. A223 (1954) pp 29-40.
34. F. F. Ling and S. L. Pu: *Probable Interface Temperatures of Solids in Sliding Contact*. Air Force Material Laboratory Report RTD-TDR-63-4184, February 1964. AD-433,587. Unclassified.
35. F. F. Ling and S. L. Pu: *Probable Interface Temperatures of Solids in Sliding Contact*. *Wear* 7 (1964) pp 23-34.
36. F. F. Ling: *On Thermal and Mechanical Effects at Sliding Interfaces*. Air Force Materials Laboratory Report AFML-TR-69-91, April 1969. AD-693,207. Unclassified.
37. F. F. Ling and T. E. Sinkins: *Measurement of Pointwise Junction Condition of Temperature at the Interface of Two Bodies in Sliding Contact*. *Trans. Am. Soc. Mech. Engrs.* 85 481-485 (1963).
38. F. F. Ling and E. Saibel: *Thermal Aspects of Galling of Dry Metallic Surfaces in Sliding Contact*. *Wear* 1 80-89 (1957/58).

39. M. J. Furey: *Surface Temperatures in Sliding Contact*. ASLE Transactions 7 133-146 (1964).
40. J. C. Jaeger: *Moving Sources of Heat and the Temperature at Sliding Contacts*. Proc. Roy. Soc. (N.S.W.), Vol. 76, Pt. 3, pp 203-224. 1942.
41. H. A. Francis: *Interfacial Temperature Distribution within a Sliding Hertzian Contact*. Paper 70-AM IC-1, presented at the 25th ASLE Annual Meeting in Chicago, 4-8 May 1970. To be published. Preprint in the Appendix of This Report.
42. S. W. E. Earles and D. G. Powell: *Surface Temperature and its Relation to Periodic Changes in Sliding Conditions between Unlubricated Steel Surfaces*. ASLE Transactions 11 109-120 (1968).
43. D. A. Barlow: *A Thermal Size Effect in Friction Tests*. Wear 11 No. 3, 229-232 (1968).
44. F. F. Ling and J. S. Rice: *Surface Temperature with Temperature-Dependent Thermal Properties*. ASLE Transactions 9 195-201 (1966).
45. R. J. Heighway and D. S. Taylor: *Transient Temperature Rises During the Rubbing of Metals on Glass*. Wear 9 310-319 (1966).
46. J. E. Gerrard, F. E. Steidler and J. K. Appeldoorn: *Viscous Heating in Capillaries - The Adiabatic Case*. I&EC Fundamentals Vol. 4 pp 332-339 (1965).
47. J. E. Gerrard, F. E. Steidler and J. K. Appeldoorn: *Viscous Heating in Capillaries - The Isothermal-Wall Case*. I&EC Fundamentals Vol. 5 pp 260-263 (1966).

STUDIES ON EXPLOSIVES

48. J. Zinn: *Initiation of Explosions by Hot Spots*. J. Chem. Phys. 36 1949 (1962).
49. J. Zinn and C. L. Mader: *Thermal Initiation of Explosives*. J. Applied Physics, Vol. 31, No. 2, pp 323-328 (1960).
50. T. Boddington: *The Growth and Decay of Hot Spots and the Relation Between Structure and Stability*. 9th Int. Combustion Symposium (1963) pp 287-293.

51. G. R. Walker, Editor: *Manual of Sensitiveness Tests*. TTCP Panel O-2 (Explosives) Working Group on Sensitivity. Published by the Canadian Armament Research and Development Establishment, February 1966.
52. Universal Match Corporation: *Development of Method for Measurement of Sensitivity of Explosives to Friction*. Contract DA-23-072-ORD-1397; 20 Feb 1961. AD-258,012. Unclassified.
53. K. G. Hoge: *Friction and Wear of Explosive Materials*. UCRL-50134, 1 Sept 1966, available from CFSTI.
54. K. G. Hoge: *Friction and Viscoelastic Properties of Highly Filled Polymers: Plastic-Bonded Explosives*. UCRL Preprint 70588. 27 July 1967.
55. J. A. Brown, et.al.: *Sensitivity and Rheology Studies on Lead Azide - RDX - Silica Mixtures*. Contract DAAA21-67-C-1108, January 1969.
56. R. H. Richardson: *Hazards Evaluation of the Cast Double-Base Manufacturing Process*. Allegany Ballistics Laboratory Report ABL/X-47, December 1960. Presented at the 16th JANAF Solid Propellant Group Meeting held in Dallas, Texas, June 14-16, 1960.
57. R. H. Richardson: *Friction Sensitivity*. Allegany Ballistics Laboratory Research Progress Report 7-2-15, 29 Aug 1960.
58. R. H. Richardson: *Friction Sensitivity*. Allegany Ballistics Laboratory Research Progress Report 7-2-15, 21 Sept 1960.
59. W. D. English, et.al.: *Material-Propellant Reaction Initiation by Rotational Friction*. Paper presented to the 23rd Meeting of the ICRPG Test Methods Working Group at Monterey, California, 28-29 March 1968.
60. J. G. Rankine and H. C. Turner: *A Design for a Rotary Machine to Assess the Friction Sensitiveness of Explosives and Propellants*. Technical Note No. 16, February 1970. Available from Mintech Reports Centre, Station Square House, St. Mary Cray, Orpington, Kent.
61. A. S. Dyer and J. W. Taylor: *Initiation of Detonation by Friction on a High Explosive Charge*. ONR Report DR-163, presented to 5th Symposium on Detonation, 18-21 Aug 1970.
62. L. Green: *(Analysis of Panter Skid Test)*. Private communication. Work to be published.

63. F. P. Bowden and K. Singh: *Size Effects in the Initiation and Growth of Explosion*. *Nature*, Vol. 172 (29 Aug 1953) pp 378-380.
64. F. P. Bowden and O. A. Gurton: *Initiation of Explosions by Grit Particles*. *Nature*, Vol. 162 (23 Oct 1948) pp 654-655.
65. J. Eadie: *A Possible Relationship Between the Shock Sensitivity and Crystal Frangibility of High Explosives*. Australian Defence Standards Laboratories Report 337, April 1969. AD-855,624. Unclassified.
66. J. A. Brown, et.al.: *Annual Report, Contract AF04(611)-9969*. Air Force Rocket Propulsion Laboratory Report TR-65-156, 1965, AD-366,083. Confidential report.
67. J. A. Brown, et.al.: *Final Report, Contract AF04(611)-9969*. Air Force Rocket Propulsion Laboratory Report TR-66-329, 1966. AD-379,575. Confidential report.

RUBBER AND POLYMERIC SOLIDS

68. E. M. Bevilacqua and E. P. Percarpio: *Friction of Rubber on Wet Surfaces*. *Science*, Vol. 160, No. 3831, pp-959-964. (1968).
69. H. W. Kummer: *Unified Theory of Rubber and Tire Friction*. Pennsylvania State University Engineering Research Bulletin B-94. July 1966. Available from CFSTI, PB-184,487.
70. A. Schallamach: *The Load Dependence of Rubber Friction*. *Proc. Royal Society*, Vol. 65, Pt. 9, No. 393B, pp 657-661, (1952).
71. K. V. Shooter and D. Tabor: *The Frictional Properties of Plastics*. *Proc. Royal Society*. Vol. 65, Pt. 9, No. 393B, pp 661-671. (1952).
72. K. C. Ludema and D. Tabor: *The Friction and Visco-elastic Properties of Polymeric Solids*. *Wear*, 9 pp 329-348 (1966).
73. D. G. Flom: *Rolling Friction of Polymeric Materials*. I. *Elastomers*. *J. Appl. Phys.* Vol. 31, No. 2, pp 306-314 (1960).
74. J. Beshara: *An Introductory Survey of Internal Friction as a Source of Energy Loss in Solids*. (Canadian) Defence Research Telecommunications Establishment Report No. 1181, April 1967. AD-813,578. Unclassified.
75. H. Domandl: *A Comparison of the Operation and Friction Characteristics of Airplane and Dragster Tires*. Boeing Company Technical Note D6-58384-4TN (1969). AD-688,669. Unclassified.

LUBRICATION

76. D. Godfrey: *Lubrication*. ASTM Symposium on Properties of Surfaces, Los Angeles, 4 Oct 62. ASTM Special Technical Publication No. 130, ASTM.
77. W. H. Roberts: *Lubrication Without Oils*. Paper No. 6 presented 30 Sept - 1 Oct 1969 at National Center of Tribology symposium UKAEA, Risley, Warrington, Lancs, England.
78. P. M. Ku, editor: *Interdisciplinary Approach to the Lubrication of Concentrated Contacts*. Proceedings Preprint of NASA Symposium held 15-17 July 1969 at Rensselaer Polytechnic Institute.
79. F. F. Ling, et.al.: *BOUNDARY LUBRICATION, An Appraisal of World Literature*. American Society of Mechanical Engineers, NY 1969. 11 synoptic reviews and 2711 abstracts.
80. A. Beerbower: *Army Research Office Scientific and Technical Applications Forecast on [the prospects for extraordinary improvements in boundary lubrication]*. Contract DAHCl9-69-C-0033 in progress. Final Report available some time in 1971.

CRUSHING AND FRACTURE

81. P. G. Fox and J. Soria-Ruiz: *Fracture-induced Thermal Decomposition in Brittle Crystalline Solids*. Proc. Roy. Soc. London, A317, 79-90, (1970).
82. D. C. Drucker and J. J. Gilman, editors: *Fracture of Solids. (the Proceedings of an international conference at Maple Valley Washington, 21-24 Aug 1962. 28 papers, on the subjects of: Continuum Mechanics, Microstructural Phenomena, Atomistic Mechanisms and Environmental Effects.)* Interscience Publishers NY, 1963.
83. O. Imanaka: *Surface Energy and Fracture of Materials*. Kinzoku Hyomen Gijutsu, 19 No. 10, pp 424-429 (1968).
84. E. N. Pugh: *The Brittle Fracture of Non-Metals*. Final Report Contract DA-31-124-ARO-D-388, 1966. AD-802,241. Unclassified.
85. F. Wittmann: *On the Influence of the Surface Energy on the Strength of a Porous Solid*. (in German). Z. Angew. Phys. 25 pp 160-163 (1968).
86. A. K. Schellinger: *Solid Surface Energy and Calorimetric Determinations of Surface-Energy Relationships for Some Common Minerals*. Mining Engineering 4 No. 4, 369-374 (1952).

87. J. C. Dutertre, et.al.: *Shear Phenomena in Natural Granular Materials*. Contract AF 19(628)-5805, 1966. AD-646,865. Unclassified.
88. M. K. Kassir, et.al.: *Griffith's Theory of Brittle Fracture in Three Dimensions*. Contract Nonr-610(06), 1967. AD-659,306. Unclassified.
89. Y. P. Gupta and A. T. Santhanam: *On Cleavage Surface Energy of Calcite Crystals*. Acta Metallurgica Vol. 17, April 1969. pp 419-424.
90. S. M. Wiederhorn, et.al.: *Critical Analysis of the Theory of the Double Cantilever Method of Measuring Fracture-Surface Energies*. J. Appl. Phys. Vol 39, No. 3, 1968. pp 1569-1572.
91. R. L. Barnett, et.al.: *Fracture of Brittle Materials under Transient Mechanical and Thermal Loading*. Air Force Flight Dynamics Laboratory report AFFDL-TR-66-220, 1967. AD-649,978. Unclassified.
92. G. W. Patterson and T. O. Mulhearn: *The Fracture of Idealized Abrasive Particles*. Wear, 13 (1968) pp 175-182.
93. J. Nakayama: *Direct Measurement of Fracture Energies of Brittle Heterogeneous Materials*. J. Am. Ceram. Soc. 48 pp 583-587 (1965).
94. S. M. Wiederhorn: *Fracture Surface Energy of Glass*. J. Am. Ceram. Soc. 52 pp 99-105 (1969).
95. V. Weiss, et.al.: *A Study of the Effect of Superimposed Stress Concentrations and Fracture of Inhomogeneous Brittle Solids*. Air Force Materials Laboratory report AFML-TR-66-235, 1967. AD-813,728. Unclassified.
96. R. W. Davidge and G. Tappin: *The Effective Surface Energy of Brittle Materials*. J. Materials Sciences 3 (1968) pp 165-177.
97. J. J. Gilman: *Direct Measurements of the Surface Energies of Crystals*. J. Appl. Phys. 31, No. 12, pp 2208-2218 (1960).
98. D. Tabor: *Mohs's Hardness Scale - A Physical Interpretation*. Proc. Phys. Soc. LXVII, 3-B, pp 249-257, (1954).

ELECTRIFICATION

99. W. R. Harper: Book: *Contact and Frictional Electrification*. Oxford University Press, NY, 1967.
100. J. N. Maycock and D. E. Grabenstein: *Piezoelectricity in Secondary Explosives*. Science 152 pp 508-509 (1966).

ABRASION

101. J. Kramer: *A Wave Radiation Originating in the Transformation of Amorphous Metal Modifications*. Naturwissenschaften v.27, 1089 (1939).
102. J. Kramer: *Point Counter and Counter Tube in Metallographic Investigations of Surfaces*. Z. Physik v.125 739-756 (1949).
103. J. Kramer: *Studies with the Geiger Point Counter on Worked Non-Metals*. Z. Physik V.128, 538-545 (1950).
104. J. Kramer: *Investigations with the Geiger Point Counter on Irradiated Crystals*. Z. Physik, v.129, pp 34-44 (1951).
105. J. Kramer: *Surface Examination of Metals and Non-Metals with X-ray Photoelectrons*. Z. Physik, v.133, pp 629-646 (1952).
106. G. L. Kennan: *Substances which Affect Photographic Plates in the Dark*. Chem. Reviews, v.3, pp 95-111 (1926-27).
107. M. C. Shaw: *Mechanical Activation - A Newly Developed Chemical Process*. J. Appl. Mech. v.15, pp 37-44 (1948).
108. L. Grunberg and K. H. R. Wright: *Crystal Defects in Freshly Worked Surfaces*. Nature, V.174, pp 656-657 (1954).
109. L. Grunberg and K. H. R. Wright: *A Study of the Structure of Abraded Metal Surfaces*. Proc. Roy. Soc., v.A232, pp 403-423 (1955).
110. E. Ferroni: *A Chemical Test to Reveal the Kramer Effect*. Research, v.8, pp S49-S50 (1955).

OTHER

111. D. Tabor and J. C. F. Walker: *Creep and Friction of Ice*. Nature. v.228, pp 137-139 (1970).
112. D. Atack and D. Tabor: *The Friction of Wood*. Proc. Royal Soc. London. v.A246, pp 539-555 (1958).

113. L. Da Vinci: In Il Codice Atlantico, Academia dei Lincei, Milano, 1960.
114. G. Amontons: Histoire de l'Academie Royale des Sciences, Anne MDCXCIX, Amsterdam, 1734. pp 259-282.
115. C. A. Coulomb: Memoires de l'Academie des Sciences, p 161.
116. L. Euler: Historie de l'Academie Royale a Berlin, iv (1784), 313.
117. H. Hertz: Z. Reine u. Angew. Math., 92, 156 (1881).
118. A. Beerbower: Private communication.
119. L. Green: Private communication.
120. J. Hershkowitz: Private communication.
121. Private communications. Sensitivity data from Lockheed personnel; hardness data from Thiokol personnel.

Interfacial Temperature Distribution Within a Sliding Hertzian Contact

-55-

Preprint 70 AM 1C-1

H. A. FRANCIS

Dept. of Chemical Engineering & Chemical Technology
Imperial College, London, S. W. 7

An analytic expression for the steady-state interfacial temperature field in a sliding circular Hertzian contact is derived, taking into account the ellipsoidal distribution of the frictional power and the difference between the bulk temperatures of the two bodies, for the case where one surface is stationary and the other rapidly moving with respect to the contact. Other cases may be treated in a similar manner. It is shown that the temperature at any point on the interface can be approximated, to an accuracy improving with velocity, by half the harmonic mean of the two surface temperatures attained at that point if each body were to receive all the frictional power. The resulting maximum flash temperature is 33-38% higher than that given by Blok's widely used formula.

INTRODUCTION

To characterize completely the interface between two sliding bodies, one must be able to determine the temperature distribution over the area of contact due to frictional heating or, lacking this, the maximum and/or mean temperatures. Measurement of these temperatures

is a notoriously difficult problem, hence there is considerable demand for reliable mathematical techniques. Several methods for calculating interfacial temperatures have been devised (1-7) for the case in which the power density (i.e., the rate of frictional heat production per unit area) is constant over the contact area. However, in engineering systems the area of sliding contact is often formed by elastic deformation of curved bodies in nominal point or line contact, in which cases the pressure is exactly or approximately elliptically distributed over the contact area according to the classic equations of Hertz (8). Even if the load exceeds the elastic limit, the interfacial pressure distribution is still fairly close to elliptical (9). Thus, given that the friction force contributed by a differential element of area is proportional to the normal load on that element, the power density in a sliding Hertzian contact will be elliptically distributed. An important example, and the principal application for the results of this paper, is the 4-ball machine, (or a pin-on-disc machine with a hemispherical slider), widely used in tribology research and lubricant testing, which effects sliding contact between two spheres such that the contact area is stationary on one of them.

Presented at the 23th ASLE Annual Meeting
in Chicago, May 4-8, 1970

NOMENCLATURE

α = thermal diffusivity
 B = dimensionless parameter $\sqrt{R/\alpha}$
 E, K = complete elliptic integrals
 G = dimensionless bulk temperature difference $\pi R \Delta\theta_b / Q$
 k = thermal conductivity
 L = heat source half-width in the direction of motion
 q = frictional power density (heat per unit time per unit area)
 q_b = heat flux across the interface due to the bulk temperature difference
 Q = total frictional power
 Q_b = power transferred across the interface as a result of the bulk temperature difference
 r = distance from the center of the heat source
 R = radius of the heat source
 T = temperature at the sliding interface minus the bulk temperature

T_s = surface temperature within a stationary heat source on a single surface minus the bulk temperature
 T_m = surface temperature within a moving heat source on a single surface minus the bulk temperature
 u = dimensionless coordinate $\frac{1}{2}(1 + x/L)$
 v = velocity with respect to the heat source
 x, y = Cartesian coordinates denoting position within the heat source
 x_m, y_m = x, y coordinates of the maximum interfacial temperature
 α = true heat partition coefficient
 β = effective heat partition coefficient
 $\Delta\theta$ = local deviation from α
 θ = absolute temperature at the sliding interface
 θ_s, θ_m = bulk temperatures of the stationary and moving bodies, respectively
 $\Delta\theta_b$ = bulk temperature difference $\theta_m - \theta_s$
 Ω = dimensionless function of u

In this paper, an analytic expression for the steady-state interfacial temperature distribution in a radially symmetric Hertzian contact sliding under unlubricated or boundary-lubricated conditions is derived taking into account the ellipsoidal power density distribution. The treatment is presented for the case in which one surface is stationary with respect to the contact area but is valid as well for certain other cases which will be discussed. We will first derive the temperature distribution on a single surface for (a) a stationary heat source and (b) a moving heat source. The temperature distribution for sliding contact will then be obtained from these two distributions, initially for the case where the two bodies have the same bulk temperature and subsequently for the more general case of unequal bulk temperatures.

In this paper, the symbol T will always represent the surface temperature increase above the temperature in the body(s) far from the heat source. The subscripts s and i will refer to the single surface stationary and moving sources, respectively.

STATIONARY HEAT SOURCE ON A SINGLE SURFACE

The steady-state (i.e., after an infinitely long time) surface temperature due to a stationary point heat source on a plane surface is given by (10)

$$dT = \frac{dQ}{2\pi bk}, \quad [1]$$

where b is the distance from the heat source, dQ is its power, and k is the thermal conductivity. An identical relationship holds for the elastic normal deflection of a plane surface due to a normal point force dW acting on the surface (11);

$$dw = \frac{dW}{2\pi bE'}, \quad [2]$$

where $E' = E/2(1 - \nu^2)$, E is Young's modulus, and ν is Poisson's ratio. Therefore the normal deflection $w(x, y)$ of a plane surface due to a pressure distribution $p(x, y)$, obtained by double integration of Eq. [2], is an exact analogue of the steady-state surface temperature field $T_s(x, y)$ resulting from a stationary heat source of power density $q(x, y)$ distributed over a finite area on the surface, which is given by double integration of Eq. [1].

An analytic expression is required for $T_s(r)$ resulting from the ellipsoidal power density distribution

$$q(r) = \frac{3Q}{2\pi R^2} [1 - (r/R)^2]^{1/2}, \quad [3]$$

where Q is the total power produced by the heat source, R is its radius, and r is the distance from its center. This is plotted in Fig. 1 in the dimensionless form $(2\pi R^2/3Q) q(r/R)$. For comparison, the uniform power density distribution $q = Q/\pi R^2$ is plotted as well. Using the analogy presented above, the surface temperature fields $T_s(r)$ for these two heat distributions can be written directly from

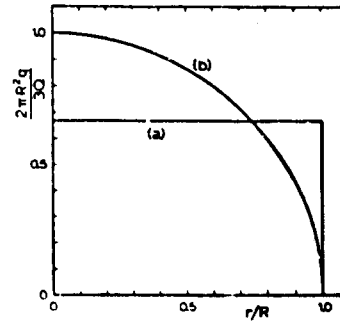


Fig. 1—(a) Uniform and (b) ellipsoidal power density distributions. Both distributions have the same total power Q .

the elastic deflections $w(r)$ for the corresponding pressure distributions (11). For the ellipsoidal power density [3],

$$T_s(r) = \frac{3\pi}{8} \left[1 - \frac{1}{2} \left(\frac{r}{R} \right)^2 \right] \frac{Q}{\pi Rk} \quad (r \leq R), \quad [4]$$

and, for the uniform power density,

$$T_s(r) = \frac{2}{\pi} E(r/R) \frac{Q}{\pi Rk} \quad (r \leq R), \quad [5]$$

where $E(r/R)$ is the complete elliptic integral of the second kind whose modulus is r/R . In Fig. 2, the two temperature distributions are plotted in the dimensionless form $(\pi Rk/Q) T_s(r/R)$. The average temperature over the source area ($r < R$) for the ellipsoidal distribution is

$$T_{s,avg} = \frac{9\pi}{32} \frac{Q}{\pi Rk}, \quad [6]$$

which is 4.1% greater than that for the commonly employed uniform heat source.

FAST MOVING HEAT SOURCE ON A SINGLE SURFACE

Let (x, y) be a Cartesian coordinate system in the surface with its origin at the center of the heat source,

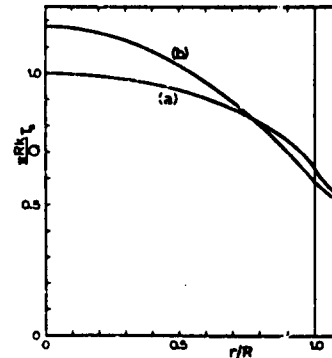


Fig. 2—Surface temperature field within a stationary heat source for (a) uniform and (b) ellipsoidal power density distributions.

where $+x$ is the direction of motion with velocity v of the surface with respect to the source. Archard (3) has shown that when the dimensionless parameter $vR/a > \sim 10$, where a is the thermal diffusivity, the heat flow in the y direction may be neglected, and the temperature distribution in a heat source of finite area can be determined by dividing the area into differential strips parallel to the sliding direction; the temperature profile along any strip is the same as that for an infinitely long (in the y direction) band source (for which naturally there is no heat flow in the y direction) of width equal to the strip length and having the same power density profile as the strip. The situation is illustrated in Fig. 3 which shows the ellipsoidal power density distribution, a differential strip, and its equivalent semi-infinite band source.

To apply this method to our fast moving ellipsoidal heat source, we require an analytic expression for the temperature profile across a band source having an ellipsoidal power density profile (a vertical section through an ellipsoid being an ellipse). An exact analytic solution is not possible (2), however Blok (12) has derived an approximate expression whose accuracy improves asymptotically with increasing vL/a , where the band width is $2L$. Blok's relationship can be expressed most conveniently, after a change of variable and rearrangement, as

$$T_v(u) = \frac{2}{k} \left(\frac{2aLu}{\pi v} \right)^{1/2} \int_0^1 q(x) ds, \quad [7]$$

where $u = \frac{1}{2}(1 + x/L)$, and the x in $q(x)$ is replaced by $L[2u(1 - s^2) - 1]$. Since $q(x) = q_{x=0}[1 - (x/L)^2]^{1/2}$, Eq. [7] is an elliptic integral which reduces to (13)

$$T_v(u) = \frac{4q_{x=0}}{3k} \left(\frac{2aL}{\pi v} \right)^{1/2} \Omega(u), \quad [8]$$

where $\Omega(u) = (1 - u)K(u^{1/2}) + (2u - 1)E(u^{1/2})$, and $K(u^{1/2})$, $E(u^{1/2})$ are the complete elliptic integrals of the first and second kind, respectively, both of whose moduli have the value $u^{1/2}$. The function $\Omega(u)$ is plotted in Fig. 4.

Cameron, et al. (6) showed that for a uniform ($q(x) = \tau$ constant) band source, the temperature profile $T_v(u)$ is

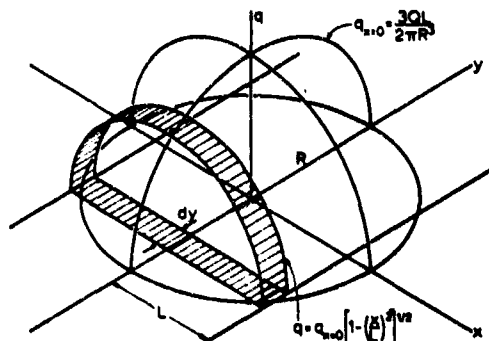


Fig. 3—Isometric view showing the fast moving ellipsoidal power density distribution, a differential strip (width dy , length $2L$), and its equivalent semi-infinite band source (width $2L$).

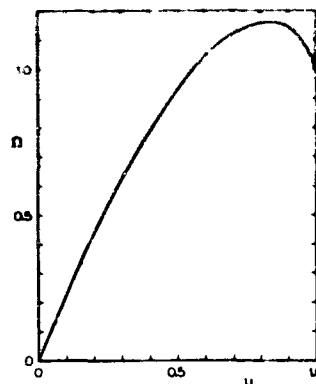


Fig. 4—The dimensionless function $\Omega(u)$ which prescribes the shape of the surface temperature profile across an infinitely fast moving band source having an elliptical power density profile. The leading edge of the band is on the left.

given almost exactly for $10 < vL/a < \infty$ by multiplying the asymptotic ($vL/a = \infty$) expression by the factor $1 + u^{-1/2}[0.65(a/vL) + 0.44(a/vL)^{3/2}]$. Assuming this correction factor to be valid for the elliptical case as well, Eq. [8] becomes

$$T_v(u) = \frac{4Lq_{x=0}}{3k} \left(\frac{2}{\pi} \right)^{1/2} \left(\frac{a}{vL} \right)^{1/2} \left(1 + u^{-1/2} \left[0.65 \left(\frac{a}{vL} \right) + 0.44 \left(\frac{a}{vL} \right)^{3/2} \right] \right) \Omega(u). \quad [9]$$

As vL/a decreases, the correction factor effectively increases the maximum temperature and moves it toward the origin.

Following Archard's method, we now can write directly the temperature distribution within a fast moving circular heat source having an ellipsoidal power density distribution by setting $L(y) = (R^2 - y^2)^{1/2}$ and $q_{x=0} = (3Q/2\pi R^2)[1 - (y/R)^2]^{1/2} = [3QL(y)/2\pi R^3]$ (see Fig. 3). Thus we have, from Eq. [9]

$$T_v(x, y) = \frac{2Q}{\pi^{3/2}kR^3} \left(\frac{2a}{v} \right)^{1/2} \left(1 + u^{-1/2} \left[0.65 \left(\frac{a}{vL(y)} \right) + 0.44 \left(\frac{a}{vL(y)} \right)^{3/2} \right] \right) L^{3/2}(y) \Omega(u). \quad [10]$$

This expression holds for $B = vR/a > \sim 10$. For $B \approx 10$, vL/a for the outer strips will be less than 10, however this would not be expected to contribute a serious error because (a) the correction factor will hold approximately for $vL/a < 10$, and (b) the outer strips are only a small fraction of the area of the source; e.g., $L < R/2$ for only 6% of the total area.

The maximum temperature and its location (x, y) are

$$T_{v,\max} = 1.852 \frac{Q}{\pi R k B^{1/2}} \text{ at } (0.652R, 0) \text{ for the asymptotic case,} \quad [11]$$

$$T_{v,\max} = 2.013 \frac{Q}{\pi R k B^{1/2}} \text{ at } (0.633R, 0) \text{ for } B = 10. \quad [12]$$

The average temperature over the source area $x^2 + y^2 \leq B^2$ is given by

$$T_{v,avg} = \frac{2}{\pi R^2} \int_0^R \phi \int_{-\sqrt{B^2-x^2}}^{\sqrt{B^2-x^2}} T_v(x, y) dy dx$$

$$= 1.016 \frac{Q}{\pi R A B^{1/2}} \left[1 + \frac{1.047}{B} + \frac{0.774}{B^{3/2}} \right] \quad [13]$$

For $B = 10$,

$$T_{v,avg} = 1.148 \frac{Q}{\pi R A B^{1/2}} \quad [14]$$

Thus, over the range of applicability of Eq. [10], the effect of the correction factor is chiefly amplification of the temperature; the translation of the maximum is negligible. For the asymptotic case, the maximum and average temperatures are 16.1% and 4.3% higher, respectively, than those (3) for a circular uniform heat source, where the maximum temperature occurs at the trailing edge ($R, 0$).

SLIDING HERTZIAN CONTACT

Now that we have both the stationary and high velocity surface temperature fields within an ellipsoidal heat source on a single surface, the task remains to determine the steady-state interfacial temperature field for sliding Hertzian contact. We assume here that the two bodies have the same bulk temperature (i.e., the temperature far from the contact); the more general case will be treated in the next section.

Assuming that within the contact area the gap between the surfaces is sufficiently small, which obtains for "dry" sliding or boundary lubrication,¹ there will be no temperature discontinuity across the interface. The moving² body will receive a greater fraction α of the total frictional power³ Q than the stationary body, because the stationary side of the interface needs only enough power $(1 - \alpha)Q$ to maintain the steady-state temperature field, while the moving side of the interface requires the greater amount of power αQ to raise its temperature from the ambient value to the higher values at the interface. As v increases, a proportionately greater area of the moving surface must be "brought up to temperature" per unit time, and thus the heat partition coefficient α increases to accommodate the increased power requirement; for the asymptotic case, $\alpha = 1$.

Interfacial Temperature

If the frictional power density $q(r)$ were to divide itself between the two bodies in the ratio $\alpha/(1 - \alpha)$ everywhere

within the contact area, the temperature fields of the moving and stationary surfaces at the interface would be $\alpha T_v(x, y)$ and $(1 - \alpha)T_s(x, y)$, respectively, where T_v and T_s are as defined by Eqs. [10] and [1]. However, it was pointed out by Blok (1) that if the temperature fields on the two surfaces are to coincide over the entire contact, the ratio of the two heat fluxes into the surfaces cannot be constant over the contact: assuming that the interfacial temperature field lies between $\alpha T_v(x, y)$ and $(1 - \alpha)T_s(x, y)$, then, in the regions where $\alpha T_v < (1 - \alpha)T_s$, the fraction of the local frictional power entering the moving body will have values greater than α , and conversely for the rest of the contact area. Thus the distributions over the contact of αQ and $(1 - \alpha)Q$ will in fact be $(\alpha + \Delta\alpha)q(r)$ and $[1 - (\alpha + \Delta\alpha)]q(r)$, where $\Delta\alpha$ is some unknown function of x, y which expresses the deviation from the ellipsoidal heat flux distributions $\alpha q(r)$ and $(1 - \alpha)q(r)$. However, a reasonable and mathematically practical approximation to the resulting interfacial temperature field $T(x, y)$ may be had by assuming that, since at a given point αT_v and $(1 - \alpha)T_s$ are linearly dependent on αQ and $(1 - \alpha)Q$, the deviations in the two surface temperatures caused by the heat flux deviations $\pm \Delta\alpha(x, y)q(r)$ are similarly proportional to $\Delta\alpha(x, y)Q$. Then

$$[\alpha + \Delta\alpha(x, y)]T_v(x, y) = T(x, y)$$

$$= [1 - \alpha - \Delta\alpha(x, y)]T_s(x, y), \quad [15]$$

and

$$T(x, y) = \frac{1}{\frac{1}{T_v(x, y)} + \frac{1}{T_s(x, y)}} \quad (B > \sim 10). \quad [16]$$

Thus the interfacial temperature field in the circle of contact can be approximated by half the harmonic mean of the two "single surface" temperature fields—that is, the temperature fields which would exist if each body were to receive all of the frictional power Q . Note that, due to the assumption leading to Eq. [15], $T(x, y)$ is independent of α .

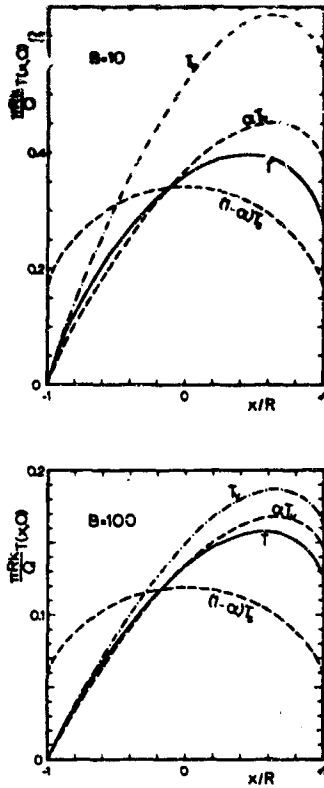
The subsequent presentation will be restricted for simplicity to the case where the two contacting bodies have the same thermal constants k, a but can easily be followed through for dissimilar materials; the same arguments hold.

$T_v(x, y)$ is a decreasing function of B , while $T_s(x, y)$ is independent of B . Thus from Eq. [15], as $B \rightarrow \infty$, $\Delta\alpha T_v / \Delta\alpha T_s \rightarrow 0$, and $T(x, y) \rightarrow \alpha T_v(x, y)$, while $\alpha T_v(x, y) \rightarrow T_v(x, y)$. For the asymptotic case, $T(x, y) = T_v(x, y)$. This is apparent in Fig. 5 which shows the profiles along the x axis to $T, T_v, \alpha T_v, (1 - \alpha)T_s$ plotted in the dimensionless form $(\pi R k / Q) T(x, 0)$ for $B = 10, 100$. The value of α was calculated using Eq. [23] derived below. Thus for high velocities the temperature field of the stationary surface is forced to conform to $\alpha T_v(x, y)$, and the form of $(1 - \alpha)T_s(x, y)$ is of little consequence. Stated another way, the power which flows across the interface in order to equalize the two temperature fields is, for large values of B , a negligible fraction of the power αQ received by

¹Thicker elastohydrodynamic lubricant films present a more complex problem (14, 15)

²The terms "moving" and "stationary" are defined with respect to the contact area.

³Given here by the product of velocity, normal load, and coefficient of friction.



Figs. 5a, 5b—Surface temperature profiles along the centerline of a sliding Hertzian contact for two different sliding velocities. The leading edge of the contact circle is on the left. T is the interfacial temperature, T_s the temperature of the moving body if it were to receive all the frictional heat, and αT_s , $(1 - \alpha)T_s$ are the two single surface temperatures taking into account the partition of the heat. As B increases, $T \rightarrow \alpha T_s$.

the moving body, and thus $T(x, y)$ does not significantly depart from $\alpha T_v(x, y)$. Consequently the accuracy of the approximation [16] increases with B .

Since $T_{s,max}$ and $T_{v,max}$ both lie on the x axis, it can be seen from Eq. [16] that the maximum interfacial temperature T_{max} will occur on the x axis as well. Putting $y = 0$, $L = R$, $r = |x| = R|2u - 1|$, Eqs. [4] [10] [16] give

$$\frac{\pi R k}{Q} T(x, 0) = \frac{1}{\frac{8/3\pi}{1 - \frac{1}{2}(2u - 1)^2} + \frac{(\pi B/8)^{1/2}}{\Omega(u) \left[1 + \frac{\frac{0.65}{B} + \frac{0.44}{B^{3/2}}}{u^{1/2}} \right]}} \quad [17]$$

which is plotted in Fig. 5 for $B = 10, 100$. The position x_m at which T_{max} occurs, obtainable from Eq. [17], depends only on B and is equal to $0.652R$, $0.396R$ for $B = \infty, 10$, respectively. Over the range $\infty > B > 10$, $T_s(x_m, 0)$ varies by 14% and can be approximated by the expression

$$Q/\pi R k T_s(x_m, 0) = 1.078 - 0.290B^{-0.271} \quad [18]$$

Similarly, $B^{1/2} T_v(x_m, 0)$ varies by 5% and can be approximated by

$$Q/\pi R k B^{1/2} T_v(x_m, 0) = 0.540 - 0.589B^{-1.118} \quad [19]$$

Finally, from Eqs. [16] [18] [19],

$$T_{max} = T(x_m, 0) = \frac{1.852Q/\pi R k}{1.996 - 1.091B^{-0.818} - 0.537B^{-0.271} + B^{1/2}} \quad (B \geq 10), \quad [20]$$

which provides a working formula for computing T_{max} .

Heat Partition Coefficient

Over the element $dx dy$, the power entering the moving body is $(T/T_v)q dx dy = q dx dy/[1 + (T_v/T_s)]$. Thus the heat partition coefficient α is given by

$$\alpha Q = \iint \frac{q}{1 + \frac{T_v}{T_s}} dx dy \quad [21]$$

However, since this expression cannot be integrated analytically, and, besides, it is only as good an approximation as Eq. [16], we offer the following alternate method for determining α .

The best approximation to the true value of α will be the value which best satisfies the condition that the temperature fields of the two surfaces be identical over the contact area. Thus an analytic approximation can be obtained by equating the mean temperatures of the two surfaces, as did Jaeger (2), giving

$$\alpha T_{v,avg} = (1 - \alpha) T_{s,avg} \quad [22]$$

Substituting Eqs. [6] [13] yields

$$\frac{\alpha}{1 - \alpha} = \frac{0.870B^{1/2}}{1 + \frac{1.047}{B} + \frac{0.774}{B^{3/2}}} \quad (B \geq 10) \quad [23]$$

which expresses the manner in which α approaches unity as $B \rightarrow \infty$. At the lower limit $B = 10$, $\alpha = 0.709$; the moving body receives roughly twice as much power as the stationary body.

UNEQUAL BULK TEMPERATURES

In the preceding section, the bulk temperatures of the two sliding bodies were taken to be equal. In practice, however, this condition seldom occurs. If the heat partition coefficient α is greater than $1/2$, and/or if the thermal masses or heat loss characteristics of the two bodies are unequal, the difference between the bulk temperature will increase asymptotically with time due to the frictional heating. In addition, of course, external heating can contribute to the bulk temperature difference.

We now consider the effect of unequal bulk temperatures on the interfacial temperature field. In addition to the frictional power flowing into both bodies from the interface, there is now an amount of power Q_b which flows from the hotter body across the interface into the colder body. The situation is illustrated in Fig. 6 where, remembering that the symbol T refers to the temperature increase above the bulk temperature and designating absolute temperature by the symbol θ , $\theta(x, y)$ is the absolute interfacial temperature field, and θ_{bv} , θ_{bs} are the two bulk temperatures (assumed to be uniform far from the interface). The form of the heat flux distribution $q_b(x, y)$ is indeterminate. However, if we assume $q_b(x, y)$ to be ellipsoidal, then Q_b and Q become additive, greatly simplifying the mathematics; effectively Q_b only alters the heat partition coefficient α . As long as Q_b is sufficiently less than Q , the error due to assuming an arbitrary specific $q_b(x, y)$ distribution will be small. Taking Q_b to be positive when it flows from the moving body to the stationary body, we define a parameter β such that

$$Q_b = (\alpha - \beta)Q \quad [24]$$

Thus, when $\theta_{bv} - \theta_{bs} = \Delta\theta_b = 0$, $Q_b = 0$ and $\beta = \alpha$. Q_b and hence $\alpha - \beta$ have the same sign as $\Delta\theta_b$. The net heat flow from the interface into the moving body is

$$\alpha Q - Q_b = \beta Q \quad [25]$$

and the net heat flow into the stationary body is

$$(1 - \alpha)Q + Q_b = (1 - \beta)Q \quad [26]$$

Thus β is the effective heat partition coefficient. Note that, whereas α ranges only from $1/2$ (when $B = 0$) to unity (when $B = \infty$), β can have any value, positive or negative, depending on $\Delta\theta_b$.

The absolute interfacial temperature field $\theta(x, y)$ can be derived as in the preceding section; the same arguments apply. Eq. [15] becomes

$$\begin{aligned} [\beta + \Delta\alpha(x, y)]T_v(x, y) + \theta_{bv} &= \theta(x, y) \\ &= [1 - \beta - \Delta\alpha(x, y)]T_s(x, y) + \theta_{bs} \end{aligned} \quad [27]$$

Note that the single surface temperature fields $\beta T_v(x, y)$ or $(1 - \beta)T_s(x, y)$ will be negative (cooler than the bulk temperature) when heat flows out of the respective body—

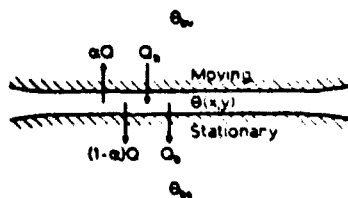


Fig. 6—Schematic representation of the heat flow at the sliding interface. Q is the frictional power, and Q_b is the heat flow resulting from the bulk temperature difference $\Delta\theta_b = \theta_{bv} - \theta_{bs}$.

equivalent to an ellipsoidal heat unit on that surface. From Eq. [27],

$$\theta(x, y) = \theta_{bv} + \frac{1 - \frac{\Delta\theta_b}{T_s(x, y)}}{\frac{1}{T_s(x, y)} + \frac{1}{T_v(x, y)}} \quad (B > \sim 10) \quad [28]$$

As before, $\theta(x, y)$ is independent of β .

As $B \rightarrow \infty$, $\theta(x, y) - \theta_{bv} \rightarrow [1 - (\Delta\theta_b/T_s(x, y))]T_v(x, y)$. Thus when the bulk temperatures are unequal, the interfacial temperature field for the asymptotic case no longer conforms to $T_v(x, y)$. In addition, $T_v(x, y) \rightarrow 0$, hence $\theta(x, y) \rightarrow \theta_{bv}$.

In Fig. 7 the relative values of θ_{\max} , θ_{bv} , θ_{bs} are plotted as functions of the dimensionless bulk temperature difference $G = \pi R k \Delta\theta_b / Q$ over the range $-1.3 < G < 1.3$ for $B = 10, 100$. The horizontal line is the average bulk temperature $1/2(\theta_{bv} + \theta_{bs})$. As $B \rightarrow \infty$, $\theta_{\max} \rightarrow \theta_{bv}$, and this trend may be seen in the plot. The location x_m of the maximum interfacial temperature on the x axis varies with G as shown in Fig. 8. When $G = +1.178$, $\theta_{\max} = \theta_{bv}$ for all values of B , and θ_{\max} is situated at the center of

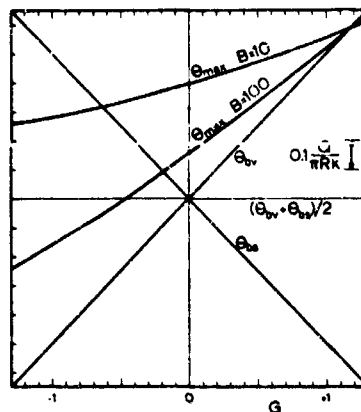


Fig. 7—Relative values of the maximum interfacial temperature and the two bulk temperatures plotted as functions of the dimensionless bulk temperature difference G for two different sliding velocities.

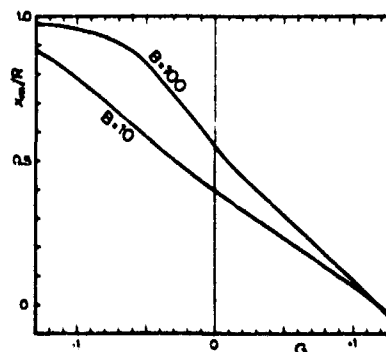


Fig. 8—Location of the maximum interfacial temperature on the centerline as a function of the bulk temperature difference. The ordinate 1.0 is the trailing edge, and 0 is the center.

the contact or. As G decreases, θ_{\max} moves toward the trailing edge of the contact ($R, 0$).

The effective heat partition coefficient β is given by

$$\beta Q = \iint_{r < R} \frac{\theta - \theta_{bv}}{T_v} q \, dx \, dy = \iint_{r < R} \frac{T_s - \Delta\theta_b}{T_s + T_v} q \, dx \, dy. \quad [29]$$

However, as in the preceding section, we can obtain an analytic expression for β by equating the average temperatures of the two surfaces over the contact area. Thus,

$$\beta T_{v,avg} + \theta_{bv} = (1 - \beta) T_{s,avg} + \theta_{bs} \quad [30]$$

which, together with Eqs. [22] [6], gives

$$\frac{\beta}{1 - \beta} = \frac{1 - 1.132G}{\frac{1 - \alpha}{\alpha} + 1.132G}, \quad [31]$$

where $(1 - \alpha)/\alpha$ is as given by Eq. [23]. Rearranging Eqs. [24] and [31],

$$Q_b/Q = \alpha - \beta = 1.132\alpha G, \quad [32]$$

$$\beta = \alpha - 1.132\alpha G; \quad [33]$$

thus both β and the ratio Q_b/Q are linear in G , the constants depending only on B .

DISCUSSION

A number of cases where both surfaces move with respect to the contact can be treated by the method of this paper. Jaeger (2) showed that for low velocities ($B < \sim 0.2$) the moving single surface temperature distribution may be approximated by that for a stationary source. Thus, designating the velocities of the two bodies with respect to the contact area by v_1, v_2 , we can determine $\theta(x, y)$ for any combination of values of B_1, B_2 greater than +10, less than -10, and from -0.2 to +0.2. When $B_2 > 10$, B_1 can range from -0.2 to +0.2 without invalidating the results of the previous sections. When both $|B_1|, |B_2| < 0.2$, T_v is replaced by T_s , and Eq. [28] becomes

$$\theta(x, y) = \frac{1}{2}(\theta_{bv} + \theta_{bs}) + \frac{1}{2}T_s(x, y). \quad [34]$$

When both $|B_1|, |B_2| > 10$, $\theta(x, y)$ will be given by

$$\theta(x, y) = \theta_{bv} + \frac{1 - \frac{\Delta\theta_b}{T_{v1}(x, y)}}{\frac{1}{T_{v1}(x, y)} + \frac{1}{T_{v2}(x, y)}}. \quad [35]$$

If v_1, v_2 are of opposite sign, $T_{v2}(x, y)$ must be replaced by $T_{v2}(-x, y)$. For the case of pure rolling contact⁴ ($v_1 = v_2$), Eq. [35] becomes

⁴It should be noted that, for pure rolling in the absence of a hydrodynamic lubricant film, the frictional power consists primarily of the hysteresis in the elastic deformation cycle and is distributed nonuni-

$$\theta(x, y) = \frac{1}{2}(\theta_{bv} + \theta_{bs}) + \frac{1}{2}T_v(x, y) \quad [36]$$

Eq. [35] is also applicable to the one-dimensional problem of a sliding/rolling Hertzian contact band such as would result from contact between gear teeth or cylinders, here, $T_{v1}(x), T_{v2}(x)$ are of the form of Eq. [9].

The maximum interfacial temperature T_{\max} is usually the most useful single quantity and the one most often referred to as the flash temperature. In his landmark paper on flash temperature, Blok (1) derived, for a circular contact area with a uniform power density distribution, an expression for T_{\max} based on the two assumptions

$$\alpha T_v(R, 0) = (1 - \alpha) T_s(0, 0) \quad [37]$$

and

$$T_{\max} = \frac{1}{2}[\alpha T_v(0, 0) + (1 - \alpha) T_s(0, 0)]. \quad [38]$$

Although the heat partition criterion [37] is convenient in that it does not require knowledge of the complete functions $T_s(x, y)$ and $T_v(x, y)$, it seems a rather poor approximation to the condition that the temperature distributions of the two surfaces must coincide over the entire contact area. The assumption [38] neglects the fact that at high velocities T approaches T_v , as shown earlier, and, in addition, it is likely that T_{\max} occurs at a point nearer to the trailing edge ($R, 0$) than to the center ($0, 0$). However, as Blok's equation is the one commonly used to calculate flash temperatures, it is the logical equation with which to compare our Eq. [20].

The equation derived by Blok (1) for $B > \sim 20$ is

$$T_{\max} = \frac{1.362Q/\pi Rk}{1.596 + B^{1/2}}. \quad [39]$$

The ratio of Eq. [20] to Eq. [39] is 1.33 for $B = 100$ and 1.38 for $B = 10$, the lower limit of applicability of Eq. [20].

Experimental support for the validity of Eq. [20] is contained in data presented by Fein (17, 18), who found a discrepancy between lubricant transition temperatures in a slow speed pin-on-disc machine and those determined by calculating, using Blok's equation, T_{\max} at the transition point in a 4-ball machine where the parameter B was in the vicinity of 10. He further showed that this discrepancy could be eliminated by multiplying the numerator of Eq. [39] by 1.33 which compares favorably with the ratio 1.38 between Eqs. [20], [39] at $B = 10$.

It should be noted in passing that a commonly overlooked factor in the calculation of flash temperature is the fact that the value of the thermal conductivity k (to which the thermal diffusivity a is proportional) can vary markedly with composition, thermal history, and temperature. For example, the values of k for various typical iron alloys listed in Table 1 (19) are seen to vary through-

formly over a volume whose effective radius from the center of contact is perhaps 2 or 3 times R (16). The ellipsoidal planar heat source may therefore be a less accurate approximation when there is no sliding.

Table 1 THERMAL CONDUCTIVITY OF VARIOUS IRON ALLOYS

Alloy Type	Composition (weight %)						Thermal Conductivity (cal/cm sec °C)
	C	Mn	Si	Cr	Ni	Other	
Pure iron							.178
Cast iron	3.16	.57	1.54				.112
Carb steel	23	.64					.124
Carbon steel	1.22	.35					.108
Alloy steel	.34	.55		.78	3.53	Mo .39	.079
						Cu .05	
						W18.0	
T1 tool steel	.70			4.0		V1.0	.058
Stainless type 410	.15	1.0	1.0	11.5-13.5			.057
Stainless type 304	.08	2.0	1.0	18.0-20.0	8.0-12.0		.036

a factor of 5. For EN 31 or AISI 52100 steel, generally used in the fully hardened state for bearing components, tempering due to frictional heating could result in as much as a 67% increase in k above its value for the as-received fully hardened condition (20).

CONCLUSIONS

An analytic expression for the steady-state interfacial temperature field within an unlubricated (or boundary-lubricated) sliding circular Hertzian contact has been derived in terms of the total frictional power, velocity, contact radius, the thermal properties of the materials, and the bulk temperature of each body. The detailed analysis has been presented for the case where one of the surfaces does not move with respect to the contact area ($v_1 = 0$), as, for example, in the 4-ball machine, and where $v_2 > 10a/R$, although the relationships derived would hold, to a lesser degree of accuracy, for lower velocities. The basic method presented in this paper, however, can be applied to any combination of v_1, v_2 outside of the range $0.2a/R < |v| < 10a/R$.

Although not an exact solution to the problem, the results of this paper are more reliable than previously reported approximations in the following respects: (a) Account is taken of the fact that the power density is ellipsoidally distributed over the contact circle. (b) A factor is introduced into the asymptotic expression for the temperature distribution $T_p(x, y)$ within a moving heat source on a single surface which extends the range of validity of the results down to $B = 10$. (c) It was shown that the interfacial temperature distribution $T(x, y)$ can be approximated by half the harmonic mean of the two single surface temperature fields $T_1(x, y), T_2(x, y)$ and that the accuracy of this approximation improves with increasing velocity as $T(x, y)$ approaches $T_p(x, y)$. The expression for T_{max} was obtained directly from $T(x, y)$.

In addition, the problem and its analytic solution have been extended to include the more general case of unequal bulk temperatures of the two sliding bodies. This

alters the heat partition coefficient and the magnitude and shape of the interfacial temperature field. As $B \rightarrow \infty$, the interfacial temperature approaches the bulk temperature of the moving body.

The expression derived for the maximum flash temperature T_{max} gives a value from 33% to 38% greater (depending on the value of B) than Blok's widely used formula (1).

ACKNOWLEDGMENTS

This work was performed as part of a research program supported by Castrol, Ltd. to whom the author is indebted. Thanks are also due to Dr. A. E. B. Presland for useful discussion and to Professor A. R. Ubbelohde for providing facilities in the Dept. of Chemical Engineering & Chemical Technology.

REFERENCES

- (1) Blok, H., "Theoretical Study of Temperature Rise at Surfaces of Actual Contact under Oiliness Lubricating Conditions," *Int. Mech. Engrs., General Discussion on Lubrication* 2, 222-235 (1937).
- (2) Jaeger, J. C., "Moving Sources of Heat and the Temperature at Sliding Contacts," *J. Proc. Roy. Soc. A, S. B.* 76, 203-224 (1912).
- (3) Archard, J. F., "The Temperature of Rubbing Surfaces," *Wear* 2, 438-455 (1958-59).
- (4) Ling, F. F., "A Quasi-Iterative Method for Computing Interface Temperature Distributions," *Z. Angew. Math. Phys.* 10, 461-474 (1959).
- (5) Allen, D. N. deG., "A Suggested Approach to Finite Difference Representation of Differential Equations, with an Application to Determine Temperature Distributions Near a Sliding Contact," *Quant. J. Mech. Appl. Math.* 15, 11-33 (1962).
- (6) Cameron, A., Gordon, A. N., and Symm, G. T., "Contact Temperatures in Rolling Sliding Surfaces," *Proc. Roy. Soc. A286*, 43-61 (1965).
- (7) Symm, G. T., "Surface Temperatures of Two Rubbing Bodies," *Quant. J. Mech. Appl. Math.* 20, 381-391 (1967).
- (8) Hertz, H., "On the Contact of Elastic Bodies," *J. Reine Angew. Math.* 92, 156-171 (1886).
- (9) Tabor, D., "The Hardness of Metals," Oxford Press, 1951, pp. 88-89.
- (10) Carslaw, H. S., and Jaeger, J. C., "Conduction of Heat in Solids," Oxford Press, 2nd ed., 1959, p. 261.

- (11) Timoshenko, S., and Goodier, J. N., "Theory of Elasticity," McGraw-Hill Book Co., Inc., New York, 2nd ed., 1951, pp. 362-377.
- (12) Blok, H., "Les températures de surface dans des conditions de graissage sous pression extrême," 2nd World Petroleum Congress, Section 4, Paris, 471-486 (1937).
- (13) Byrd, P. F., and Friedman, M. D., "Handbook of Elliptic Integrals for Engineers and Physicists," Springer-Verlag, Berlin, 1st ed., 1954, p. 51, §214.12.
- (14) Cheng, H. S., "A Refined Solution to the Thermal-Elastohydrodynamic Lubrication of Rolling and Sliding Cylinders" *ASLE Trans.* 8, 397-410 (1965).
- (15) Manton, S. M., O'Donoghue, J. P., and Cameron, A., "Temperatures at Lubricated Rolling Sliding Contacts," *Proc Instn Mech Engrs* 182, Part 1, 813-824 (1967-68).
- (16) Greenwood, J. A., Minshall, H., and Tabor, D., "Hysteresis Losses in Rolling and Sliding Friction," *Proc Roy Soc* A259, 480-507 (1961).
- (17) Fein, R. S., "Transition Temperatures with Four Ball Machine," *ASLE Trans.* 3, 34-39 (1960).
- (18) Fein, R. S., "Effects of Lubricants on Transition Temperatures," *ASLE Trans.* 8, 59-68 (1965).
- (19) "Metals Handbook," Amer. Soc. Metals, Metals Park, Ohio, 8th ed., 1961, p. 55.
- (20) Powell, R. W., and Tye, R. P., "The Effect of Oil Quenching and Tempering on the Thermal Conductivities and Electric Resistivities of Three Steels," *J. Iron Steel Inst.* 184, 10-17 (1956).

INTENTIONALLY

BLANK

A Critical Survey of Mathematical Models for Boundary Lubrication

A. BEERBOWER

Government Research Laboratory
Esso Research and Engineering Co., Linden, New Jersey 07036

Presented at the ASME/ASLE Lubrication
Conference, Cincinnati, Ohio, Oct. 13-15, 1970

This paper is the literary property of the American Society of Lubrication Engineers. The press may summarize freely from this manuscript after presentation, citing source; however, publication of material constituting more than 20% of the manuscript shall be construed as a violation of the Society's rights and subject to appropriate legal action. Manuscripts not to be published by the Society will be released in writing for publication by other sources.

Statements and opinions advanced in papers are understood to be individual expressions of the author(s) and not those of the American Society of Lubrication Engineers.

AMERICAN SOCIETY OF LUBRICATION ENGINEERS

838 BUSSE HIGHWAY

PARK RIDGE, ILLINOIS 60068

Discussion of this paper will be accepted at
ASLE Headquarters until November 15, 1970.

A Critical Survey of Mathematical Models for Boundary Lubrication

A. BEERBOWER

Government Research Laboratory

Esso Research and Engineering Co., Linden, New Jersey 07036

The various equations representing special cases of boundary lubrication are examined and grouped as "models". The study indicates that there are no serious inconsistencies, but that each model is so seriously limited in its coverage that large gaps exist in coverage. Methods for closure of these gaps are suggested and numerically explored to a limited extent. Hope is extended that in the near future it will be possible to compute wear rates from basic physical properties without actual experimentation on the specific lubricant and surfaces. This would constitute a useful new system for machine element design.

INTRODUCTION

Elastohydrodynamic lubrication models form a reasonably well integrated matrix, but those related to boundary lubrication are isolated and apparently inconsistent. However, there are enough of them to justify a serious attempt at unification. The scope of this project was selected to exclude dry solid film lubrication and gas

bearings, and to include all liquid lubrication even when the liquid is thickened to a grease or a solid additive is present. The load regime is defined by the zone XY in Fig. 1, where "relative load" may be taken as the force, generalized in regard to geometry required to produce the wear effects illustrated.

As study proceeded, it became necessary to recognize additional regimes. The first of these is AX , in which the original asperities interfere with the elastohydrodynamic regime in OX , at least until they are smoothed out by one or more "break-in" processes. This "running in" regime is transitory in time but of vital importance. If the processes include chemical reactions, the regime of "corrosive wear" extends from A to B . The position of B is highly variable; with very inert systems it may lie at X , while with very active EP (extreme pressure) agents it shifts all the way to Z' . In ordinary systems, it lies between X and Y , and the BY regime is known as "adhesive wear." Finally, at Y , there is an abrupt transition to "scuffing wear" or "scoring." The YZ regime is of little interest to the operator of successfully lubricated machines, but the exact location of Y is of great interest to designers.

Presented as an American Society of Lubrication Engineers paper at the ASM-ASLE Lubrication Conference held in Cincinnati, Ohio, October 13-15, 1970

NOMENCLATURE

α = tractional film defect (for additive in Model II C)
 A_t = cross-sectional area of wear track (cm^2)
 A_{12} = work of adhesion (ergs/cm^2)
 β = fractional base fluid film defect
 B = electric charging energy of metal (ergs/cm^2)
 $\gamma = (1 + 3\mu^2)^{0.5}$
 γ_0 = surface free energy of liquid extrapolated to 0°K (ergs/cm^2)
 γ_1 = surface free energy of solid (ergs/cm^2)
 γ_2 = surface free energy of liquid (ergs/cm^2)
 γ_{12} = interfacial free energy (ergs/cm^2)
 c = additive concentration in mol/l action
 C, C^* = constants in finite wear equations
 C_o = oxygen concentration in lubricant (gm/gm)
 δd = London force solubility parameter ($\text{cal}/\text{cm}^3)^{0.5}$

$\delta\mu$ = polar solubility parameter ($\text{cal}/\text{cm}^3)^{0.5}$
 δ_H = hydrogen bonding solubility parameter ($\text{cal}/\text{cm}^3)^{0.5}$
 d = sliding distance (cm)
 d_0 = zero wear sliding distance (cm)
 D = surface roughness, peak to peak (μ in or μ m)
 ϵ = dielectric constant of lubricant
 E = heat of adsorption (cal/mol or ergs/cm^2)
 ΔE = difference in heat of adsorption of additive (E_a) and base fluid (E_b)
 E_1, E_2 = Young's modulus of solids (psi)
 G = allowable fraction of τ_y for zero wear
 G_R = G for 2000 passes
 h = Planck's constant (6.6×10^{-27} erg sec)
 H = Hertz contact dimension (in or cm)
 k = Boltzman's constant (1.4×10^{-16} ergs/deg C)
 k_m = "wear coefficient" for metal-metal contact area
 k_1, k_2 = thermal conductivities ($\text{cal}/\text{sec-cm}^\circ\text{C}$)

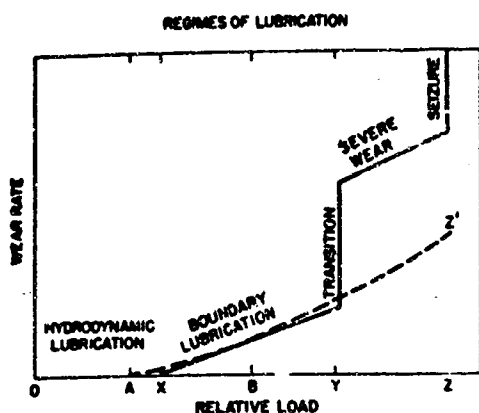


Fig. 1—Regimes of lubrication.

As a useful simplification, it was decided to eliminate, at least for the present analysis, the possibility of foreign abrasive contaminants reaching the wearing surfaces. It was also assumed that the lubricant was adequately inhibited against bulk oxidation and that changes due to thermal decomposition were negligible. However, a full range of atmospheres was accepted as a necessary part of the job, with those more corrosive than humid air being set aside temporarily. Also temporarily, the ambient atmospheric pressure was set at one atmosphere. Thus, the scope includes break-in, (1) corrosive wear due to lubricant or to atmospheric $O_2 + H_2O$, (2) adhesive wear and transition point location (3). The effect of lubrication on fatigue, except as it marks a limiting condition, does not seem to be ready for this type of consideration.

MODELS

Strictly speaking, any equation relating to boundary lubrication could be considered a "model" and, therefore, deserving of separate handling. Fortunately, many of

these have been rounded up and screened into some coherence by MacGregor et al (4) and by Rowe (5). These will be referred to as Model I and Model II respectively. In addition to these, it is necessary to consider a third model which has not yet been completely formulated. Model III is based on the general concept of irreversible reactions. These include the formation of "friction polymer" a material generated under conditions of low wear from the base stocks, apparently by catalytic action of freshly sheared metal surfaces. A fourth model came to the writer's attention too late for complete analysis at present, and a fifth is given minor attention as a special-purpose matter.

BASIS OF MODEL I

This model is the result of a great deal of experimental work at IBM, an account of which is given by Bayer (6, 7, 8). It may be described as essentially geometric and empirical, though a definite relationship to the Archard wear and Palmgren fatigue equations has since been established. Only four (sometimes three) "grades" of lubricant are considered. These were selected to cover the range of oils commonly encountered, along with the dry situation. Of course, this constraint is very irksome to those concerned with lubricant development, especially since no means is provided for interpolation or extrapolation to other grades of oil or grease beyond assuming that the change will not be for the better. Another serious limitation is that it is not possible to adjust the model for environmental conditions, these being preselected as air at one atmosphere, 30% relative humidity, and a temperature of about 22 C. It is assumed that speeds will be kept low enough that surface temperatures will not be significantly above ambient, so there is no adjustability for speed. A fourth limitation is that parameters must be looked up for specific material pairs or couples. There is

K_{12} = interfacial wetting factor

λ = mass diffusivity (cm^2/sec)

L = number of revolutions or strokes

$L_0 = L$ for zero wear period

F = coefficient of friction

n = exponent in finite wear equation

M = molecular weight (g/mole)

ν_1, ν_2 = Poisson's ratio of solids

σ = number of molecules per unit area (cm^{-2})

N = number of passes

$N_0 = N$ for zero wear

P = partial pressure of preferred component

P_m = flow pressure of metal under static loading (gm/cm^2 or kg/mm^2)

ϕ = fractional surface coverage by additive

q = maximum stress in Hertz contact area (psi)

Q_s = heat of surface formation ($ergs/cm^2$)

r = radius of spherical member (in or cm)

R = molar gas constant ($cal/mole \cdot ^\circ K$)

ρ = density of oil (gm/cc)

$\rho_0 = \rho$ at $60^\circ F$ ($15^\circ C$)

ΔS = total entropy change associated with adsorption (eu)

N_A = Avogadro's number

S = distance traveled per revolution or stroke (in or cm)

τ_{max} = maximum shear stress in contact area (psi)

τ_y = yield stress in shear of solid (psi)

t = time (sec)

t_0 = vibrational time of adsorbed molecule (sec)

t'_0 = ratio of t_0 values for additive and base fluid

T_c = critical temperatures of lubricant ($^\circ K$)

T_b = bulk temperature of lubricant ($^\circ K$)

T_m = melting point of lubricant ($^\circ K$)

T_s = temperature of surface ($^\circ K$)

T_t = transition temperature at scuffing ($^\circ K$)

θ = contact angle (deg)

U = sliding velocity (cm/sec)

U_a = lubricant flow velocity, average, into gap (cm/sec)

V = wear volumes (cm^3)

V_m = molar volume (cm^3/mol)

W = load (gms or lbs)

w = width of wear track (cm or in)

$w_0 = w$ for end of zero wear period

x = ratio of molar diameters

X = diameter of adsorbed molecule (cm)

ξ = clearance of bearing (cm)

a wide selection of alloys, and also plastics for one member of the pair, but only three metals are available for the other member: 52100 steel, 302 stainless steel and a 65/35 brass. It is possible to make limited adjustments in this part of the model; for instance, the same alloy heat-treated to a different hardness, or plated on a different metal substrate can be handled. However, this requires the assumption that the coefficient of friction is the same as for the material listed, which is hard to justify.

The reasons for these limitations lie partly in the history of the model. It was developed primarily for use in designing business machines to operate in air-conditioned offices. Release to the general engineering public was a later consideration, and apparently sufficient warnings of its limited applicability were not included. As a result, lubrication engineers have tended to criticize Model I for not serving purposes clearly outside its scope, rather than looking to see in what directions it needs to be extended. The authors (9) do not plan to extend the model as it already serves the original purpose at IBM. However, they suggested that anyone interested in doing so could prepare tables for other temperatures and humidities. Plastics in particular need such special handling.

The limited version available has two levels. Model IA is for design at the "zero wear" level, defined as damage low enough not to change the original surface roughness. This may be considered to be a means of locating point A in Fig. 1. Model IB is for finite wear, and is further subdivided into two types of wear apparently corresponding to regimes AB and BY.

Both models are tied to a concept of unit travel called a "pass" and defined as the distance of sliding equal to the Hertz contact area dimension in the direction of motion.

ANALYSIS OF MODEL IA

This model uses the criterion for zero wear that the maximum shear stress in the contact area τ_{\max} must be smaller than a certain fraction, G , of the yield stress in shear of the material, τ_y . Hence, the following inequality defines "zero wear conditions":

$$\tau_{\max} \leq G\tau_y \quad [1]$$

change to 1

When the number of passes (N) is 2000 G has the reference value G_R . G_R can have one of three possible values, depending on the materials and lubricant. For full hydrodynamic lubrication $G_R = 1.00$. For boundary lubrication $G_R = 0.54$ designates systems with low susceptibility to transfer and $G_R = 0.20$ for those with high susceptibility. No systems showing G_R values intermediate between 0.20 and 0.54 have ever been detected, indicating that these represent different sub-regimes. Values of G_R are tabulated (4) for over 500 systems, and for unlisted systems $G_R = 0.20$ is usually assumed. For $N \geq 2000$ passes,

$$G = \left(\frac{2000}{N}\right)^{1/9} G_R \quad [2]$$

Use of the model is by stepwise calculation. First, the contact stress τ_{\max} is calculated from the Hertz formula appropriate to the geometry, the load, the radii of curvature, the Young's modulus and Poisson's ratio of the materials and the coefficient of friction of the system, F . A stress concentration factor may be used to correct the Hertz formula for sharp corners, and non-Hertz cases can also be handled. Values of F must be looked up from the same table as G_R , obtained experimentally or estimated by analogy from listed systems.

The number of passes for zero wear (N_0) in passes may be estimated by combining Inequality [1] and Equation [2].

$$N_0 = 200 \left(\frac{\tau_y G_R}{\tau_{\max}} \right)^9 \quad [3]$$

However, the lifetime of each member must be considered separately. For the "fixed spot" member, on which the contact spot does not move, the zero-wear travel d_0 in inches of relative travel is given by

$$d_0 = SL_0 = HN_0 \quad [4]$$

where H is the length of the Hertz contact spot in the direction of travel, S the distance traveled per revolution or stroke and L_0 the lifetime in revolutions or strokes.

For the "moving spot" member, on which the contact spot keeps moving,

$$d_0 = SL_0 = SN_0 \quad [5]$$

The lower of these d_0 values is taken as the lifetime of the system. Failure at this point is believed to be by fatigue (8).

It is not possible to do a great deal of mathematical testing on Model IA, as the only inputs are load, geometry, properties of the two materials and F . The value of G_R is automatically selected from the tables (4) or estimated to be 0.20. For an example, the ball-on-plane geometry of Rowe (5) and Bayer (6) may be put through some computations. Unfortunately, no fixed F value for Rowe's copper (hemi-)sphere is available, but the range 0.26 to 0.57 can be reconstituted from his paper. He gives hardness values for his copper and steel of 88 and 220 kg/mm² respectively.

The equations for the sphere are (13)

$$\tau_{\max} = q_0 \sqrt{[1 - 2\nu_1]^2/16 + F^2} \quad [6]$$

where q_0 is the maximum stress in the τ_{\max} Hertz contact area and ν_1 is Poisson's ratio for the metal of the sphere. For this geometry

$$q_0 = \left[\frac{6W'}{\pi^3 \left[\frac{1 - \nu_1^2}{E_1} + \frac{1 - \nu_2^2}{E_2} \right]^2 r^2} \right]^{1/3} \quad [7]$$

Where W is the load, E_1 , and E_2 are Young's modulus for sphere and plane, and r is the radius of the sphere (0.312 cm or 0.123 in).

By definition

$$q\phi_0 = 6 W/H^2 \quad [8]$$

For Copper, $E_1 = 16.5 \times 10^6$, $\nu_1 = 0.34$, $\tau_y = 12,800$ pse; for Steel, $E_2 = 30 \times 10^6$, $\nu_2 = 0.30$; System $G_R = 0.20$ (the conservative assumption).

With these inserted, the minimum zero wear travel of this system in inches is

$$d_0 = \frac{8.68 \times 10^{-15}}{W^{2.67} (0.0064 + F^2)^{4.50}} \quad [9]$$

This was evaluated for the loads and F values shown in Table 1. The loads are considerably below Rowe's range, to avoid the criterion $d_0 < H$ (16). This is not clearly expressed in the published versions (4,7) though it is implicit in inequality [1]. The μ values cover the entire range from MacGregor's lowest to Rowe's highest.

We may conclude that Model IA is useful in locating point A in Fig. 1 but needs generalization. The extreme sensitivity of d_0 to F creates a problem, and a more sophisticated method for estimating F would be highly desirable.

EVALUATION OF MODEL IB

This model (7) requires an immediate decision as to the type of wear anticipated, not by an analytic or computer process, but based on the experience of the user or on a quick simulative experiment. There are two possible modes; one involves high transfer of material from one surface to the other. If this corresponded to regime YZ in Fig. 1, it would be outside the scope of this study. However, as shown under Model IIIA, it corresponds to the "Archard wear law" under conditions obviously related to corrosive wear. The other, with little or no transfer, can be analysed by using many of the factors already considered in Model IA. It must be recognized at the start that only one of the surfaces is expected to show finite wear, while the other one is expected to remain in the

zero-wear condition described in Equation [3]. The wear on the first surface is predicted by a differential equation which is basically a statement that wear is a function of the energy dissipated per pass:

$$d[A_1/\tau_{\max} W)^{9/2}] = C' dN \quad [10]$$

This equation can be integrated only for specific situations, of which only the Rowe example used above will be illustrated. Converting A_1 , the cross-sectional area of the wear track, to the more useful wear track width (in this case, equal to ball scar diameter) is done by an approximation based on a triangular area formula

$$A_1 \approx \frac{w^3}{16r} \quad [11]$$

Wear on the ball results in a flat-to-flat geometry, so that

$$\tau_{\max} H = \frac{4W(0.25 + F^2)^{0.5}}{\pi w} \quad [12]$$

Making these substitutions and integrating for ball wear,

$$w = C(LrS)^{0.118} P^{0.530} (0.25 + F^2)^{0.265} \quad [13]$$

where C includes the original C' times several numerical constants. Neither C' nor C can be developed directly from material properties.

By establishing a formalization of the definition of zero wear, it is possible to establish a useful relationship between Models IA and IB. This is done by defining the depth of the "zero" wear scar as half the surface roughness, D . From this and the triangle approximation, the zero wear scar width

$$T_0 = (8rD)^{1/2} \quad [14]$$

Assuming that all the other factors in Equation [14] remain constant

$$T = T_0 \left(\frac{L}{L_0} \right)^m \quad [15]$$

TABLE 1 - PREDICTED ZERO WEAR TRAVEL (in) FOR COPPER BALL ON STEEL DISK

COEFFICIENT OF FRICTION (F):	.08	.16	.24	.32	.40	.48	.56	.64
LOAD (lb) POUNDS								
.001	286.	4.63	0.205	1.88×10^{-2}	2.78×10^{-3}	5.68×10^{-5}	1.46×10^{-5}	4.50×10^{-5}
.004	7.10	0.115	2.08×10^{-3}	4.66×10^{-4}	6.89×10^{-5}	1.41×10^{-5}	3.63×10^{-6}	1.16×10^{-6}
.015	0.209	3.38×10^{-3}	1.50×10^{-4}	1.37×10^{-5}	2.03×10^{-6}	4.15×10^{-7}	1.07×10^{-7}	3.29×10^{-8}
.065	4.19×10^{-3}	6.78×10^{-5}	3.00×10^{-6}	2.75×10^{-7}	4.06×10^{-8}	8.31×10^{-9}	2.14×10^{-9}	6.58×10^{-10}
.250	1.15×10^{-6}	1.86×10^{-8}	8.24×10^{-9}	7.57×10^{-9}	1.12×10^{-9}	2.29×10^{-10}	5.90×10^{-11}	1.81×10^{-11}

Note: All values below the line are unreliable by the criterion $d_0 < H$ (16).

where m is 0.118 for ball wear and 0.133 for plane wear. In the high transfer regime, these exponents are 0.25 and 0.33 respectively. As shown under Model IIIA, $m = 0.25$ is equivalent to the "Archard wear law."

It has been demonstrated that L_0 is independent of surface finish (14). It is proper to substitute the L_0 value obtained from Equation [3] into Equation [13] as this point represents the intersection of the zero wear line with the finite wear curve. This is a discontinuity, where the ball ceases to have a spherical contact on the plane. Another discontinuity comes when the second member starts to wear, and Equation [13] is not applicable above this point.

It is evident that Equation [13] shows a much greater dependence of wear on surface finish than most investigators find in the boundary regimes (10). Bayer's tying D to the coarser surface (7) has been reconsidered and the writer believes it best to use the roughness of the surface expected to first show wear. This is necessary by the definition [14] and is compatible with the general nature of adhesive wear. It is important to use peak-to-peak values for D . If only root-mean-square values are available, they should be multiplied by $2\sqrt{2}$ to convert them.

There is a case in which the roughness of the non-wearing surface is significant, but it is so special as to be outside the scope of this study. It is usually the result of very poor design in which the harder member acts as a file on the softer one. This is known as "two-body abrasive wear", and is set aside along with the similar case in which hard foreign matter embeds in one surface to create the "file."

The result of computation using Model IB with the same conditions as for zero wear in Table 1 are shown

in Table 2. Rowe's copper sphere roughness of 1 micro-inch RMS was converted to 2.8 microinches peak-to-peak. To provide results comparable to him, the program was set up to read out in V/d , using the proper geometrical formula to convert T to V . The d values were selected to cover Rowe's ranges of 3 to 20 hours at 0.1 to 100 cm/sec.

The results compare very favorably with Rowe's Fig. 4, where the lightest load gives a value of $V/dW\gamma$ of 1.2×10^{-12} cc/cm-g. Transforming Table II to the same units, we find that for $F = 0.24$ and $d = 10^4$ cm (3900 in), the values of this function vary from 1.3×10^{-12} at the lightest load to 2.3×10^{-12} at the first load beyond the $d_0 < H$ criterion. Similar calculations for $m = 0.250$ gave values of 2×10^{-11} and 3×10^{-8} , respectively, indicating that $m = 0.118$ was the proper choice despite Rowe's assumption of the "Archard law."

BASIS OF MODEL II

The Rowe model was presented in three papers of increasing degrees of sophistication (5, 11, 12). It is based on reversible adsorption. The basic equation is an adaptation of the "Archard wear law"

$$\frac{V}{d} = \frac{k_m \gamma \alpha W}{P_m} \quad [16]$$

where k_m is a dimensionless wear coefficient descriptive of the surfaces, W the load and P_m the flow pressure under static loading. The other factors are obtained as follows:

$$\gamma = (1 + 3F^2)^{0.5} \quad [17]$$

TABLE 2—PREDICTED WEAR RATES FOR MODEL IB (cm³/cm)

LOAD (lbs)	SLIDING DISTANCE (in)	COEFFICIENT OF FRICTION (F)							
		.08	.16	.24	.32	.40	.48	.56	.64
0.001	3,900	9.5×10^{-13}	8.0×10^{-13}	7.1×10^{-13}	2.2×10^{-12}	4.6×10^{-12}	9.4×10^{-12}	1.7×10^{-11}	2.9×10^{-11}
0.004	3,900	4.2×10^{-13}	1.4×10^{-11}	3.7×10^{-11}	1.0×10^{-11}	2.4×10^{-11}	5.0×10^{-11}	9.5×10^{-11}	1.6×10^{-10}
0.015	3,900	7.4×10^{-13}	4.3×10^{-12}	1.7×10^{-11}	5.1×10^{-11}	1.2×10^{-10}	2.6×10^{-10}	5.0×10^{-10}	8.7×10^{-10}
0.065	3,900	4.3×10^{-12}	2.4×10^{-11}	1.0×10^{-10}	3.2×10^{-10}	7.8×10^{-10}	1.7×10^{-9}	3.2×10^{-9}	5.5×10^{-9}
0.250	3,900	1.8×10^{-11}	1.3×10^{-10}	5.6×10^{-10}	1.7×10^{-9}	4.3×10^{-9}	9.2×10^{-9}	1.8×10^{-8}	3.1×10^{-8}
0.001	39,000	4.6×10^{-14}	5.1×10^{-14}	2.1×10^{-13}	5.2×10^{-13}	1.3×10^{-12}	2.6×10^{-12}	4.8×10^{-12}	8.6×10^{-12}
0.004	39,000	1.0×10^{-13}	2.5×10^{-13}	9.8×10^{-13}	2.9×10^{-12}	7.0×10^{-12}	1.5×10^{-11}	2.8×10^{-11}	4.9×10^{-11}
0.015	39,000	1.7×10^{-13}	1.1×10^{-12}	4.8×10^{-12}	1.5×10^{-11}	3.7×10^{-11}	7.8×10^{-11}	1.5×10^{-10}	2.6×10^{-10}
0.065	39,000	1.1×10^{-12}	7.0×10^{-12}	3.0×10^{-11}	9.4×10^{-11}	2.3×10^{-10}	5.0×10^{-10}	9.5×10^{-10}	1.7×10^{-9}
0.250	39,000	5.5×10^{-12}	3.8×10^{-11}	1.7×10^{-10}	5.2×10^{-10}	1.3×10^{-9}	2.8×10^{-9}	5.3×10^{-9}	9.4×10^{-9}
0.001	390,000	6.5×10^{-15}	1.4×10^{-14}	5.2×10^{-14}	1.6×10^{-13}	3.6×10^{-13}	7.6×10^{-13}	1.5×10^{-12}	2.5×10^{-12}
0.004	390,000	1.7×10^{-14}	6.9×10^{-14}	2.7×10^{-13}	8.3×10^{-13}	2.1×10^{-12}	4.4×10^{-12}	8.3×10^{-12}	1.4×10^{-11}
0.015	390,000	5.0×10^{-14}	3.3×10^{-13}	1.4×10^{-12}	4.4×10^{-12}	1.1×10^{-11}	2.3×10^{-11}	4.4×10^{-11}	7.7×10^{-11}
0.065	390,000	3.0×10^{-13}	2.1×10^{-12}	9.1×10^{-12}	2.8×10^{-11}	7.0×10^{-11}	1.5×10^{-10}	2.8×10^{-10}	5.0×10^{-10}
0.250	390,000	1.6×10^{-12}	1.1×10^{-11}	5.0×10^{-11}	1.6×10^{-10}	3.9×10^{-10}	8.4×10^{-10}	1.6×10^{-9}	3.0×10^{-9}

Note: All values below the line are unreliable by the criterion $d_0 < H$ (16).

The constant 3 is from the von Mises equation for two dimensional plastic flow. Spurr (13) has further justified this value.

The fractional surface film defect is

$$\alpha = 1 - \exp \left[\frac{-X \exp(-E/RT_s)}{Ut_0} \right] \quad [18]$$

where X is the diameter of the spot associated with an adsorbed molecule, E the heat of adsorption, R the gas constant and U the sliding velocity.

The surface temperature is

$$T_s = T_b + 1.040 \times 10^{-5} F U \frac{(WP_m)^{0.5}}{(k_1 + k_2)} \quad [19]$$

where T_b is the bulk lubricant temperature and k_1 and k_2 the thermal conductivities of both surfaces. This is the well-accepted "surface temperature rise" equation.

The fundamental time of vibration of an adsorbed molecule is

$$t_0 = 4.75 \times 10^{-13} \left(\frac{MV_m^{2/3}}{T_m} \right)^{0.5} \quad [20]$$

where M is the molecular weight of the lubricant, V_m its molecular volume and T_m its melting point.

ANALYSIS OF MODEL IIA

All of these input values can be estimated or are known quite precisely. Rowe tested this equation by back-calculating from wear experiments, but the present plan is to use it for design purposes and then judge the results against both general and anomalous experience. For this purpose one may regard H , U , M , V_m and t_0 as preselected parameters. P_m is obtainable from the Diamond Pyramid Hardness, Vickers Hardness Number, etc. or from MacGregor's Table III-4 (4). k_m has a theoretical value for hemispherical wear particles of 0.33, shown by Rowe to be of the right order of magnitude.

The values of E are not so generally available, and it is proposed to use a simpler parameter, $(6V_m^{1/3})^{1/3}$, which has proved to be of great value in predicting surface free energies. This is the diameter of the sphere associated with the surface molecule. Hence,

$$\alpha = 1 - \exp \left(\frac{-\exp(-E/RT_s)}{3.83 \times 10^{-14} U(M/T_m)^{0.5}} \right) \quad [21]$$

Values of T_m are readily available for pure compounds, but for mixtures such as lubricating oils they simply do not exist. (The pour point only indicates that enough wax has coagulated to gel the liquid.) Hence, in such cases a generalized melting point based on the critical or pseudocritical point will be used,

$$T_m = 0.40 T_c \quad [22]$$

It must be mentioned that de Boer (14) has recently taken considerable exception to the practice of regarding t_0 as the vibration time. He finds that for adsorbed gases, $t_0 = h/kT$ where h is Planck's and k Boltzmann's constant. Liquids show lower values by a multiplier which is very difficult to predict.

Values of F cannot be predicted with any degree of certainty. Many values can be picked up from MacGregor's Table III-3. Fortunately, values of γ are not subject to even as much variation as those of F , which range only from 0.08 to 0.29 in MacGregor's lubricated systems. (Values up to 0.39 on Be-Cu seem to be a rare exception.) Hence, $\gamma = 1.06$ covers all his data with $\pm 5\%$ error, though Rowe found $1.1 < \gamma < 1.4$ for his system.

To predict the effects of this variation on T_s , we may use Rowe's example of copper on steel at 10 cm/sec, 4000 g and 311°K. The temperature rise would be only 1.5 to 5.5°K over the range of γ from 0.08 to 0.29. At his maximum speed of 100 cm/sec, the rise would be 15 to 55°K, so that T_s would be $346 \pm 17.5^\circ\text{K}$. Thus, again a fixed value of $\gamma = 0.175$ would only result in about $\pm 5\%$ error. We cannot be complacent about this, however, as processing these values through Eq. [18] results in a seven-fold range in α , the fraction of lubricant film defects, and hence in wear rate.

Some hope for a more exact input may be derived from Spurr (15), who arrived at an equation

$$F = \frac{(\tau_y \cos \theta_r \cos \theta_s)}{P_m^{0.7}} \quad [23]$$

where τ_y is the yield stress in shear of the softer material, θ_r and θ_s are the contact angles of water on the rider and specimen, or "fixed" and "moving spot" respectively, when lubricated with a partial film of stearic acid. His measurement of P_m by Vickers hardness number is presumably equivalent to Rowe's Diamond Pyramid Hardness and MacGregor's Microhardness. If so, τ_y is obtained from P_m by MacGregor's Fig. III-3.

Spurr's reasoning points up a weak spot in Rowe's, in that the latter proceeded as if E were the same for copper and iron, and that only the film on one side of the contact need be considered. To fulfill Rowe's definition of α , which is the same as Spurr's for $\cos \theta_r \cos \theta_s$, it can be proved by elementary probability theory that it must be the product of α_r and α_s which are equal to the $\cos \theta_r$ and $\cos \theta_s$ respectively. These can be calculated by Equation [18] or [21] by using the appropriate E_r and E_s , the heats of adsorption on rider and specimen. While this change in definition will not affect cases near $\alpha = 1$, at the level $\alpha < 0.01$ which Rowe indicated to be of most interest it will produce a drastic change. In effect, $\exp(-E/RT_s)$ is replaced by $\exp(-(E_r + E_s)/RT_s)$ which for similar metals is $\exp(-2E/RT_s)$. Thus, Rowe's eminently satisfactory value of $E = 11700$ is cut in half. The alternative is to accept a geometric mean definition $\alpha = \sqrt{\alpha_r \alpha_s}$ which would preserve the value of E at some expense of logic. Both alternatives will be explored numerically.

Obviously, the simultaneous solution of Equations [19, 21 and 23] is beyond an algebraic manipulation, but it is certain that an iterative computer program can be set up to handle it.

Evaluation of E is the most difficult task, and also the most important in testing Model II. Very few values are available in the literature, and Rowe was forced to compare his experimental heats (or energies) of adsorption with other authors' works of adhesion. These are not the same, though the 40% or so difference may be trivial compared to other uncertainties.

The heat of adsorption is equal to the energy of adhesion, and according to Philippoff (16)

$$E = \frac{A_{12} - T_s dA_{12}}{dT_s} = \frac{(1 - K_{12})Q_2 - \gamma_2 T_s dK_{12}}{dT_s} \quad [24]$$

where A_{12} is the work of adhesion, K_{12} is a relationship defined by

$$K_{12} = \left(\frac{A_{12}}{\gamma_2} \right) - 1 = \frac{(\gamma_1 - \gamma_{12})}{\gamma_2} \quad [25]$$

and is numerically equal to $\cos \theta$ until it exceeds 1.000, γ_1 and γ_2 the surface free energies of the solid and liquid, and γ_{12} their interfacial free energy. Other definitions are:

$$Q_2 = \frac{\gamma_2 - T_s d\gamma_2}{dT_s} \quad [26]$$

$$A_{12} = \gamma_1 + \gamma_2 - \gamma_{12} = \gamma_2(1 + K_{12}) \quad [27]$$

The important difference between this treatment and that used by many authors is that K_{12} is able to assume values greater than 1. This avoids the usual trivial solution $A_{12} = 2\gamma_2$, which merely states that the joint will part between liquid layers rather than at the interface. It should be noted that the Philippoff equations do not provide a value of E from the values of γ_1 and γ_2 even when full wetting ($K > 1$) exists. Thus, a further measurement of K_{12} or γ_{12} is necessary.

A solution to the γ_{12} problem is advocated by Fowkes (17), who sets up as his basic equation

$$\gamma_{12} = \gamma_1 + \gamma_2 - 2\sqrt{\gamma_1^d \gamma_2^d} \quad [28]$$

where γ_1^d and γ_2^d are the surface-free energies of solid and liquid due to "dispersion" forces alone. He tested this against interfacial free energies between mercury and water, and found need for a correction for polarity. There is some question of the validity of this approach, but it will be used as one alternative. It is especially useful in a modified form using Hansen's (18) partial solubility parameters, in which

$$\gamma_2^d = 0.0715 V_m^{1/3} (\delta_d^2 + \delta_p^2) \quad [29]$$

where δ_d^2 and δ_p^2 are the contributions to the energy of vaporization per unit volume by the London and polar forces, respectively. For the metals

$$\gamma_1^d = \frac{0.0715(\Delta H_s - RT_s)}{V_s^{2/3}} \quad [30]$$

where ΔH_s is the heat of sublimation of the metal. This is the same as γ_1 for all cubic metals, but not for mercury, antimony, zinc, cadmium, or magnesium, which require special handling. Values for γ_1 are listed by Grosse (19) for the liquid metals; these must be multiplied by 1.14 to obtain γ_1 for the solid, to correct for heat and volume change of fusion. A very interesting but less accurate procedure is based on Rabinowicz' (20) observation that γ_1 is proportional to $P_m^{1/3}$, again excluding the above anomalous metals. From this it may be deduced that

$$A_{12} \approx \gamma_2 + 500(P_m^{1/3} - P_{m2}^{1/3}) \quad [31]$$

where P_{m2} is the hardness of the metal measured while it is submerged in the liquid. While this is dimensionally unbalanced it offers a most convenient experimental method for A_{12} , never explicitly published though implied by Inanaka (21).

To obtain E , it is also necessary to have the entropy (dA_{12}/dT_s). Fortunately, this can be obtained from the relation cited by Duga (22):

$$\gamma_2^d = \gamma_0^d \left(1 - \frac{T_s}{T_c} \right)^{1.2} \quad [32]$$

where γ_0 is the surface free energy extrapolated to 0°K. The expression for E obtained by substituting [32] into [28] and [27], differentiating and substituting into [24] is cumbersome but workable. The justification for Equations [29], [30], and [32] is unpublished but has been verified for mercury.

An alternative approach has been developed by Karashaev (23), who uses the simpler formula

$$A_{12} = \frac{B(\epsilon - 1)}{(\epsilon + 2)} \quad [33]$$

where ϵ is the dielectric constant of the liquid and B is a constant depending only on the electronic structure of the metal. A method for calculating B from the contact potential is given by Zadumkin (24). Differentiating Equation [33], simplifying by the approximation $\epsilon^2 \gg \epsilon$ and assuming that the temperature dependence of E is entirely due to thermal expansion,

$$E = B \left(\frac{\epsilon - 1}{\epsilon + 2} \right) - \frac{3P}{\epsilon} \left(\frac{1}{V_m} \frac{dV_m}{dT_s} \right) \quad [34]$$

Equation [33] has been verified by Karashaev for specially purified gallium at 20°C as well as the anomalous mercury, and the results are in accord with Philippoff's predictions (16). However, Equation [31] gives a larger value of E than Rowe's experiments (5), so that it must be used with caution. This is probably due to neglect of a temperature dependence of B , which presumably can be corrected.

Computation of a wear rate by Model IIA is somewhat complicated by the iterative procedure for μ , and the necessity to decide between the two possible definitions of $\alpha = \alpha_a \alpha_s$ or $\sqrt{\alpha_a \alpha_s}$. Another decision must be reached on the use of Equation [34] to replace the more cumbersome Equations [24, 27, 28, and 32], or further development of the empirical Equation [31], to obtain E . Obviously, such decisions must be made on a performance basis, and Bayer's data (7) on eight metal combinations and one plastic/metal pair appears suitable for such testing. Additional testing might be based on using Equation [23] in comparison with MacGregor's tables of $F(\phi)$. Once these decisions are made, there is no shortage of any of the required data, listed in Table 3, on a wide variety of surfaces and lubricants.

TABLE 3—INPUT DATA FOR MODEL IIA

Engineering Data:	W, U, T_0, F^*, r_1
Lubricant Data:	$M, V_m, \delta_d, \delta_p, \gamma, T_c, \epsilon^*$
Metals Data:	$P_m, \gamma, B, \Delta H_s^*, V_m^*$
(Two sets required)	

* Redundant, for alternate paths.

MODEL IIB

Rowe also published (11) the application of Model IIA to the lubrication of graphite by gases and vapors, which falls outside the scope of this paper and so will not be further discussed.

ANALYSIS OF MODEL IIC

Model IIA was designed only for pure liquids, and IIB for pure gases. These limitations were removed by development of the idea of temporary residence of both additive and base fluid on the metal surface in a dynamic equilibrium. If α and β represent the fractional film defects of the area occupied at rest by the two species, respectively

$$\frac{V}{d} = \frac{k_m[\beta + (\alpha - \beta)\phi]\gamma W}{P_m} \quad [35]$$

where ϕ is the area fraction occupied at rest by additive. Since each of these develops a film defect related to its heat of adsorption as in Equation [18], this becomes

$$\frac{V}{d} = \frac{k_m \gamma}{P_m} \left[1 + \left(\frac{x}{r_0} e^{-\Delta E/RT_0} - 1 \right) \phi \right] \frac{W}{U} \frac{x}{t_0} e^{-E/RT_0} \quad [36]$$

where ΔE is the difference in heats of adsorption, x the ratio of molecular areas, r_0 the ratio of vibration times, A the molecular area of the base fluid, and t_0 its vibration time.

It is now necessary to evaluate ϕ , and Rowe chose one of the several possible ways. He set up an equilibrium

constant for the adsorption-desorption processes of both species which will eventually result in ϕ satisfying the Gibbs-Duhem requirement of minimum free energy in the system. This results in a special expression for $x = 1$, relating the wear rate to friction function ratio $(V/\gamma d)$ for a lubricant with concentration c of an additive, to the same ratio $(V/\gamma d)_b$ for the base fluid:

$$\left(\frac{V}{\gamma d} \right)_c = \frac{e^{-\Delta E/RT_c}}{c e^{\Delta S/R}} \left[\left(\frac{V}{\gamma d} \right)_b - \left(\frac{V}{\gamma d} \right)_c \right] + \left(\frac{V}{\gamma d} \right)_b \frac{e^{-\Delta E/RT_c}}{t'_0} \quad [37]$$

where ΔS is the entropy change of the entire system.

For the case where x values are not similar, Rowe ran into more difficulty in eliminating ϕ . This arose largely because his goals included evaluating x from wear data. If the approach shown under Model IIA is taken, this problem is minimized since x simply equals the cube root of the ratio the molar volumes for additive and base fluid. In addition, t'_0 becomes the ratio of the critical temperatures of the two species. When, as often happens, T_c for the additive is not known, it can usually be estimated by the Lyderson method as discussed in Reid and Sherwood (25).

It is also quite possible to avoid these difficulties by precalculating the composition of the adsorbed layer at equilibrium. Everett (26) provides means for doing this from activity coefficients, which can be derived from solubility parameters as described by Prausnitz (27). Another approach is to apply the necessary x corrections to Equation [37] and to evaluate the entropy change from Equation [32] or [34]. Grozek (28) gives a procedure for the direct determination of ΔE in a flow microcalorimeter.

In any case, the tools are available to perform the necessary manipulation on binary or multicomponent systems. The choice of going into Model IIC with corrections for $x \neq 1$ or into Model IIA with a weighted average value of E would be largely one of convenience.

One factor completely ignored in Model II is the fact that pure metals are rarely, if ever, encountered in lubrication engineering. This is not particularly hard to deal with in the case of solid-solution alloys. Buckley (29) has shown that even 1 atomic percent or less of aluminum alloyed in copper or iron will diffuse to the surface to produce a highly enriched layer. This is not any specific reaction of aluminum but merely the same principle that causes soap to coat the surface of water. It is commonly believed that Gibbs postulated attraction of low energy components to the surface, but this is not the case. This principle merely states that when they are brought to the surface by any process, they will tend to remain there because their departure would cause an increase in free energy, a Second Law violation. The Gibbs-Duhem equation merely predicts equilibrium, and the rate of attaining it is controlled by relatively sluggish solid diffusion.

This raises the question of the time scale of Model IIC. When two asperities impact as in Fig. 2, there can be two

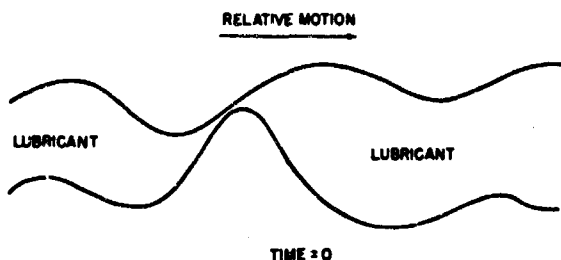


Fig. 2—The adhesive wear process—start.

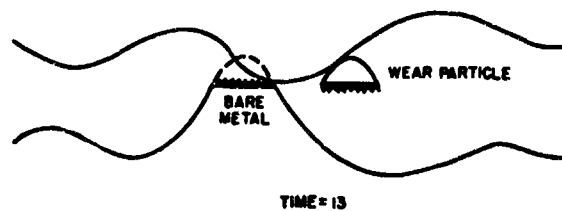


Fig. 5—The adhesive wear process—end.

different outcomes. Either the film survives by elastic deformation of the asperities (Fig. 4) or welding takes place (Fig. 3) with the generation of a hemi-ellipsoidal wear particle (Fig. 5). (The vertical scale in all these drawings is exaggerated by 50X. The times indicated may be regarded as arbitrary, though for the mechanism the writer had in mind they are approximately milliseconds.) Assuming that even the survival case requires renewal of the film due to partial rupture, we may calculate certain times on any reasonable set of parameters. Table 4 shows a typical case. The "wearing" members were calculated on the basis of time to wear a depth of $D/2$ peak-to-peak (RMS $\sqrt{2}$), and the "non-wearing" members on Model 1A. It is evident that the time for diffusion of additive from solution is very limited for the "fixed spot" (ball) member, and quite generous for the "moving spot" (plane) member, regardless of where the wear is taking place. Whether the time is sufficient for metallic diffusion on the "moving spot" member remains to be investigated. If it is, such alloys can be handled simply by calculating γ_1 by the Shain method (30). This may be a metal, or sometimes a carbide, etc.

Table 4 represents an example of the sort of new information that arises from this type of analysis. Neither Model I nor II alone would lead to the valuable conclusion that additives must be tailored to fit the "moving

TABLE 4—TIME SCALE FOR FILM RENEWAL	
Conditions: Wear Rate	$V/d = 10^{-8} \text{ cm}^3/\text{cm}$
Surface Finish	$D = 3 \times 10^{-6} \text{ cm}$ peak-to-peak
Wear Scar	$w = 0.02 \text{ cm}$ diameter or width
Hertz Diameter	$H = 0.02 \text{ cm}$
Speed	$U = 10 \text{ cm/sec}$
Path on Plate	$S = 20 \text{ cm}$
Ball Not Wearing	Ball Wearing
$t_b = \frac{H}{U} = 0.0020 \text{ sec}$	$t_b = \frac{\pi H^2 D/2}{UV/d} = 0.0024 \text{ sec}$
Plate Wearing	Plate Not Wearing
$t_p = \frac{7SD/2}{UV/d} = 3.0 \text{ sec}$	$t_p = \frac{S}{U} = 2.0 \text{ sec}$

spot" member if they are to be effective. As far as the writer knows, this principle has never been recognized before, but there is every reason to accept it as valid based both on its derivation and on practical experience. On this basis, ΔE must be calculated for the "moving spot" member, but E_b for the *hander* member, for use in Equation [37]. A more rigorous solution in terms of α and α_1 may be justifiable in the future.

Model II may also be useful in predicting the transition point at Y in Fig. 1, by reason of the rapid rise of the double exponential in Equation [18], as pointed out by Kingsbury (31) whose early work led to Model 1A. He went so far as to set up an equation for this "characteristic temperature," T_i :

$$T_i = \frac{E}{2R} \left(1 - \frac{X}{U t_0} e^{K/RT_i} \right) \quad [38]$$

which defines the conditions for a maximum da/dT . While this model does not produce a vertical line transition as shown in Fig. 1, the latter must be regarded as schematic. Data in the Y region scatter enough to fit a very steep sigmoid curve equally well.

In conclusion, it can be said that Model II opens up the whole area of reversible surface energetics to the prediction of lubrication performance. Obviously, the geometry of Model I can be put into it with very little difficulty. This would produce a design program with the additional inputs shown in Table 5. How incomplete this picture is will be shown below, under Model III.

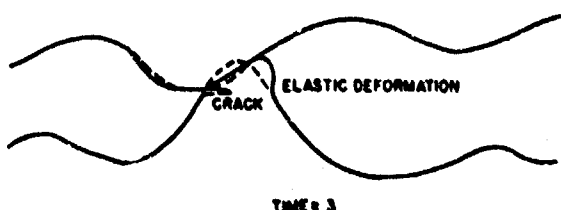


Fig. 3—The adhesive wear process—welding and cracking.

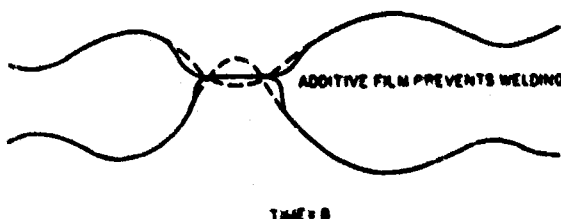


Fig. 4—Successful boundary lubrication.

TABLE 5—ADDITIONAL INPUT DATA FOR COMPLETE MODEL II

Engineering Data:	$r_2, r_3, r_4, E_1, E_2, \nu_1, \nu_2$
Additive Data:	$M, V_m, \delta_d, \delta_p, \gamma, T_c$

BASIS OF MODEL III

Neither of the models considered so far in this study have really come to grips with the irreversible chemical reactions which are known to take place at wearing surfaces, let alone those that are merely suspected. These may be put into three groups—corrosion of the metals by the atmosphere, reactions of the additives with the metals (and their corrosion products) and polymerization of the lubricant, with the metal as a catalyst. The general nature of these competitive phenomena is illustrated in Figure 6. Truly, lubrication can be described as "a very intense process in a very small reactor," to quote Dr. David Tabor.

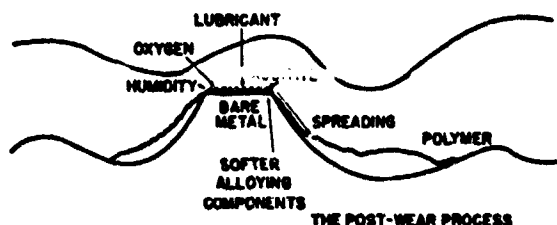


Fig. 6—The post-wear process.

ANALYSIS OF MODEL IIIA

Only a few papers seem to have taken up the mathematics of corrosive wear by oxygen and/or humidity. Tao (32) has made a fairly detailed study, based on the diffusion rate of oxygen through hydrocarbons. He started with the basic differential equations for two-dimensional steady-state diffusion, and some simplifying assumptions about the ball-on-cylinder apparatus. These included smooth surfaces, a uniform clearance (ξ), fresh oil saturated with oxygen and humidity brought in by viscous drag, instantaneous reaction of the surface followed by immediate removal of the $FeO(OH)$, and wear only at the upper (ball) surface. From these an eigenvalue and eigenfunction problem was built up and solved as

$$\xi = \frac{1}{1.64 C_0 U_o \rho} \int_H^T \frac{T^2 dt}{1 - 1.08 \exp(-3.718 \lambda T / \xi^2 U)} \quad [39]$$

where t is the time, C_0 the initial oxygen concentration, U_o the mean oil flow velocity, ρ the oil density, H the Hertz contact diameter, w the scar width on the ball (measured parallel to the cylinder axis), λ the mass diffusivity and U the sliding velocity.

Tao was able to use this equation to compute clearances, and obtained quite plausible values based on wear rates in air by neglecting the exponential term and substituting a value of W from a run of known duration. This was based on the fact that the exponential becomes negligibly small as the concentration of oxygen in the oil leaving the action zone approaches zero. With this simplification,

$$w^3 - H^3 = 0.082 \rho \xi C_0 t U \quad [40]$$

The value of C_0 was shown to be a function of the oxygen partial pressure (p), the density of the lubricant at 60°F (ρ_0) and other factors as defined above, by the writer (33).

$$C_0 = \frac{3.00 p \rho (0.980 - \rho_0)}{T_b^2 \exp \left(\frac{1.041 (T_b - 700)}{T_b} \right) + 5.347} \quad [41]$$

No equations were set up to handle humidity as it appeared that air of $\geq 50\%$ RH would provide an adequate supply of H_2O to keep the reaction supplied. Tao demonstrated in fact, that Equation [40] was only in error by about 10% regardless of the humidity.

A tentative dependence of w on the "compliance", a complex term involving B' and D , was demonstrated but the relationship to Model IB cannot be established without a good deal more work.

Obviously, this is only a partial model, as Equation [40] would indicate that no wear takes place at $C_0 = 0$. This is not true, as shown in subsequent work by the same group (2) with argon. However, no attempt was made then to incorporate this observation into Model IIIA.

A very recent paper by Schatzberg (34) led to some comments by Tao and the writer which might be considered to constitute an extension to inert atmospheres. The observation was that the dry argon had a low but measurable wear rate, consistent with (2). Schatzberg reduced all of his wear rates to the form.

$$\log W = m \log t + C'' \quad [42]$$

where C'' is a constant for any given system. He was somewhat surprised to find that only four of his sixteen cases fit the pattern of Equation [16] which Feng (35) had shown to be equivalent to Equation [12] with $m = 0.25$. Eight of the cases showed $m = 0.08$ to 0.10, four showed $m = 0.16$ to 0.18, and four showed $m = 0.23$ to 0.29. These results seem to be strongly related to those of Bayer (7), since L is proportional to t . Allowing for the difference in geometry due to Schatzberg's use of the 4-ball machine (for which Equation [10] has not yet been integrated), it seems noteworthy that his data fall into two modes near Bayer's predictions of $m = 0.118$ for low-transfer wear and $m = 0.230$ for high transfer wear of the ball. Bayer also reported (9) that a few combinations seemed to have an unstable mode with m taking

intermediate values. Schatzberg's low values were associated with dry oxygen and argon, and his high ones with wet oxygen. Thus, the "Archard Wear Law" of Equation [16] may need to be generalized to the form

$$V = \frac{k_m \gamma \alpha W d^{1m}}{P_m} \quad [43]$$

where m will vary with the atmosphere in two or three steps.

So far, all the tests of Model IIIA have involved 52100 steel. The possibility of a mathematical basis for extending this to other metals and alloys is implied by Fowle (36). He studied the ratios of oxides formed on alloys and found that the fraction coated with each oxide was more closely related to the free energy of formation of the oxide than to the composition of the alloy. This may not be helpful, as rates of oxide formation are not readily predictable from these free energies according to Kubaschewski (37). Also, in all of Fowle's five examples, the Gibbs-Duhem principle cited at the end of Model IIC would have predicted similar oxide ratios. However, the possibility of extending Equation [43] to other metals is very real.

While Tao assumed for model purposes that the corrosion product was removed as fast as formed, this is not really the case. As a result, there will be a need for surface free energies of such compounds in the solid state. Duga (22) has made an exhaustive study of these materials and his results can be applied to a hybrid Model IIC-III. Bewig and Zisman (38) have studied metal surfaces polished under water with what may be presumed to be an oxide-hydroxide-water film left on them. The data are quantitatively suitable for insertion into Equation [24]. Studt (39) has studied the displacement of one additive by another; this can be explained by Model IIC, but may involve IIIA concepts to complete it as Anderson (40) shows similar displacement by humidity.

The concept of additives forming covalent compounds with the metal surface is at least as old as that of reversible adsorption (1). However, no mathematical model has been suggested up to now. The nearest approach has been that of Kreuz (41) who demonstrated that such films can be removed by the solvent action of the base fluid. This had always been a strong argument for reversible adsorption, as it was hard to explain how a covalent film could ever fail. However, Kreuz did not carry his work to its logical conclusion by applying the Hildebrand theory of regular solutions (42). This may have been because Kreuz found quite sharp "solubilization" temperatures for his soap films, which were essentially independent of concentration; in fact, they could be related to the transition point at T in Fig. 1. Such behavior is not predicted by the Hildebrand theory because it relates only to London forces and the soaps include major polar and hydrogen bonding. Prediction of the behavior of such systems requires the Hansen modification (43), which predicts a rather sharp miscibility when the molar volume of the solid is very large with respect to that of the base fluid, V_2 .

$$(\delta_{d1} - \delta_{d2})^2 + 0.25(\delta_{p1} - \delta_{p2})^2 + 0.25(\delta_{H1} - \delta_{H2})^2 < \frac{RT_i}{2V_m} \quad [44]$$

where δ_{H1} is the hydrogen bonding parameter of the soap, δ_{H2} that of the base fluid and the other variables are as previously defined under Model IIA. This method will require more work, especially since δ_p and δ_H for soaps are not so easily calculated as for polymers, but it does offer design possibilities. It also has the complication that it leads back to Model IIC, since the soaps are still "additives" and must be treated according to their E values on the metals.

ANALYSIS OF MODEL IIIC

The "friction polymer" concept is a relatively new one, and is still far from computable. It was so named in 1958, but Fein (43) was the first to put it into general use. The general nature of the reaction seems to be clear; it consists of the highly energetic surface of the metal, made even more active by recent abrasion, acting as a catalyst in the decomposition of the base fluid. The fragments then recombine, with atmospheric oxygen if available (more slowly without it) to form a low molecular weight polymer, or oligomer by the usual standards of polymer chemistry. Chemical analyses of the product are rare and incomplete, but Fein found that it showed ketone and ester groups, and even (when nitrogen was available) amides in the infrared spectra. This phenomenon has the possibility of explaining some of the anomalies not handled by any other model (44) and also may shed light on some modes of bearing failure, outside the scope of this study, due to "lacquer" etc.

Fein had little to offer in the line of a mathematical model. Bond (45, 46), who has done much pioneer work in clarifying the rank of metals as catalysts, has not been able to provide quantitative prediction methods. This is partly because the metals do not rank in quite the same order for different reactions. For example, in hydrogen chemisorption energy they rank as follows:

$$W > Ta > Mo > Fe \approx Ni > Pd > Rh$$

while for chemisorption of ethylene they rank:

$$Pt \approx Ir > Pd > (Fe, Co, Ni) \approx Rh > Ru \approx Os > Cu$$

Both orders follow rather closely that of the surface free energies (26). Obviously, the nature of the base fluid makes a great difference, and Tabur has found (47) that even copper will rapidly polymerize dimethylsilicone. Bond (48) predicted that the order of activity of hydrocarbon would tend to be:

$$olefins > isoparaffins > naphthenes \\ \approx aromatics > paraffins$$

The work of the catalyst chemists is based on aged surfaces, and may not reveal the full extent of the prob-

TABLE 6—PREDICTIONS OF SCORING RESISTANCE ON IRON

AT. No.	METAL	CRYSTAL	RATING FROM LITERATURE				MISCIBILITY TEMPERATURE EQUATION ($V - 1^\circ$) (48)	
			(54)	(54 ^a)	(55)	(55 ^a)	deg K	SUCCESS
4	Be	HCP	Very Poor	—	—	—	210	+ ^c
12	Mg	HCP	Poor	—	Good ^a	Good/Fair	10873	± ^c
13	Al	FCC	Poor	Poor	—	Fair	2010	± ^b
14	Si	DIA	Very Poor	—	—	—	1976	—
20	Ca	FCC	Very Poor	—	—	—	24531	—
22	Ti	HCP	Very Poor	—	—	Fair	1141	— ^c
24	Cr	BCC	Very Poor	—	Good	—	146	± ^b
26	Fe	BCC	Very Poor	—	—	—	0	+
27	Co	HCP	Very Poor	Poor	—	—	139	+
28	Ni	FCC	Very Poor	—	Poor	—	84	+
29	Cu	FCC	Fair/Poor	Poor	—	Poor	179	+
30	Zn	HCP	Poor	Poor	Fair	Fair	7004	± ^c
32	Ge	DIA	Good	—	—	—	4370	+
40	Zr	HCP	Very Poor	—	Poor	Fair	1281	± ^c
41	Cb(Nb)	BCC	Very Poor	—	—	—	216	+
42	Mo	BCC	Very Poor	—	—	—	246	+
45	Rh	FCC	Very Poor	—	—	—	275	+
46	Pd	FCC	Very Poor	—	—	—	450	+
47	Ag	FCC	Good	—	Fair	Good	2596	± ^b
48	Cd	HCP	Good/Fair	Good	Good ^a	Fair	12170	± ^c
49	In	FCC	Good	—	—	—	8246	+
50	Sn	DIA	Good	—	—	—	6967	+
51	Sb	LAM	Good	—	—	—	10639	+
56	Ba	BCC	Poor	—	—	—	38896	—
58	Ce	HCP	Very Poor	—	—	—	15600	— ^c
73	Ta	BCC	Very Poor	—	Fair	—	808	± ^b
74	W	BCC	Poor	—	Fair	—	1609	± ^b
77	Ir	FCC	Very Poor	—	—	—	950	+
78	Pt	FCC	Very Poor	—	—	—	32	+
79	Au	FCC	Very Poor	—	—	—	1221	+
81	Tl	HCP	Good	—	—	—	14101	+ ^c
82	Pb	FCC	Good	—	Good ^a	Good/Fair	11742	± ^b
83	Bi	LAM	Good	—	Fair	—	16901	± ^b
90	Th	FCC	Very Poor	—	—	—	4226	—
92	U	BCC	Very Poor	—	—	—	715	+

FCC = Face Centered Cubic

DIA = Diamond Structure

FCC = Face Centered Cubic

LAM = Lamellar or Sheet Structure

HCP = Hexagonal Close Packed

(54) Scoring against 1015 steel at 4640 fpm, benzene lubricant

(54^a) Merchant's comments (cf 53), static coefficient of friction in vacuum

(55) Scar appearance in air and helium

(55^a) Merchant's comments based on friction in air and nitrogen or argon

— = Incorrect

a = In helium only

+ = Correct

b = Counted correct on most favorable data

± = Conflicting Data

c = Not counted, hexagonal

TABLE 7—PREDICTION OF SCORING RESISTANCE

METAL PAIR	CRYSTAL	RATING FROM LITERATURE			MISCIBILITY TEMPERATURE EQUATION (V - 1) (48)	SUCCESS
		(54*)	(55)	(55*)	deg K	
Al-Zn	FCC-HCP	Poor	—	Fair	1879	± ^c
Co-Cu	HCP-FCC	Poor	—	—	622	+ ^c
Al-Co	FCC-HCP	Poor	—	—	3214	- ^c
Cu-Cd	FCC-HCP	Poor	—	Poor	9706	- ^c
Cu-Zn	FCC-HCP	Poor	—	Poor/Fair	4867	- ^c
Sb-Zn	LAM-HCP	Poor	—	—	3	+ ^c
Al-Cd	FCC-HCP	Good	—	—	4771	+ ^c
Bi-Cd	LAM-HCP	Good	—	—	36	- ^c
Cd-Zn	HCP-HCP	Good	—	—	459	- ^c
Bi-Zn	LAM-HCP	Good	—	—	383	- ^c
Cu-Ni	FCC-FCC	—	Poor	—	498	+
Cr-Mo	BCC-BCC	—	Poor	—	825	+
Ti-Zn	HCP-HCP	—	Poor	—	0	+ ^c
Ag-Cu	FCC-FCC	—	Poor	Fair	1334	± ^b
Cr-Ni	BCC-FCC	—	Poor	—	444	+
Al-W	FCC-BCC	—	Poor	—	8526	—
Cu-Sn	FCC-DIA	—	Good ^a	—	4583	+
Ni-Sn	FCC-DIA	—	Fair	—	8580	—
Al-Zn	FCC-HCP	—	Poor	Fair	188	± ^c
Ag-Ta	FCC-BCC	—	Good	—	7720	+
Cu-Mo	FCC-BCC	—	Very Good	—	903	—
Ag-Cr	FCC-BCC	—	Fair/Good	—	1487	—
Cu-Ta	FCC-BCC	—	Good	—	1898	—
Al-Pb	FCC-FCC	—	Good ^a	Fair	4049	± ^a
Cu-W	FCC-BCC	—	Good	—	2986	—
Cu-Pb	FCC-FCC	—	—	Poor	8527	—
Cu-Ti	FCC-HCP	—	—	Poor/Fair	367	+ ^c
Al-Cu	FCC-FCC	—	—	Poor	948	+
Cu-Mg	FCC-HCP	—	—	Poor	7933	- ^c
Pb-Ti	FCC-HCP	—	—	Fair	6353	- ^c
Zn-Zr	HCP-HCP	—	—	Poor	3636	- ^c
Ti-Zn	HCP-HCP	—	—	Fair	3210	+ ^c
Ag-Zn	FCC-HCP	—	—	Fair	1401	- ^c
Ag-Al	FCC-FCC	—	—	Poor	41	+
Al-Mg	FCC-HCP	—	—	Poor	3806	- ^c
Al-Ti	FCC-HCP	—	—	Fair/Poor	166	+ ^c
Al-Ni	FCC-FCC	—	—	Fair	2901	+
Ag-Cu	FCC-FCC	—	—	Poor	1335	+
Ag-Ti	FCC-HCP	—	—	Fair	378	- ^c
Ag-Zr	FCC-HCP	—	—	Good	430	- ^c
Cd-Mg	HCP-HCP	—	—	Poor	84	+ ^c
Cd-Ti	HCP-HCP	—	—	Poor	7062	- ^c
Cd-Zr	HCP-HCP	—	—	Good	8095	+ ^c
Mg-Ti	HCP-HCP	—	—	Poor	5897	- ^c
Ag-Mg	FCC-HCP	—	—	Fair	3056	+ ^c

See Table VI for symbols and notes.

lem. Wear spots, such as shown in Fig. 6, are freshly abraded and emit electrons almost as if they were radioactive. Polymerization by electrical discharge has been studied by Bradley (49), who ranked some hydrocarbons:

styrene > naphthalene > toluene > ethylene
> hexamethylbenzene > propane

which again point up the uncertainties.

One factor not previously considered is the effect of pressure on polymerization. Weale (50) gives an equation which is adaptable as follows:

$$\ln(k/k_0) = \frac{q_0 \Delta V_m}{V_m RT_0} \quad [45]$$

where k and k_0 are the rate constants at q_0 pressure and at one atmosphere respectively, and $\Delta V_m/V_m$ is the fractional change in volume on polymerization. This predicts for a typical reaction in which $\Delta V_m/V_m = 0.20$, an acceleration of approximately 10,000 fold under $q_0 = 20,000$ atmospheres.

Regardless of the lack of consistent data and of a complete mathematical model, this line of attack looks very promising. The term "surface resin" for the material is suggested.

A very recent paper by Thompson (51) may be useful as it takes into account the fact that the anti-asperities can carry part of the load by hydrodynamic lubrication. Since Model IIIC involves partial filling of these spaces, Thompson's equation may provide a means for testing the rate of surface resin formation by following the time required to break in a pair of surfaces. This concept can also be used to predict another "transition failure" mechanism via Equation [44]. This would result from the layers of "surface resin" formed in the anti-asperities during break-in, (Fig. 6) suddenly going into solution (52) thus restoring the original surface roughness. The result would be to shift a good deal of the load to the asperities, which would fail quite rapidly.

MODEL IV

Investigation of the transition temperature has already been mentioned under Models II and III. However, there is reason to believe that when all else (including the oxide film) fails, the nature of the metal-metal contact may make the difference between corrosive wear and scoring at Y or even welding at Z (Fig. 1). Ernst (53), Roach (54), and Coffin (55) have all made experiments along this line. About 80% of their results can be predicted by a simple equation from Hildebrand (42) for the miscibility temperature of metals:

$$T_i = \frac{V_1 + V_2}{4R} (\delta_1 - \delta_2)^2 \quad [46]$$

where V_1 and V_2 are the molar volumes of the metals while δ_1 and δ_2 are their solubility parameters. If T_i is

less than T_s , scoring will take place. The results of these predictions are shown in Tables 6 and 7. The success ratings had to allow for the results from the laboratories containing contradictions, part of which may have been caused by the lack of a clear definition of "scoring". The writer attempted to bring the data to a common basis, in which "rough", "abraded", etc., were converted to "poor" scoring resistance, "smooth" or low wear rates to "good", and intermediate descriptions to "fair". Where data in helium was available, it was given preference over that in air or in air-saturated kerosene. All hexagonal (HCP) metals were excluded from the ratings; as shown by Buckley (56), these follow different rules than the common cubic metals. The criteria of success were based on an arbitrary choice of Poor = 0-2000°K, Fair = 2000-4000°K, Good = 4000+°K. These unrealistic temperatures result from their being based on complete miscibility at about 50/50% by volume. Future programs should be keyed to the fully developed version of Equation [46], where this can be set at 5/95 or 10/90. As pointed out by Hildebrand (42), perfect success is unlikely due to intermetallic compound formation and also to crystalline transitions of some metals at elevated temperatures.

ACKNOWLEDGMENT

This work was supported by U. S. Army Contract No. DAHC19-69-C-0033, administered by the Research Technology Division, Army Research Office, Arlington, Virginia. The kind assistance of over 50 people interviewed in the course of this study is gratefully appreciated, as is that of Mr. A. R. Garabrant who performed most of the calculations.

REFERENCES

- (1) Crook, A. W., "Some Studies on Wear and Lubrication," *Wear*, 2, 364 (1958/59).
- (2) Appeldoorn, J. K., Goldman, I. B. and Tao, F. F., "Corrosive Wear by Atmospheric Oxygen and Moisture," *ASLE Trans*, 12, 140 (1969).
- (3) Blok, H., "The Postulate About the Constancy of Scoring Temperature," Paper 4, Proc. Interdisciplinary Approach to the Lubrication of Concentrated Contacts, NASA, Washington (1970).
- (4) MacGregor, C. W., "Handbook of Analytical Design for Wear," Plenum Press, New York, 1961.
- (5) Rowe, C. N., "Some Aspects of the Heat of Adsorption in the Function of a Boundary Lubricant," *ASLE Trans*, 9, 100 (1966).
- (6) Bayer, R. G., Clinton, W. C., Nelson, C. W. and Schumacher, R. A., "Engineering Model for Wear," *Wear*, 5, 378 (1962).
- (7) Bayer, R. G., "Prediction of Wear in a Sliding System," *Wear*, 11, 319 (1963).
- (8) Bayer, R. G. and Schumacher, R. A., "On the Significance of Surface Fatigue in Sliding Friction," *Wear*, 12, 173 (1968).
- (9) Bayer, R. G. and Ku, T. C., Personal interview, April 22, 1970.
- (10) Begelinger, A., "Questionnaire on the Relation Between Surface Condition and Friction, Wear and Lubrication—Summary Report," Metalinstituut TNO, Delft, Netherlands.
- (11) Rowe, C. N., "A Relation between Adhesive Wear and Heat of Adsorption for the Vapor Lubrication of Graphite," *ASLE Trans*, 10, 10 (1967).
- (12) Rowe, C. N., "Role of Additive Adsorption in the Mitigation of Wear," *ASLE Trans*, 13, 179-188 (1970).
- (13) Spurr, R. T., "The Coefficient of Friction of Metals," *Wear*, 7, 330, (1964).
- (14) de Boer, J. H., "Mobility of Molecules along Adsorbing Surfaces,"

- from "Molecular Processes on Solid Surfaces," McGraw-Hill, New York, 1968.
- (15) Spurr, R. T., "Boundary Lubrication of Metals," *Wear*, 14, 207 (1969).
 - (16) Philippoff, W., "Grenzflächenerscheinungen an Kolloid," in "Kolloidchemisches Taschenbuch," 5. Aufl. Akademische Verlagsgesellschaft Geest and Portig K.-G., Leipzig, 1960.
 - (17) Fowkes, F. W., "Intermolecular and Interatomic Forces and Interfaces," in "Surfaces and Interfaces, I—Chemical and Physical Characteristics," Syracuse University Press, Syracuse, N. Y., 1967.
 - (18) Hansen, C. M., "The Universality of the Solubility Parameter," *IGEC Prod. Res. and Dev.*, 8, 2 (1969).
 - (19) Grosse, A. V., "The Relationship Between Surface Tension and Energy of Liquid Metals and Their Heat of Vaporization at the Melting Point," *J. Inorg. Nucl. Chem.*, 26, 1349 (1964).
 - (20) Rabinowicz, E., "Friction and Wear of Materials," John Wiley and Sons, New York, 1965.
 - (21) Imanaka, O., "Surface Energy and Fracture of Materials," *Kinzoku Hyomen Gijutsu* 19, 424 (1968).
 - (22) Duga, J. J., "Surface Energy of Ceramic Materials," DCIC Report 69-2, AD691019, Clearinghouse, Springfield, Va., 1969.
 - (23) Karashaev, A. A., Zadumkin, S. N. and Kuphno, A. I., "Temperature Dependence of the Surface Tension of Gallium and Its Interfacial Tension at the Interface with Some Nonpolar Organic Liquids," *Poverkhi. Yavleniya Rasplavakh*, 1968, 219-225.
 - (24) Zadumkin, S. N. and Karashaev, A. A., "Surface Energy at Metal/Dielectric Liquid Interfaces," *Soviet Materials Science* (Eng. Trans.) 1, No. 2, 86 (1965).
 - (25) Reid, R. C. and Sherwood, T. K., "Properties of Gases and Liquids," 2nd Ed. McGraw-Hill, New York, 1966.
 - (26) Everett, D. H., "Thermodynamics of Adsorption from Solution. Part 2—Imperfect Solutions," *Trans. Faraday Soc.* 61, 2478 (1965).
 - (27) Prausnitz, J. M., "Molecular Thermodynamics of Fluid-Phase Equilibria," Prentice-Hall, Englewood Cliffs, New Jersey, 1969.
 - (28) Groszek, A. J., "Heats of Preferential Adsorption of Boundary Additives at Iron and Iron Oxide/Liquid Hydrocarbon Interfaces," ASLE Preprint 70AM 2C-2 (May, 1970).
 - (29) Buckley, D. H., "A LEED Study of the Adhesion of Gold to Copper and Copper-Aluminum Alloys," NASA TND 5351, Aug. 1969.
 - (30) Shain, S. A. and Prausnitz, J. M., "Thermodynamics and Interfacial Tension of Multicomponent Liquid-Liquid Interfaces," *A. I. Ch. E. Jour.* 10, 766 (1964).
 - (31) Kingsbury, E. P., "The Heat of Adsorption of a Boundary Lubricant," *ASLE Trans.* 3, 30 (1960).
 - (32) Tao, F. F., "The Role of Diffusion in Corrosive Wear," *ASLE Trans.* 11, 121 (1968).
 - (33) ASTM Annual Book of Standards, Part 18, Method D 2779-69.
 - (34) Schatzberg, P., "Influence of Water and Oxygen in Lubricating Oils on Sliding Wear," ASLE Preprint 70AM 4D-2 (1970).
 - (35) Feng, I. M., "A New Approach in Interpreting the Four-Ball Wear Results," *Wear* 5, 275 (1962).
 - (36) Fowle, T. I., "Interaction Between Bearing Metals and Lubricants," Paper 3, Joint Course on Tribology, The Institution of Metallurgists, London (1968).
 - (37) Kubaschewski, O. and Hopkins, B. E., "Oxidation of Metals and Alloys," 2nd Ed., Academic Press, New York, 1962.
 - (38) Bewig, K. W. and Zisman, W. A., "Surface Potentials and Induced Polarization in Nonpolar Liquids Adsorbed on Metals," *J. Phys. Chem.* 68, 1804 (1964).
 - (39) Studt, P., "Correlation Between Adsorbability and Effectiveness of E. P. Additives in Lubricating Oils," *Erdoel Kohle* 21, No. 12:784 (1968).
 - (40) Anderson, J. L., "Groupsorption: Induced Cleavages of Functional Group/Surface Interactions," *J. Phys. Chem.* (to be published, 1970).
 - (41) Kreuz, K. L., Fein, R. S. and Rand, S. J., "Solubilization Effects in Boundary Lubrication," ACS Petr. Div. Preprint, A126 (Sept. 7-12, 1969).
 - (42) Hildebrand, J. H. and Scott, R. L., "The Solubility of Non-Electrolytes, 3rd Ed., Dover, New York, 1949.
 - (43) Fein, R. S. and Kreuz, K. L., "Chemistry of Boundary Lubrication of Steel by Hydrocarbons," *ASLE Trans.* 8, 29 (1965).
 - (44) Appeldoorn, J. K. and Tao, F. F., "The Lubricity Characteristics of Heavy Aromatics," *Wear*, 12, 117 (1968).
 - (45) Bond, G. C., "Catalysis by Metals," Academic Press, London and New York, 1962.
 - (46) Bond, G. C., "Adsorption and Coordination of Unsaturated Hydrocarbons with Metal Surfaces and Metal Atoms," *Disc. Faraday Soc.* No. 41, 200 (1966).
 - (47) Tabor, D. and Willis, R. F., "The Formation of Silicone Polymer Films on Metal Surfaces at High Temperatures and Their Boundary Lubricating Properties," *Wear* 13, 381 (1969).
 - (48) Bond, G. C., Personal interview (March 25, 1970).
 - (49) Bradley, A., "Organic Polymer Coating Deposited from a Gas Discharge," *Ind. Eng. Chem. Prod. Res. Develop.*, 9 = 1, 101 (1970).
 - (50) Weale, K. E., "Chemical Reactions at High Pressures," Chemical Engineering Series, Spon., London (1967).
 - (51) Thompson, R. A. and Bocchi, W., "A Mathematical Model for Lubricated Wear," *Trans. ASME, J. Lubr. Tech.* (to be published, 1970).
 - (52) Fein, R. S., "Operating Procedure Effects on Critical Temperature," *ASLE Trans.* 10, 373 (1967).
 - (53) Ernst, H. and Merchant, M. E., "Chip Formation, Friction and High-Quality Machined Surfaces," *Surface Treatment of Metals*, *Trans. ASM* 29, 299 (1941).
 - (54) Roach, A. E., Goodzeit, C. L. and Hunnicut, R. P., "Scoring Characteristics of Thirty-Eight Different Elemental Metals in High-Speed Sliding Contact with Steel," *Trans. ASME* 78, 1659 (1956).
 - (55) Coffin, L. F., Jr., "A Study of the Sliding of Metals, with Particular Reference to Atmosphere," *Lubr. Eng.* 12, 50 (1956).
 - (56) Buckley, D. H. and Johnson, R. L., "Friction and Wear of Hexagonal Metals and Alloys as Related to Crystal Structure and Lattice Parameters in Vacuum," *ASLE Trans.* 9, 121 (1966).

General Electric Co., Report No 69-C-379
(October, 1969)

Security Classification

DOCUMENT CONTROL DATA - R & D

(Security classification of title, body of abstract and indexing annotation must be entered when the overall report is classified)

1. ORIGINATING ACTIVITY (Corporate author) JOHN A. BROWN Box 145 Berkeley Heights, NJ 07922		2a. REPORT SECURITY CLASSIFICATION UNCLASSIFIED	
		2b. GROUP	
3. REPORT TITLE A STUDY OF FRICTION FUNDAMENTALS IN EXPLOSIVES			
4. DESCRIPTIVE NOTES (Type of report and inclusive dates) Final Technical Report			
5. AUTHOR(S) (First name, middle initial, last name) John A. Brown			
6. REPORT DATE December 1970		7a. TOTAL NO. OF PAGES 82	7b. NO. OF REFS 121
8a. CONTRACT OR GRANT NO. DAAA21-69-C-0558		8b. ORIGINATOR'S REPORT NUMBER(S)	
b. PROJECT NO.			
c.		8c. OTHER REPORT NO(S) (Any other numbers that may be assigned this report)	
d.			
10. DISTRIBUTION STATEMENT UNLIMITED			
11. SUPPLEMENTARY NOTES		12. SPONSORING MILITARY ACTIVITY United States Army PICATINNY ARSENAL Dover, NJ 07801	
13. ABSTRACT <p>Mechanical and lubrication engineers picture solid-solid contact as taking place only on the tips of the higher asperities of each surface, so that the contact load is borne only on a very small portion of the total surface area and all frictional heat is generated and absorbed in this small area. The size and number of the individual asperity junctions is in general not known; but averages are known, and it appears that asperity heights and spatial frequencies are described reasonably well by Gaussian statistics. This should make it possible to calculate frictional hot-spot temperatures and distributions on an explosive surface, given some laboratory measurements of factors such as coefficients of friction, frictional work expended and surface characteristics. With hot-spot statistics available, the probability of explosion can be calculated by available, published methods.</p> <p>A coordinated theoretical and empirical research program is proposed to apply the above engineering and mathematical concepts to explosives. The results should facilitate the identification of basic mechanical processes (such as metal-metal friction, or the viscous or plastic shear of explosives) which do and do not generate explosion hazards. This in turn will aid the design of more valid laboratory friction sensitivity testers and the design of safer explosive processing plants.</p>			

DD FORM 1473 REPLACES DD FORM 1473, 1 JAN 64, WHICH IS OBSOLETE FOR ARMY USE.

UNCLASSIFIED
Security Classification

UNCLASSIFIED

Security Classification

14. KEY WORDS	LINK A		LINK B		LINK C	
	ROLE	WT	ROLE	WT	ROLE	WT
Friction						
Explosives						
Testing						
Safety						
Mathematical models						
Laboratory sensitivity testers						
Programs						
Research planning						
Asperity statistics						
Hot-spots						

UNCLASSIFIED

Security Classification